FUNDAMENTALS

SUPERCONDUCTIVITY
SURFACE RESISTANCE
RF and CAVITIES
MICROPHONICS

Jean Delayen

Center for Accelerator Science
Old Dominion University
and
Thomas Jefferson National Accelerator Facility

Historical Overview

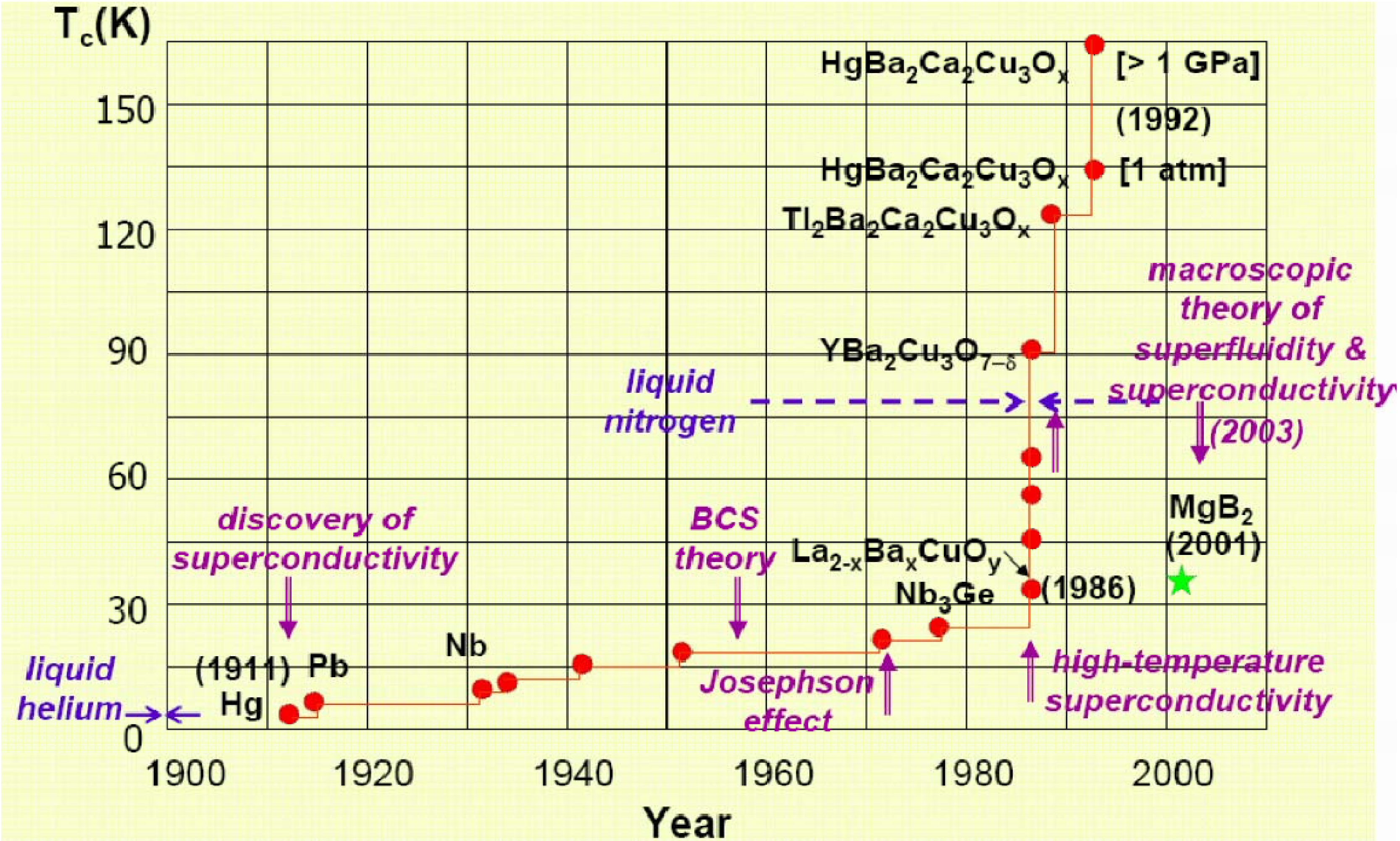

Perfect Conductivity

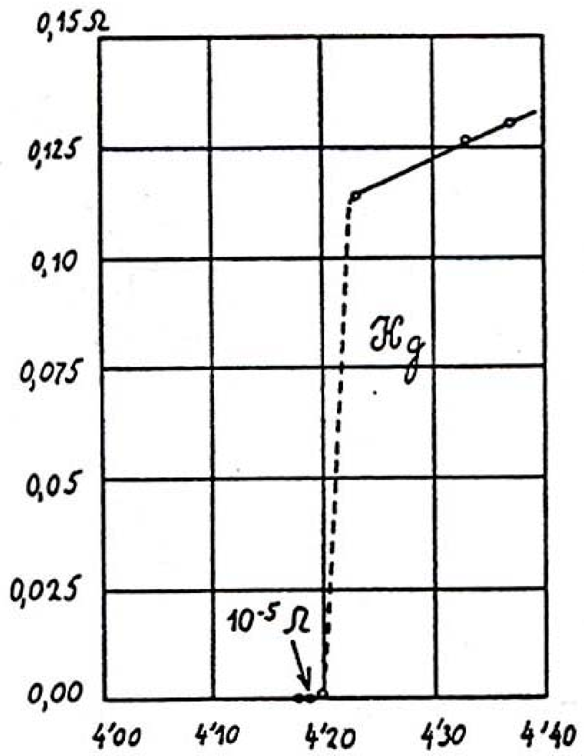

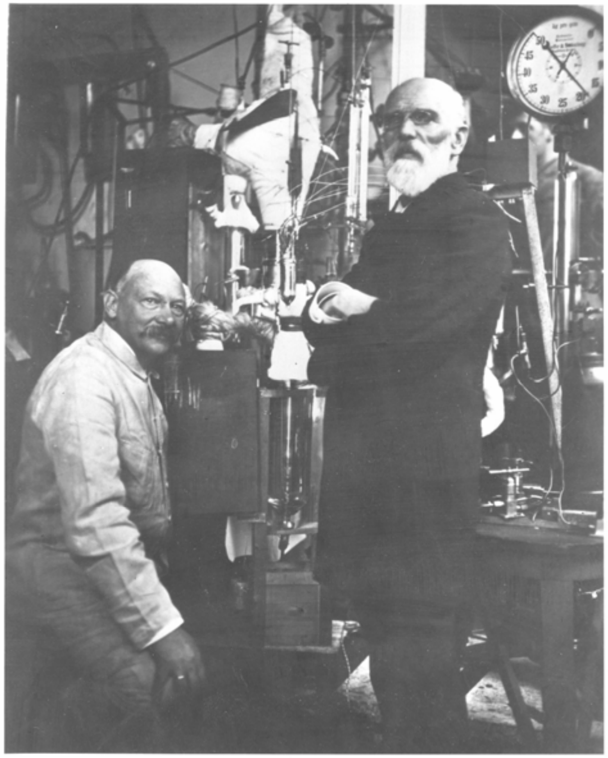

Kamerlingh Onnes and van der Waals in Leiden with the helium 'liquefactor' (1908)

Perfect Conductivity

Persistent current experiments on rings have measured

$$\frac{\sigma_s}{\sigma_n} > 10^{15}$$

Resistivity < 10^{-23} Ω.cm

Decay time > 10^{5} years

Perfect conductivity is not superconductivity

Superconductivity is a phase transition

A perfect conductor has an infinite relaxation time L/R

Perfect Diamagnetism (Meissner & Ochsenfeld 1933)

Perfect conductor

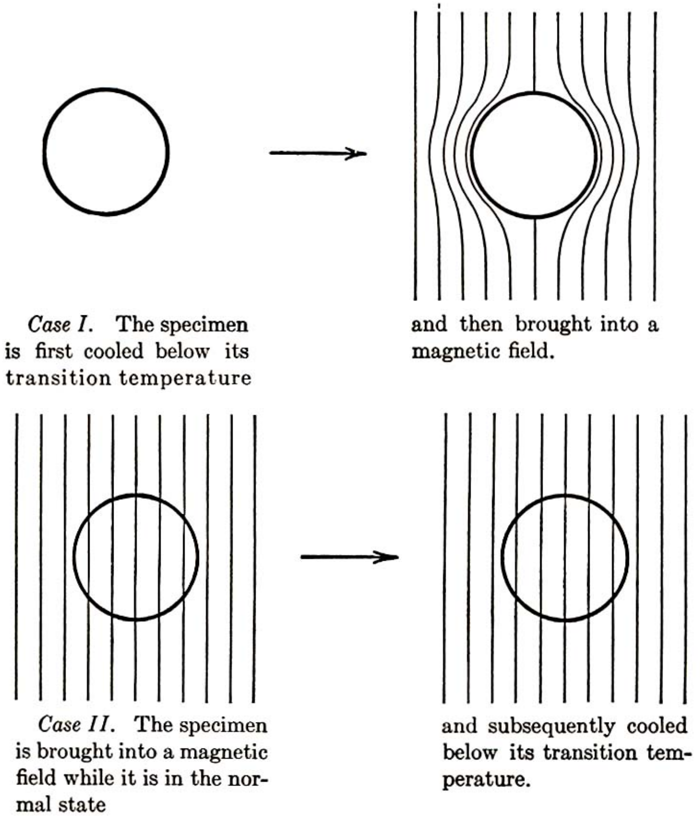

FIG. 3. The behavior expected for a transition into a state of *perfect conductivity.* The final state would depend on the *serial order* in which the specimen is brought into the same external conditions.

$$\frac{\partial B}{\partial t} = 0$$

Superconductor

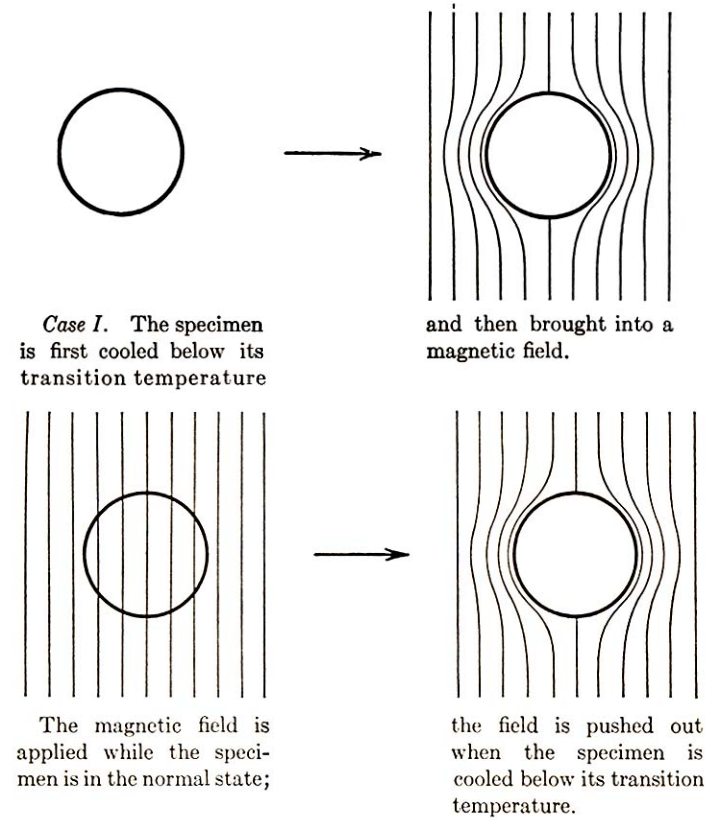

FIG. 4. Case II of Fig. 3 according to Meissner. The *superconductor,* in contrast to the perfect conductor, has zero magnetic induction independently of the way in which the superconducting state has been reached.

$$B = 0$$

Penetration Depth in Thin Films

Very thin films

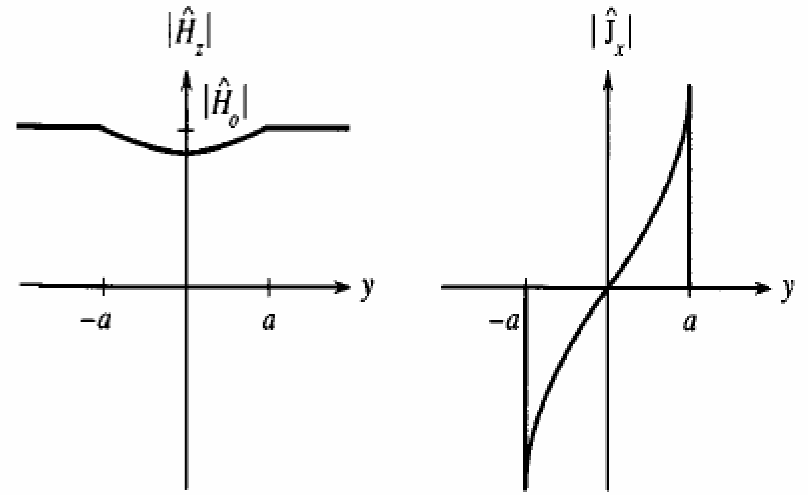

Very thick films

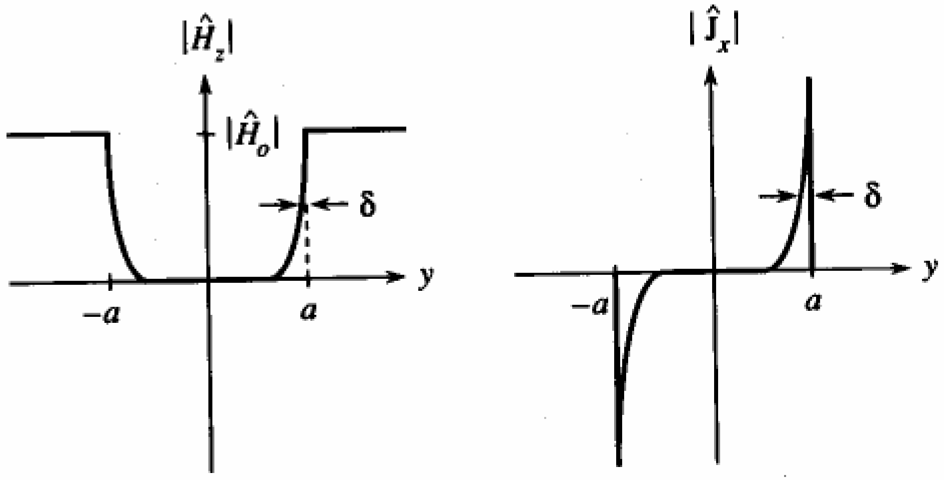

Critical Field (Type I)

Superconductivity is destroyed by the application of a magnetic field

$$H_c(T) \simeq H_c(0)\left[1-\left(\frac{T}{T_c}\right)^2\right]$$

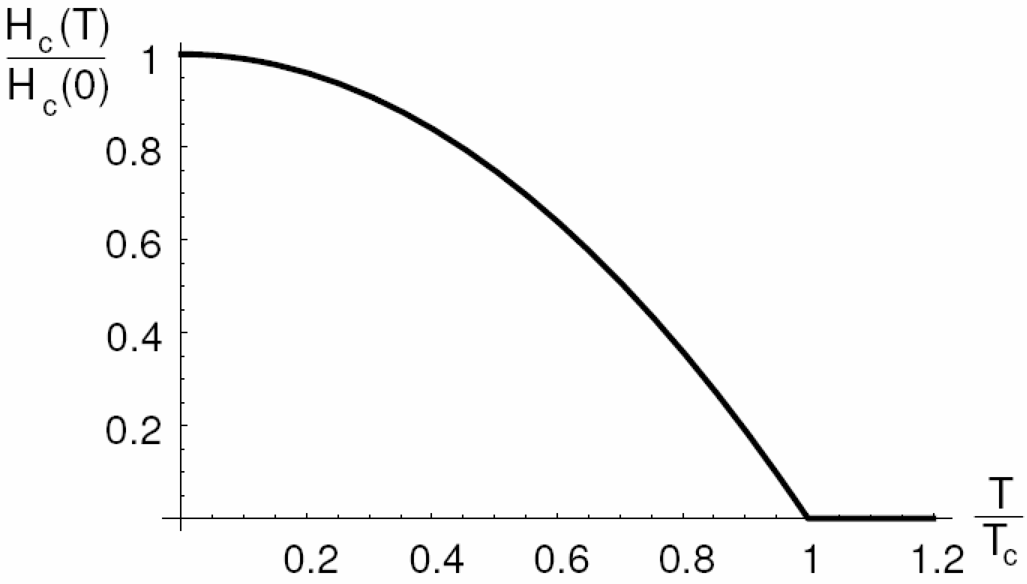

Type I or “soft” superconductors

Critical Field (Type II or “hard” superconductors)

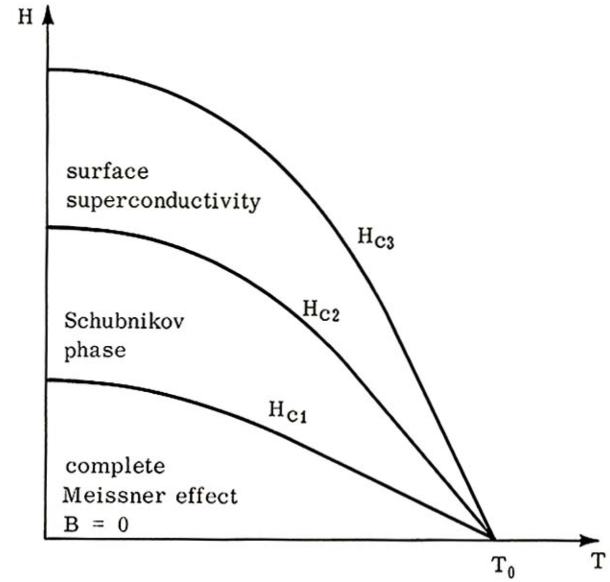

Figure 3-1
Phase diagram for a long cylinder of a Type II superconductor.

Expulsion of the magnetic field is complete up to H_{c1}, and partial up to H_{c2}

Between H_{c1} and H_{c2} the field penetrates in the form if quantized vortices or fluxoids

$$\phi_0 = \frac{\pi\hbar}{e}$$

Thermodynamic Properties

Entropy

Specific Heat

Energy

Free Energy

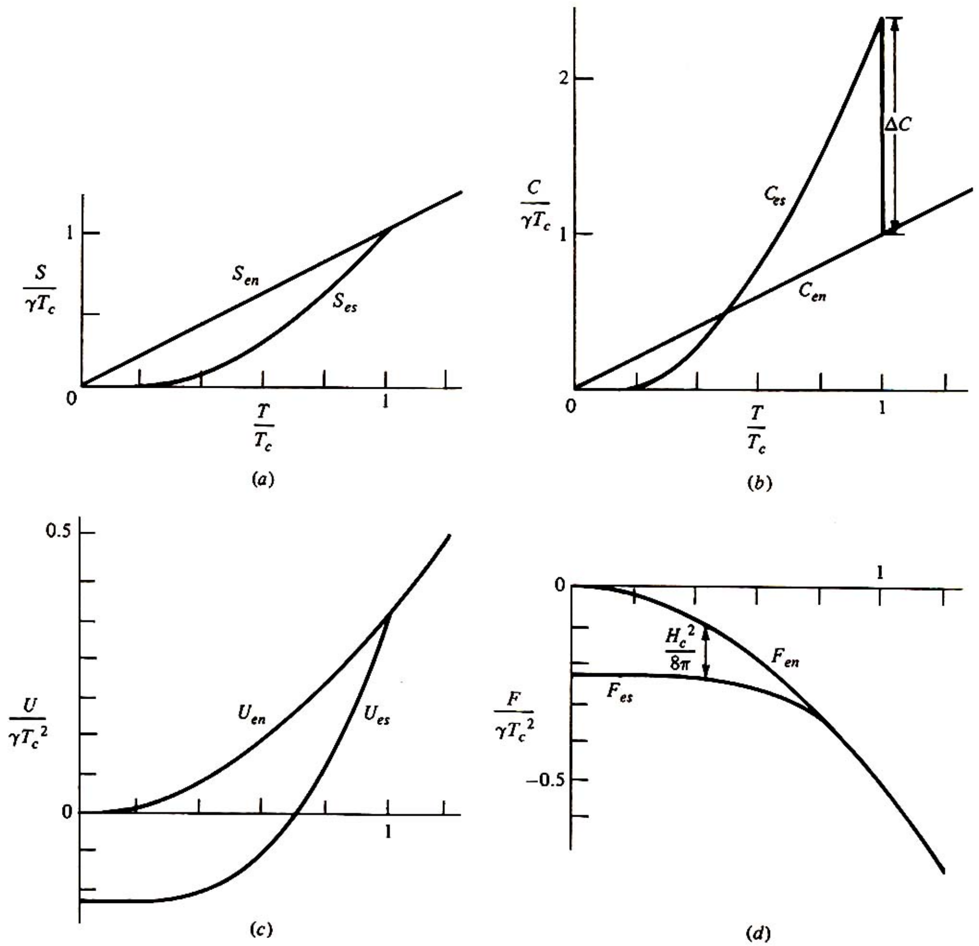

FIGURE 2-3
Comparison of thermodynamic quantities in superconducting and normal states. $U_{en}(0)$ is chosen as the zero of ordinates in (c) and (d). Because the transition is of second order, the quantities S, U, and F are continuous at T_c. Moreover, the slope of F_{es} joins continuously to that of F_{en} at T_c, since $\partial F/\partial T = -S$.

Thermodynamic Properties

When $T < T_c$ phase transition at $H = H_c(T)$ is of 1^{st} order $\Rightarrow$ latent heat

At $T = T_c$ transition is of 2^{nd} order $\Rightarrow$ no latent heat

jump in specific heat

$$C_{es}(T_c) \sim 3C_{en}(T_c)$$

$C_{en}(T) = \gamma T$ electronic specific heat

$C_{es}(T) \approx \alpha T^3$ reasonable fit to experimental data

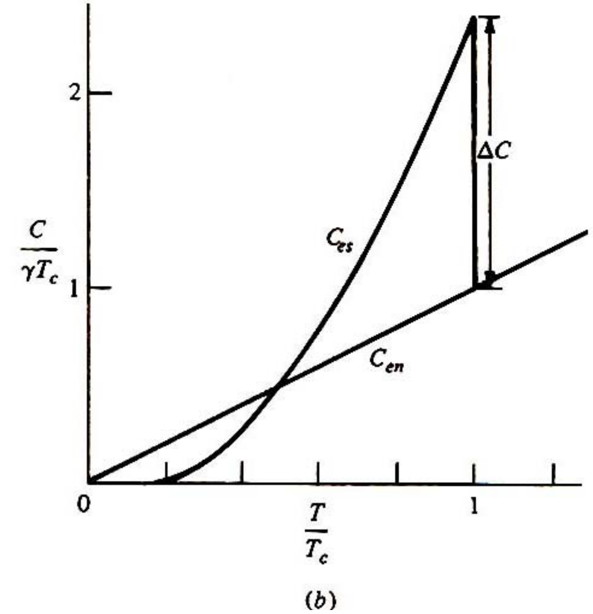

Thermodynamic Properties

At T_c : $S_s(T_c) = S_n(T_c)$ The entropy is continuous

Recall: $S(0) = 0$ and $\dfrac{\partial S}{\partial T} = \dfrac{C}{T}$

$$\Rightarrow \int_0^{T_c} \frac{\alpha T^3}{T} dt = \int_0^{T_c} \frac{\gamma T}{T} dt \rightarrow \alpha = \frac{3\gamma}{T_c^2} \qquad C_{es} = 3\gamma \frac{T^3}{T_c^2}$$

$$S_s(T) = \gamma \frac{T^3}{T_c^3} \qquad S_n(T) = \gamma \frac{T}{T_c}$$

For $T < T_c$ $S_s(T) < S_n(T)$

$\Rightarrow$ **superconducting state is more ordered than normal state**

A better fit for the electron specific heat in superconducting state is

$C_{es} = a\gamma T_c\, e^{-\frac{bT_c}{T}}$ with $a \approx 9, b \approx 1.5$ for $T \ll T_c$

Energy Difference Between Normal and Superconducting State

$$U_n(T_c) = U_s(T_c)$$ Energy is continuous

$$U_n(T) - U_s(T) = \int_T^{T_c} (C_{es} - C_{en})dt = \frac{3}{4}\frac{\gamma}{T_c^2}(T_c^4 - T^4) - \frac{\gamma}{2}\left(T_c^2 - T^2\right)$$

at $T=0$ $$U_n(0) - U_s(0) = \frac{1}{4}\gamma T_c^2 = \frac{H_c^2}{8\pi}$$

$\frac{H_c^2}{8\pi}$ is the condensation energy

at $T \neq 0$, $\frac{H_c^2}{8\pi}$ is the free energy difference

$$\frac{H_c^2(T)}{8\pi} = \Delta F = (U_n - U_s) - T(S_n - S_c) = \frac{1}{4}\gamma T_c^2\left[1 - \left(\frac{T}{T_c}\right)^2\right]^2$$

$$H_c(T) = (2\pi\gamma)^{\frac{1}{2}} T_c\left[1 - \left(\frac{T}{T_c}\right)^2\right]$$

The quadratic dependence of critical field on T is related to the cubic dependence of specific heat

Isotope Effect (Maxwell 1950)

The critical temperature and the critical field at 0K are dependent on the mass of the isotope

$$T_c \sim H_c(0) \sim M^{-\alpha} \qquad \text{with } \alpha \simeq 0.5$$

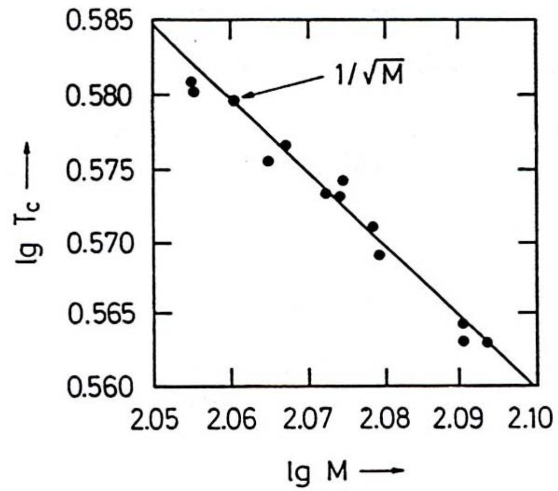

Figure 26: The critical temperature of various tin isotopes.

Energy Gap (1950s)

At very low temperature the specific heat exhibits an exponential behavior

$$c_s \propto e^{-bT_c/T} \qquad \text{with } b \simeq 1.5$$

Electromagnetic absorption shows a threshold

Tunneling between 2 superconductors separated by a thin oxide film shows the presence of a gap

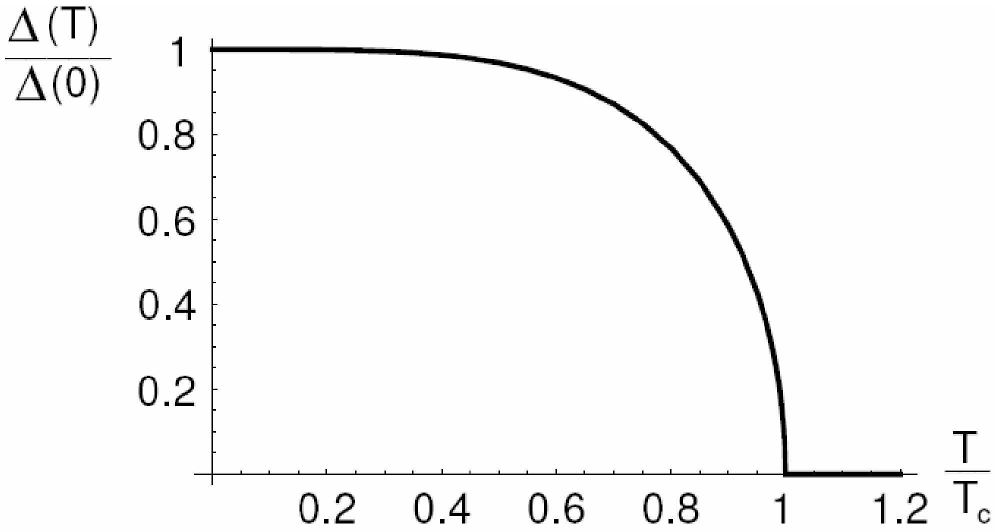

Two Fundamental Lengths

- London penetration depth λ
  - Distance over which magnetic fields decay in superconductors
- Pippard coherence length ξ
  - Distance over which the superconducting state decays

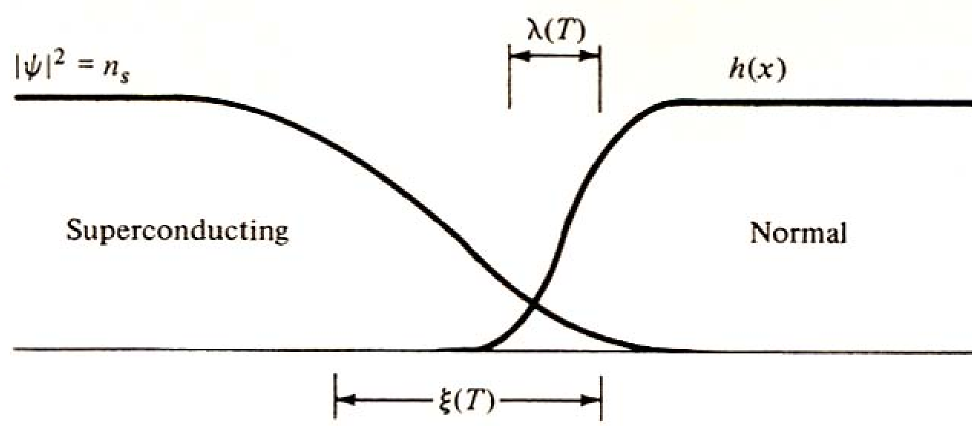

FIGURE 1-4
Interface between superconducting and normal domains in the intermediate sta

Two Types of Superconductors

- London superconductors (Type II)
  - $\lambda \gg \xi$
  - Impure metals
  - Alloys
  - Local electrodynamics

- Pippard superconductors (Type I)
  - $\xi \gg \lambda$
  - Pure metals
  - Nonlocal electrodynamics

Material Parameters for Some Superconductors

Superconductor	λ_L (0) (nm)	ξ_0 (nm)	κ	$2\Delta(0)/kT_c$	T_c(K)
Al	16	1500	0.011	3.40	1.18
In	25	400	0.062	3.50	3.3
Sn	28	300	0.093	3.55	3.7
Pb	28	110	0.255	4.10	7.2
Nb	32	39	0.82	3.5-3.85	8.95-9.2
Ta	35	93	0.38	3.55	4.46
Nb_3Sn	50	6	8.3	4.4	18
NbN	50	6	8.3	4.3	≤ 17
$Yba_2Cu_3o_x$	140	1.5	93	4.5	90

Phenomenological Models (1930s to 1950s)

Phenomenological model:
Purely descriptive
Everything behaves as though…..

A finite fraction of the electrons form some kind of condensate that behaves as a macroscopic system (similar to superfluidity)

At 0K, condensation is complete

At T_c the condensate disappears

Two Fluid Model – Gorter and Casimir

$T < T_c$ $\quad x =$ fraction of "normal" electrons

$(1-x)$: fraction of "condensed" electrons (zero entropy)

Assume: $F(T) = x^{1/2}\, f_n(T) + (1-x)\, f_s(T)$ free energy

$$f_n(T) = -\frac{1}{2}\gamma T^2$$

$$f_s(T) = -\beta = -\frac{1}{4}\gamma T_c^2$$ independent of temperature

Minimization of $F(T)$ gives $\quad x = \left(\frac{T}{T_C}\right)^4$

$$\Rightarrow F(T) = x^{1/2}\, f_n(T) + (1-x)\, f_s(T) = -\beta\left[1 + \left(\frac{T}{T_C}\right)^4\right]$$

$$\Rightarrow C_{es} = 3\gamma \frac{\mathrm{T}^3}{\mathrm{T}_\mathrm{C}^2}$$

Two Fluid Model – Gorter and Casimir

Superconducting state: $$F(T) = x^{1/2} f_n(T) + (1-x) f_s(T) = -\beta\left[1 + \left(\frac{T}{T_C}\right)^4\right]$$

Normal state: $$F(T) = f_n(T) = -\frac{\gamma}{2}T^2 = -2\beta\left(\frac{T}{T_C}\right)^2$$

Recall $\frac{H_c^2}{8\pi} =$ difference in free energy between normal and superconducting state

$$= \beta\left[1 - \left(\frac{T}{T_C}\right)^2\right]^2 \qquad \Rightarrow \qquad \frac{H_c(T)}{H_c(0)} = 1 - \left(\frac{T}{T_C}\right)^2$$

The Gorter-Casimir model is an "ad hoc" model (there is no physical basis for the assumed expression for the free energy) but provides a fairly accurate representation of experimental results

Model of F & H London (1935)

Proposed a 2-fluid model with a normal fluid and superfluid components

***n_s* : density of the superfluid component of velocity v_s**
***n_n* : density of the normal component of velocity v_n**

$$m\frac{\partial \vec{v}}{\partial t} = -e\vec{E}$$

superelectrons are accelerated by E

$$\overrightarrow{J_s} = -en_s\,\vec{v}$$

$$\frac{\partial \vec{J}_s}{\partial t} = \frac{n_s e^2}{m}\vec{E}$$

superelectrons

$$\vec{J}_n = \sigma_n \vec{E}$$

normal electrons

Model of F & H London (1935)

$$\frac{\partial \vec{J}_s}{\partial t} = \frac{n_s e^2}{m} \vec{E}$$

Maxwell: $$\vec{\nabla} \times \vec{E} = -\frac{\partial \vec{B}}{\partial t}$$

$$\Rightarrow \frac{\partial}{\partial t}\left(\frac{m}{n_s e^2} \vec{\nabla} \times \vec{J}_s + \vec{B} \right) = 0 \qquad \Rightarrow \frac{m}{n_s e^2} \vec{\nabla} \times \vec{J}_s + \vec{B} = \text{Constant}$$

F&H London postulated: $$\boxed{\frac{m}{n_s e^2} \vec{\nabla} \times \vec{J}_s + \vec{B} = 0}$$

Model of F & H London (1935)

combine with $\vec{\nabla} \times \vec{B} = \mu_0 \vec{J}_s$

$$\boxed{\nabla^2 \vec{B} - \frac{\mu_0 n_s e^2}{m} \vec{B} = 0}$$

$$B(x) = B_o \exp\left[-x / \lambda_L\right]$$

$$\lambda_L = \left[\frac{m}{\mu_0 n_s e^2}\right]^{\frac{1}{2}}$$

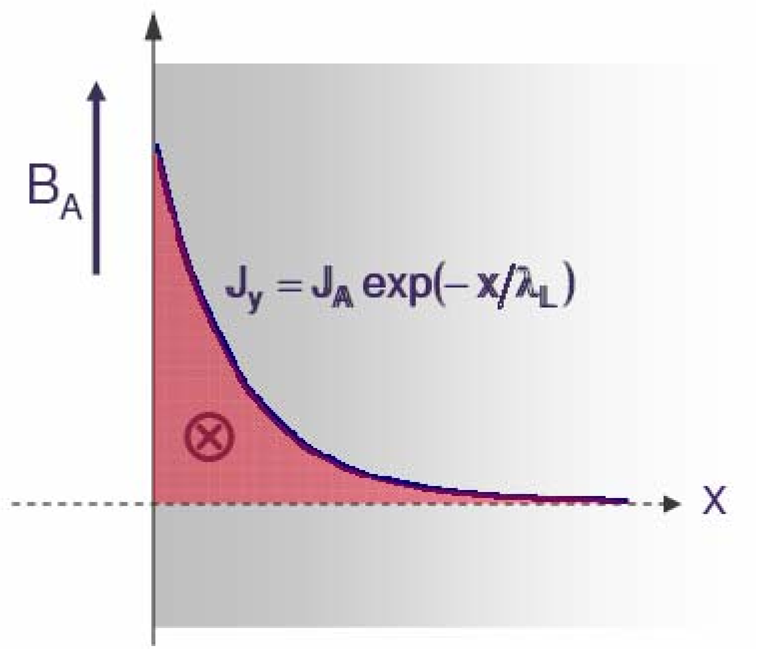

The magnetic field, and the current, decay exponentially over a distance λ (a few 10s of nm)

Model of F & H London (1935)

$$\lambda_L = \left[\frac{m}{\mu_0 n_s e^2}\right]^{\frac{1}{2}}$$

From Gorter and Casimir two-fluid model

$$n_s \propto \left[1 - \left(\frac{T}{T_C}\right)^4\right]$$

$$\lambda_L(T) = \lambda_L(0)\frac{1}{\left[1 - \left(\frac{T}{T_C}\right)^4\right]^{\frac{1}{2}}}$$

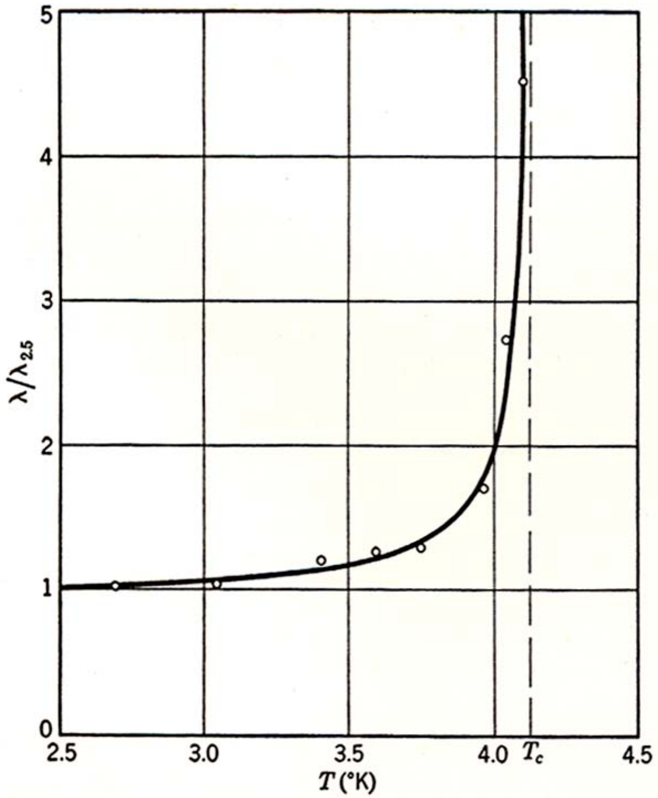

FIG. 21. Penetration depth as a function of temperature. (After Shoenberg, *Nature*, **43**, 433, 1939.)

Model of F & H London (1935)

London Equation: $\lambda^2 \nabla \times \vec{J}_s = -\dfrac{\vec{B}}{\mu_0} = -\vec{H}$

$$\nabla \times \vec{A} = \vec{H}$$

choose $\nabla \bullet \vec{A} = 0,$ $A_n = 0$ on sample surface (London gauge)

$$\boxed{\vec{J}_s = -\frac{1}{\lambda^2}\vec{A}}$$

Note: Local relationship between $\vec{J}_s$ and $\vec{A}$

Penetration Depth in Thin Films

Very thin films

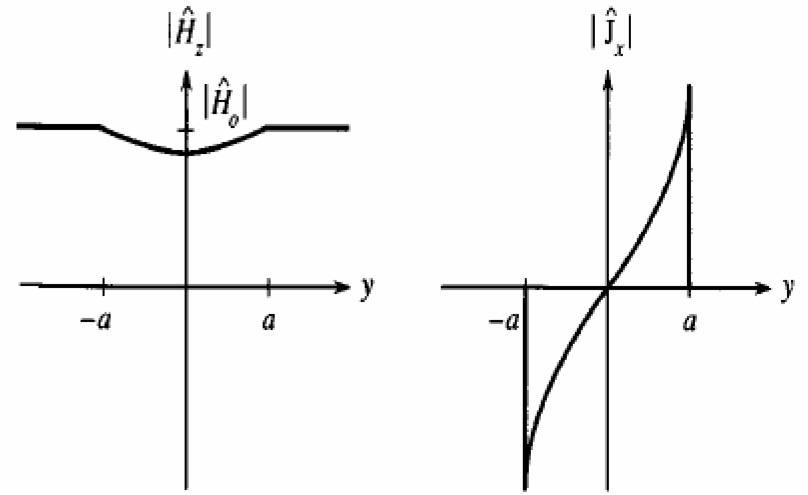

Very thick films

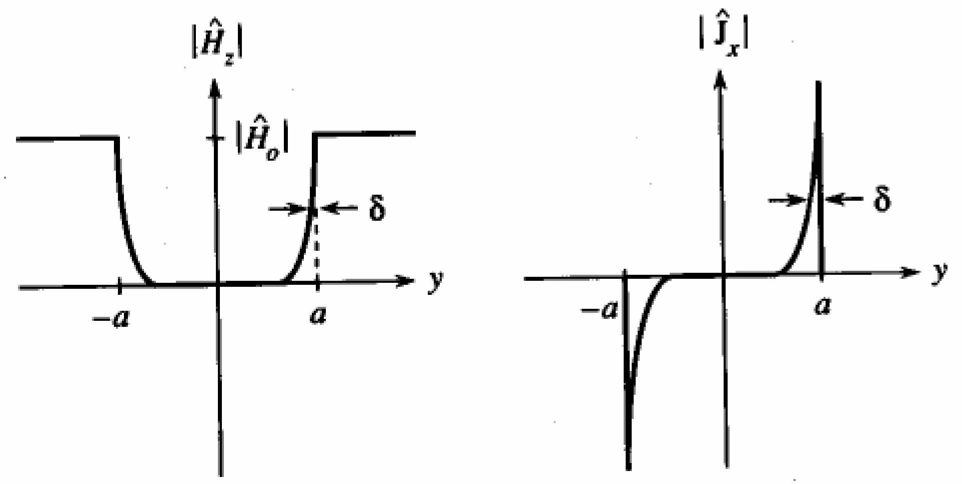

Quantum Mechanical Basis for London Equation

$$\vec{J}(r) = \sum_n \int \left\{ \frac{e\hbar}{2mi}\left[\psi^* \nabla_n \psi - \psi \nabla_n \psi^*\right] - \frac{e^2}{mc}\vec{A}(\vec{r}_n)\psi^*\psi \right\} \delta(r - r_n) dr_1 - dr_n$$

In zero field $\vec{A} = 0 \quad \vec{J}(r) = 0 \,, \qquad \psi = \psi_0$

Assume ψ is "rigid", ie the field has no effect on wave function

$$\vec{J}(r) = -\frac{\rho(r) e^2}{m\, e}\vec{A}(r)$$

$$\rho(r) = n$$

Pippard's Extension of London's Model

Observations:

-Penetration depth increased with reduced mean free path

- H_c and T_c did not change

-Need for a positive surface energy over 10^{-4} cm to explain existence of normal and superconducting phase in intermediate state

Non-local modification of London equation

Local: $$\vec{J} = -\frac{1}{c\lambda}\vec{A}$$

Non local: $$\vec{J}(r) = -\frac{3\sigma}{4\pi\xi_0\lambda c}\int \frac{\vec{R}\left[\vec{R}\bullet\vec{A}(r')\right]e^{-\frac{R}{\xi}}}{R^4}d\upsilon$$

$$\frac{1}{\xi} = \frac{1}{\xi_0} + \frac{1}{\ell}$$

London and Pippard Kernels

Apply Fourier transform to relationship between

$J(r)$ and $A(r)$: $$J(k) = -\frac{c}{4\pi} K(k)\ A(k)$$

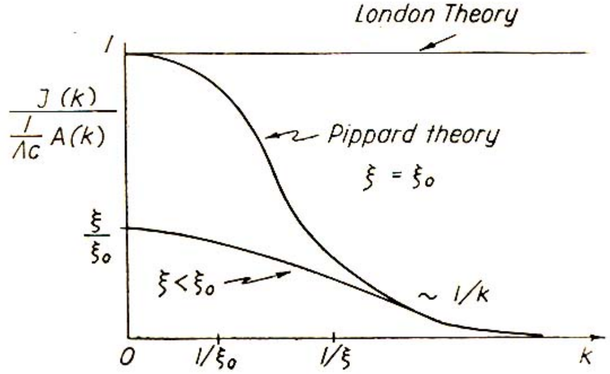

Fig. 1. Comparison of supercurrent response to vector potential in London and Pippard theories (schematic).

Effective penetration depth

Specular: $$\lambda_{eff} = \frac{2}{\pi} \int_o^\infty \frac{dk}{K(k) + k^2}$$

Diffuse: $$\lambda_{eff} = \frac{\pi}{\int_o^\infty \ln\left[1 + \frac{K(k)}{k^2}\right] dk}$$

London Electrodynamics

Linear London equations

$$\frac{\partial \vec{J}_s}{\partial t} = -\frac{\vec{E}}{\lambda^2 \mu_0} \qquad \nabla^2 \vec{H} - \frac{1}{\lambda^2}\vec{H} = 0$$

together with Maxwell equations

$$\nabla \times \vec{H} = \vec{J}_s \qquad \nabla \times \vec{E} = -\mu_0 \frac{\partial \vec{H}}{\partial t}$$

describe the electrodynamics of superconductors at all T if:

- The superfluid density n_s is spatially uniform
- The current density J_s is small

Ginzburg-Landau Theory

- Many important phenomena in superconductivity occur because n_s is not uniform
  - Interfaces between normal and superconductors
  - Trapped flux
  - Intermediate state

- London model does not provide an explanation for the surface energy (which can be positive or negative)

- GL is a generalization of the London model but it still retain the local approximation of the electrodynamics

Ginzburg-Landau Theory

- Ginzburg-Landau theory is a particular case of Landau's theory of second order phase transition
- Formulated in 1950, before BCS
- Masterpiece of physical intuition
- Grounded in thermodynamics
- Even after BCS it still is very fruitful in analyzing the behavior of superconductors and is still one of the most widely used theory of superconductivity

Ginzburg-Landau Theory

- Theory of second order phase transition is based on an order parameter which is zero above the transition temperature and non-zero below
- For superconductors, GL use a complex order parameter $\Psi(r)$ such that $|\Psi(r)|^2$ represents the density of superelectrons
- The Ginzburg-Landau theory is valid close to T_c

Ginzburg-Landau Equation for Free Energy

- Assume that Ψ(r) is small and varies slowly in space

- Expand the free energy in powers of Ψ(r) and its derivative

$$f = f_{n0} + \alpha|\psi|^2 + \frac{\beta}{2}|\psi|^4 + \frac{1}{2m^*}\left|\left(\frac{\hbar}{i}\nabla - \frac{e^*}{c}\mathbf{A}\right)\psi\right|^2 + \frac{h^2}{8\pi}$$

Field-Free Uniform Case

$$f - f_{n0} = \alpha|\psi|^2 + \frac{\beta}{2}|\psi|^4$$

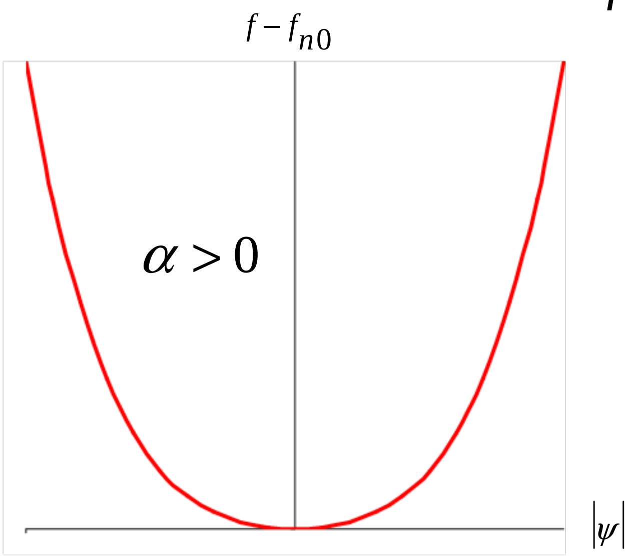

$$|\psi_\infty|^2 = -\frac{\alpha}{\beta}$$

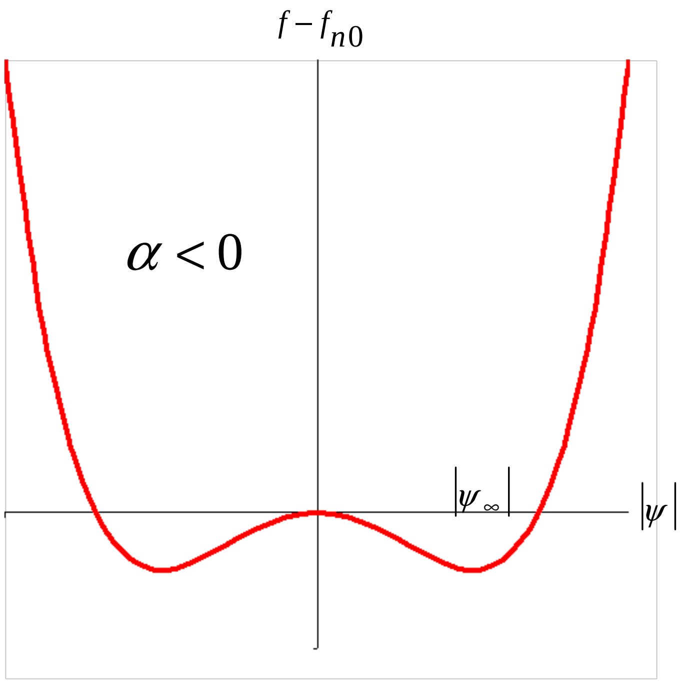

Near T_c we must have $\beta > 0$ $\alpha(t) = \alpha'(t-1)$

At the minimum $f - f_{n0} = -\frac{H_c^2}{8\pi} = -\frac{\alpha^2}{2\beta} \Rightarrow |\psi|^2$ and $H_c \propto (1-t)$

Field-Free Uniform Case

$$f - f_{n0} = \alpha|\psi|^2 + \frac{\beta}{2}|\psi|^4 \qquad\qquad |\psi_\infty|^2 = -\frac{\alpha}{\beta}$$

$$\beta > 0 \qquad \alpha(t) = \alpha'(t-1) \qquad \Rightarrow |\psi_\infty|^2 \propto (1-t)$$

It is consistent with correlating |Ψ(r)|² with the density of superelectrons

$n_s \propto \lambda^{-2} \propto (1-t)$ near T_c

At the minimum $\qquad f - f_{n0} = -\frac{\alpha^2}{2\beta} = -\frac{H_c^2}{8\pi}$ (definition of H_c)

$$\Rightarrow H_c \propto (1-t)$$

which is consistent with $\qquad H_c = H_{c0}(1-t^2)$

Field-Free Uniform Case

Identify the order parameter with the density of superelectrons

$$n_s = |\Psi|^2 \sim \frac{1}{\lambda_L^2(T)} \Rightarrow \quad \frac{\lambda_L^2(0)}{\lambda_L^2(T)} = \frac{|\Psi(T)|^2}{|\Psi(0)|^2} = -\frac{1}{n}\frac{\alpha(T)}{\beta}$$

since $\dfrac{1}{2}\dfrac{\alpha^2(T)}{\beta} = \dfrac{H_c^2(T)}{8\pi}$

$$n\alpha(T) = -\frac{H_c^2(T)}{4\pi}\frac{\lambda_L^2(T)}{\lambda_L^2(0)} \quad \text{and} \quad n^2\beta = \frac{H_c^2(T)}{4\pi}\frac{\lambda_L^4(T)}{\lambda_L^4(0)}$$

Field-Free Nonuniform Case

Equation of motion in the absence of electromagnetic field

$$-\frac{1}{2m^*}\nabla^2\psi + \alpha(T)\psi + \beta|\psi|^2\psi = 0$$

Look at solutions close to the constant one

$$\psi = \psi_\infty + \delta \quad \text{where} \quad |\psi_\infty|^2 = -\frac{\alpha(T)}{\beta}$$

To first order: $$\frac{1}{4m^*|\alpha(T)|}\nabla^2\delta - \delta = 0$$

Which leads to $$\delta \approx e^{-\sqrt{2}r/\xi(T)}$$

Field-Free Nonuniform Case

$$\delta \approx e^{-\sqrt{2}r/\xi(T)} \quad \text{where} \quad \xi(T) = \frac{1}{\sqrt{2m^*|\alpha(T)|}} = \sqrt{\frac{2\pi n}{m^* H_c^2(T)}} \frac{\lambda_L(0)}{\lambda_L(T)}$$

is the Ginzburg-Landau coherence length.

It is different from, but related to, the Pippard coherence length. $\xi(T) \simeq \dfrac{\xi_0}{\left(1-t^2\right)^{1/2}}$

GL parameter: $$\kappa(T) = \frac{\lambda_L(T)}{\xi(T)}$$

Both $\lambda_L(T)$ and $\xi(T)$ diverge as $T \to T_c$ but their ratio remains finite

$\kappa(T)$ is almost constant over the whole temperature range

2 Fundamental Lengths

London penetration depth: length over which magnetic field decay

$$\lambda_L(T) = \left(\frac{m^*\beta}{2e^2\alpha'}\right)^{1/2}\sqrt{\frac{T_c}{T_c - T}}$$

Coherence length: scale of spatial variation of the order parameter (superconducting electron density)

$$\xi(T) = \left(\frac{\hbar^2}{4m^*\alpha'}\right)^{1/2}\sqrt{\frac{T_c}{T_c - T}}$$

The critical field is directly related to those 2 parameters

$$H_c(T) = \frac{\phi_0}{2\sqrt{2}\,\xi(T)\,\lambda_L(T)}$$

Surface Energy

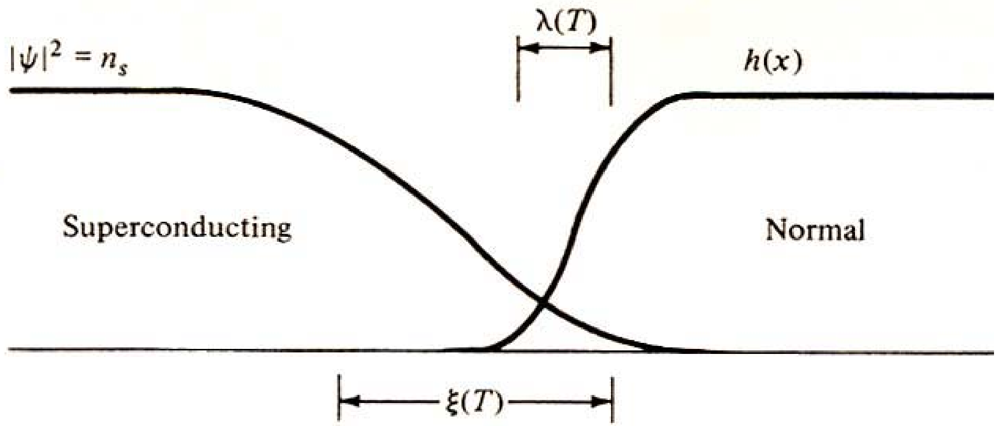

$$\sigma \simeq \frac{1}{8\pi}\left[H_c^2\xi - H^2\lambda\right]$$

$\frac{H^2\lambda}{8\pi}$: Energy that can be gained by letting the fields penetrate

$\frac{H_c^2\xi}{8\pi}$: Energy lost by "damaging" superconductor

Surface Energy $\sigma \simeq \frac{1}{8\pi}\left[H_c^2\xi - H^2\lambda\right]$

Interface is stable if σ>0

If $\xi >> \lambda$ σ>0

Superconducting up to H_c where superconductivity is destroyed globally

If λ >>ξ σ<0 for $H^2 > H_c^2 \frac{\xi}{\lambda}$

Advantageous to create small areas of normal state with large area to volume ratio

$\rightarrow$ quantized fluxoids

More exact calculation (from Ginzburg-Landau):

$\kappa = \frac{\lambda}{\xi} < \frac{1}{\sqrt{2}}$: Type I

$\kappa = \frac{\lambda}{\xi} > \frac{1}{\sqrt{2}}$: Type II

Magnetization Curves

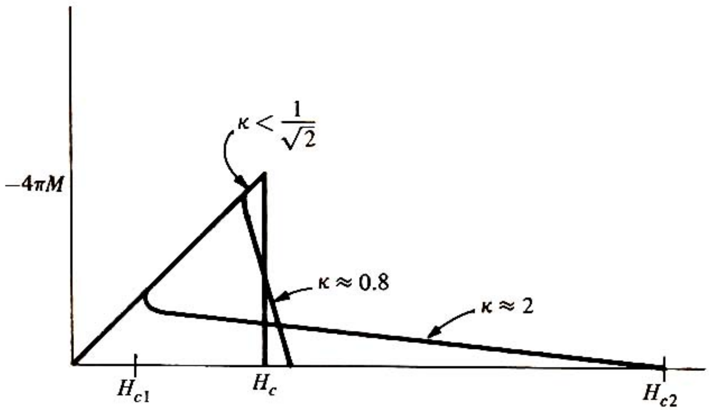

FIGURE 5-2
Comparison of magnetization curves for three superconductors with the same value of thermodynamic critical field H_c, but different values of κ. For $\kappa < 1/\sqrt{2}$, the superconductor is of type I and exhibits a first-order transition at H_c. For $\kappa > 1/\sqrt{2}$, the superconductor is type II and shows second-order transitions at H_{c1} and H_{c2} (for clarity, marked only for the highest κ case). In all cases, the area under the curve is the condensation energy $H_c^2/8\pi$.

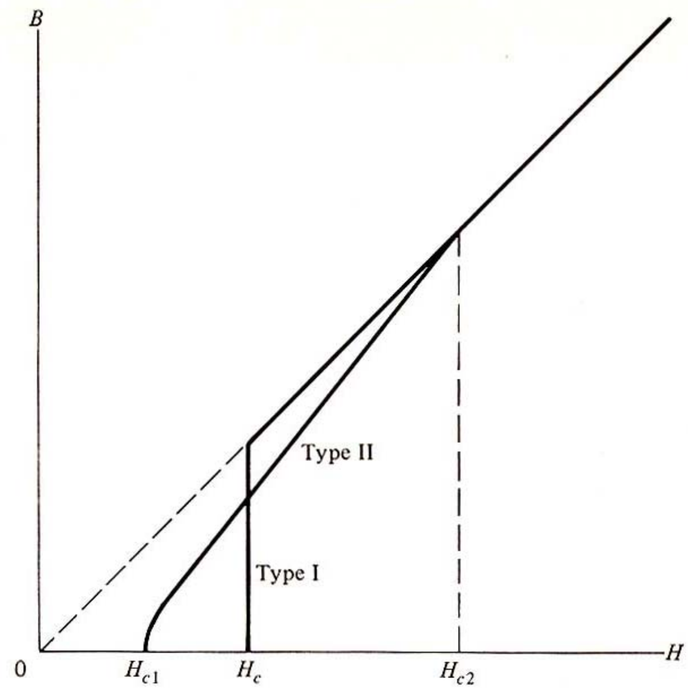

FIGURE 1-5
Comparison of flux penetration behavior of type I and type II superconductors with the same thermodynamic critical field H_c. $H_{c2} = \sqrt{2}\,\kappa H_c$. The ratio of B/H_{c2} from this plot also gives the approximate variation of R/R_n, where R is the electrical resistance for the case of negligible pinning, and R_n is the normal-state resistance.

Intermediate State

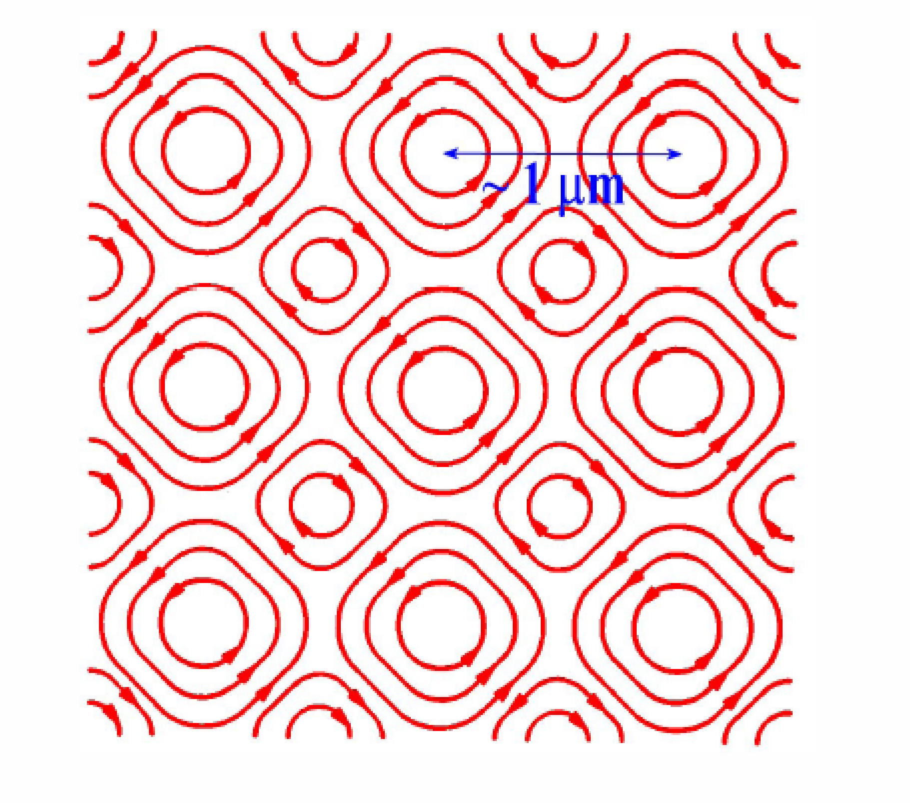

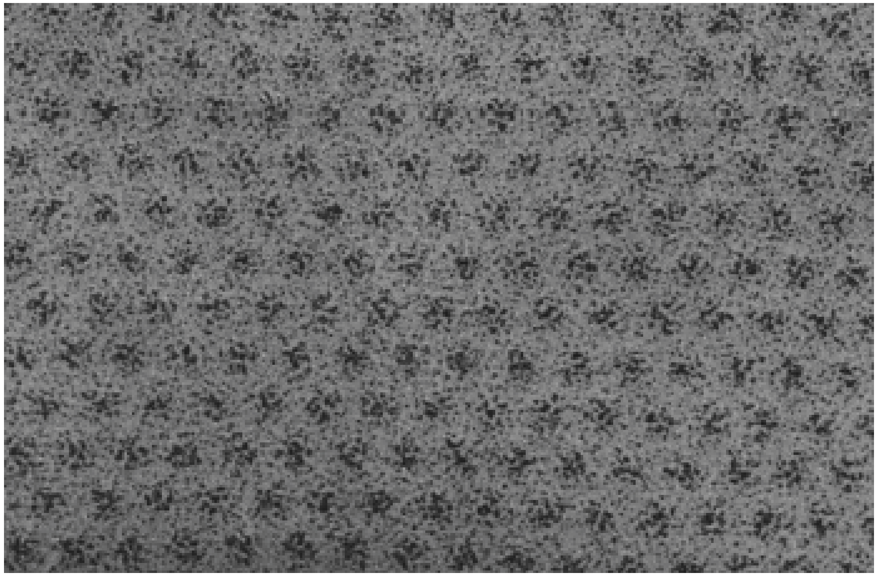

At the center of each vortex is a normal region of flux h/2e

Vortex lines in $Pb_{.98}In_{.02}$

Critical Fields

Even though it is more energetically favorable for a type I superconductor to revert to the normal state at H_c, the surface energy is still positive up to a superheating field $H_{sh}>H_c$ → metastable superheating region in which the material may remain superconducting for short times.

Type I

H_c Thermodynamic critical field

$H_{sh} \simeq \frac{H_c}{\sqrt{\kappa}}$ Superheating critical field

Field at which surface energy is

Type II

H_c Thermodynamic critical field

$$H_{c2} = \sqrt{2}\ \kappa\ H_c$$

$$H_{c1} \simeq \frac{H_c^2}{H_{c2}}$$

$$\simeq \frac{1}{2\kappa}(\ln\kappa + .008)H_c \qquad (\text{for } \kappa \gg 1)$$

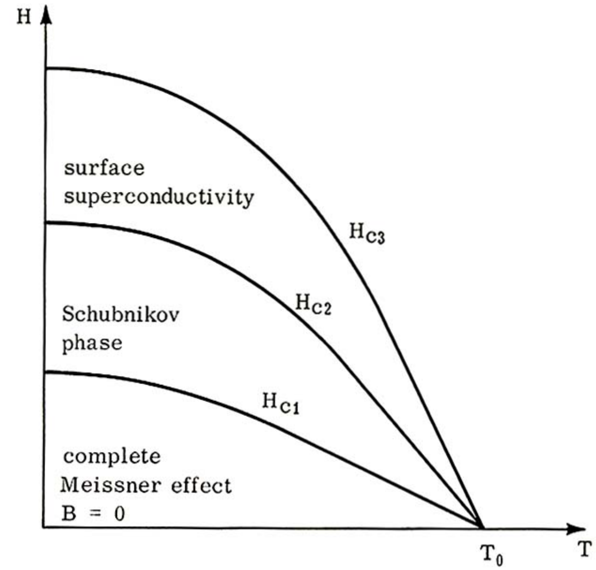

Figure 3-1
Phase diagram for a long cylinder of a Type II superconductor.

Superheating Field

Ginsburg-Landau:

$$H_{sh} \sim \frac{0.9H_c}{\sqrt{\kappa}} \quad \text{for } \kappa << 1$$

$$\sim \quad 1.2\ H_c \quad \text{for } \kappa \sim 1$$

$$\sim \quad 0.75\ H_c \quad \text{for } \kappa >> 1$$

The exact nature of the rf critical field of superconductors is still an open question

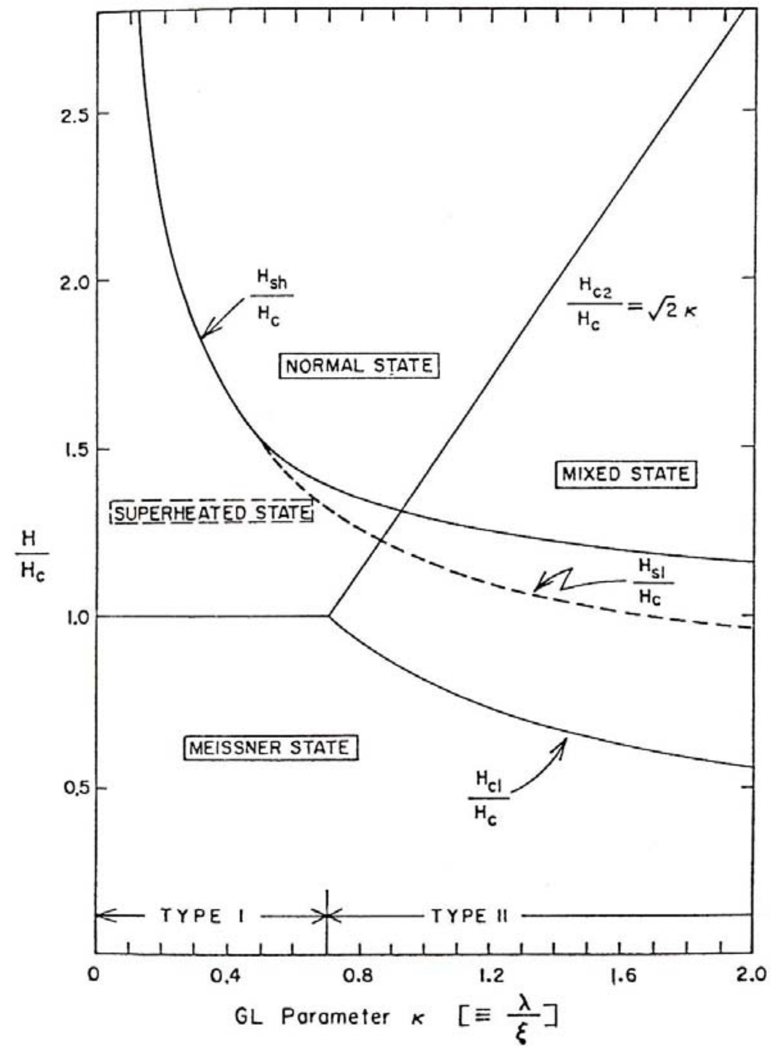

Fig. 13: Phase diagram of superconductors[42] in the transition regime of type I and II. The normalized critical fields are shown as a function of ϰ.

Material Parameters for Some Superconductors

Superconductor	λ_L (0) (nm)	ξ_0 (nm)	κ	$2\Delta(0)/kT_c$	T_c(K)
Al	16	1500	0.011	3.40	1.18
In	25	400	0.062	3.50	3.3
Sn	28	300	0.093	3.55	3.7
Pb	28	110	0.255	4.10	7.2
Nb	32	39	0.82	3.5-3.85	8.95-9.2
Ta	35	93	0.38	3.55	4.46
Nb_3Sn	50	6	8.3	4.4	18
NbN	50	6	8.3	4.3	≤ 17
$Yba_2Cu_3o_x$	140	1.5	93	4.5	90

BCS

- What needed to be explained and what were the clues?
  - Energy gap (exponential dependence of specific heat)
  - Isotope effect (the lattice is involved)
  - Meissner effect

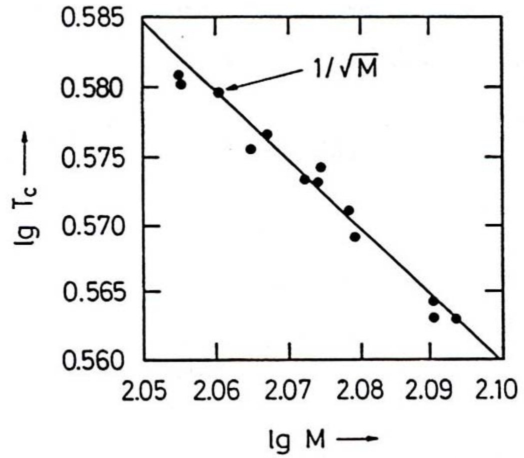

Figure 26: The critical temperature of various tin isotopes.

Cooper Pairs

Assumption: Phonon-mediated attraction between electron of equal and opposite momenta located within $\hbar\omega_D$ of Fermi surface

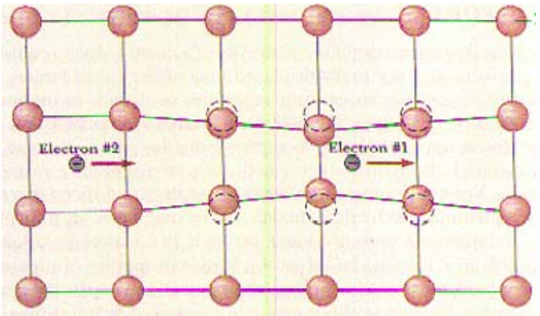

Moving electron distorts lattice and leaves behind a trail of positive charge that attracts another electron moving in opposite direction

Fermi ground state is unstable

Electron pairs can form bound states of lower energy

Bose condensation of overlapping Cooper pairs into a coherent Superconducting state

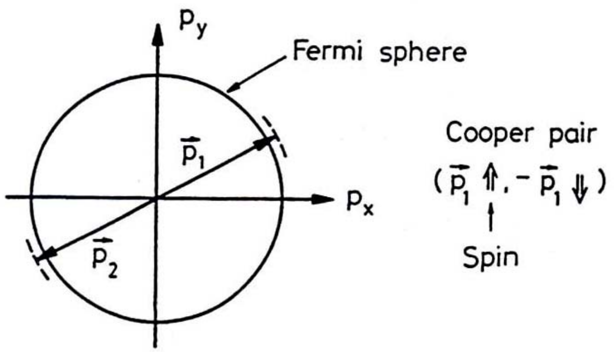

Figure 20: A pair of electrons of opposite momenta added to the full Fermi sphere.

Cooper Pairs

One electron moving through the lattice attracts the positive ions.

Because of their inertia the maximum displacement will take place

$d \approx v_F \dfrac{2\pi}{\omega_D} \approx 100 - 1000\,\mathrm{nm}$ behind.

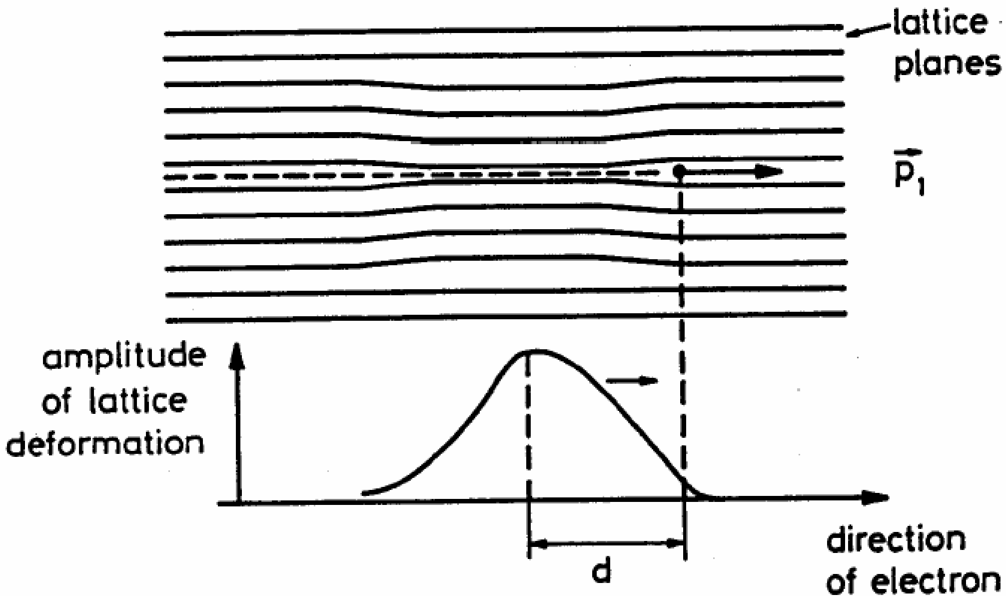

BCS

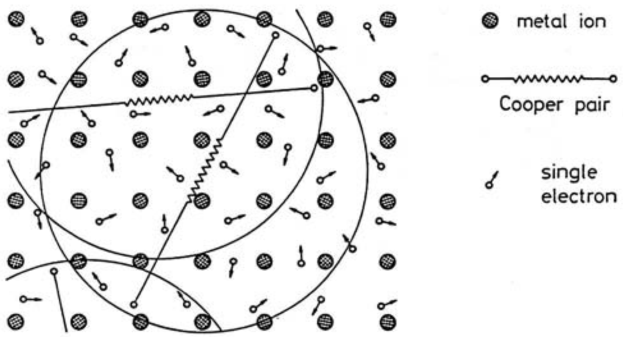

Figure 22: Cooper pairs and single electrons in the crystal lattice of a superconductor. (After Essmann and Träuble [12]).

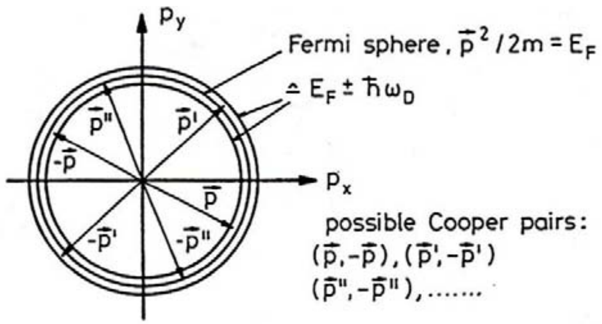

Figure 23: Various Cooper pairs $(\vec{p}, -\vec{p})$, $(\vec{p}', -\vec{p}')$, $(\vec{p}'', -\vec{p}'')$, ... in momentum space.

The size of the Cooper pairs is much larger than their spacing

They form a coherent state

BCS and BEC

BCS	BEC
weak coupling	strong coupling
large pair size **k**-space pairing	small pair size **r**-space pairing
strongly overlapping Cooper pairs	ideal gas of preformed pairs

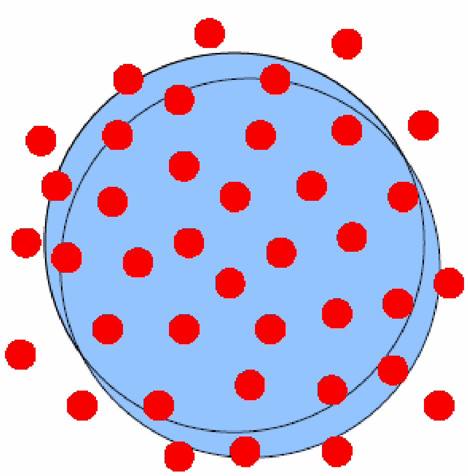

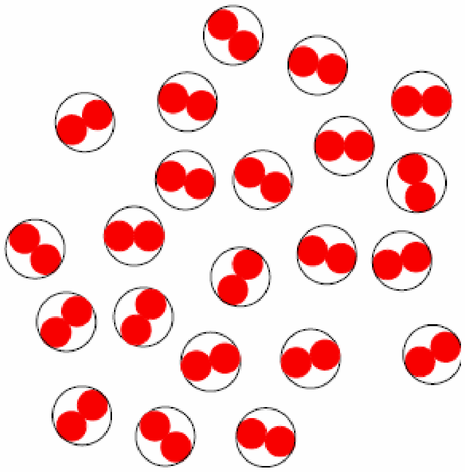

BCS Theory

$|0\rangle_q, |1\rangle_q$:states where pairs $(\vec{q},\text{-}\vec{q})$ are unoccupied, occupied

a_q, b_q :probabilites that pair $(\vec{q},\text{-}\vec{q})$ is unoccupied, occupied

BCS ground state

$$|\Psi\rangle = \prod_{\vec{q}} \left(a_q |0\rangle_q + b_q |1\rangle_q \right)$$

Assume interaction between pairs $\vec{q}$ and $\vec{k}$

$$V_{qk} = -V \text{ if } |\xi_\mathrm{q}| \le \hbar\omega_D \text{ and } |\xi_\mathrm{k}| \le \hbar\omega_D$$
$$= 0 \text{ otherwise}$$

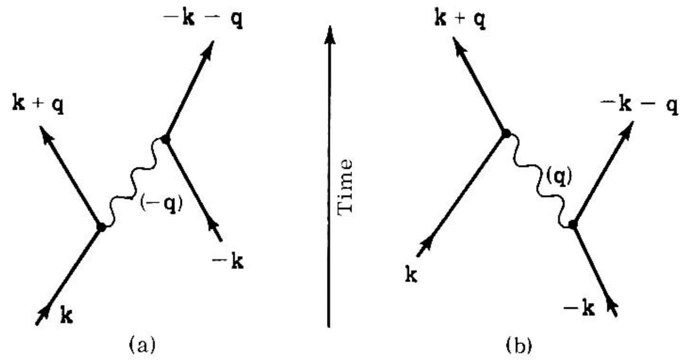

Figure 4-1
Electron-electron interaction via phonons. In process (a) the electron **k** emits a phonon of wave-vector −**q**. The phonon is absorbed later by the second electron. In process (b) the second electron in state (−**k**) emits a phonon **q**, subsequently absorbed by the first electron.

BCS

- Hamiltonian

$$\mathscr{H} = \sum_k \varepsilon_k n_k + \sum_{qk} V_{qk} c_q^* c_{-q}^* c_k c_{-k}$$

c_k destroys an electron of momentum k

c_q^* creates an electron of momentum k

$n_k = c_k^* c_k$ number of electrons of momentum k

- Ground state wave function

$$|\Psi\rangle = \prod_{\vec{q}} \left(a_q + b_q c_q^* c_{-q}^* \right) |\phi_0\rangle$$

BCS

- The BCS model is an extremely simplified model of reality
  - The Coulomb interaction between single electrons is ignored
  - Only the term representing the scattering of pairs is retained
  - The interaction term is assumed to be constant over a thin layer at the Fermi surface and 0 everywhere else
  - The Fermi surface is assumed to be spherical

- Nevertheless, the BCS results (which include only a very few adjustable parameters) are amazingly close to the real world

BCS

Is there a state of lower energy than the normal state?

$$a_q = 0,\ b_q = 1 \qquad \text{for} \quad \xi_q < 0$$

$$a_q = 1,\ b_q = 0 \ \text{for} \quad \xi_q > 0$$

yes: $$2b_q^2 = 1 - \frac{\xi_q}{\sqrt{\xi_q^2 + \Delta_0^2}}$$

where

$$\Delta_0 = \frac{\hbar\omega_D}{\sinh\left[\dfrac{1}{\rho(0)V}\right]} \simeq 2\hbar\omega_D\ e^{-\frac{1}{\rho(0)V}}$$

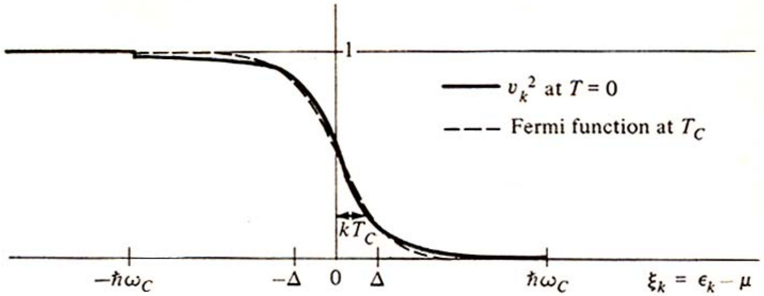

FIGURE 2-1
Plot of BCS occupation fraction v_k^2 vs. electron energy measured from the chemical potential (Fermi energy). To make the cutoffs at $\pm\hbar\omega_c$ visible, the plot has been made for a strong-coupling superconductor with $N(0)V = 0.43$. For comparison, the Fermi function for the normal state at T_c is also shown on the same scale, using the BCS relation $\Delta(0) = 1.76kT_c$.

BCS

Critical temperature

$$kT_c = 1.14\hbar\omega_D \exp\left[-\frac{1}{VN(E_F)}\right]$$

$$\Delta(0) = 1.76\, kT_c$$

element	Sn	In	Tl	Ta	Nb	Hg	Pb
$\Delta(0)/k_B T_c$	1.75	1.8	1.8	1.75	1.75	2.3	2.15

Coherence length (the size of the Cooper pairs)

$$\xi_0 = .18\frac{\hbar v_F}{kT_c}$$

BCS Condensation Energy

Condensation energy: $$E_s - E_n = -\frac{\rho(0) V \Delta_0^2}{2}$$

$$\simeq -N\Delta_0 \left(\frac{\Delta_0}{\varepsilon_F}\right) = \frac{H_0^2}{8\pi}$$

$$\Delta_0 / k \simeq 10K$$

$$\varepsilon_F / k \simeq 10^4 K$$

BCS Energy Gap

At finite temperature:

Implicit equation for the temperature dependence of the gap:

$$\frac{1}{V\rho(0)} = \int_0^{\hbar\omega_D} \frac{\tanh\left[(\varepsilon^2+\Delta^2)^{1/2}/2kT\right]}{(\varepsilon^2+\Delta^2)^{1/2}}\, d\varepsilon$$

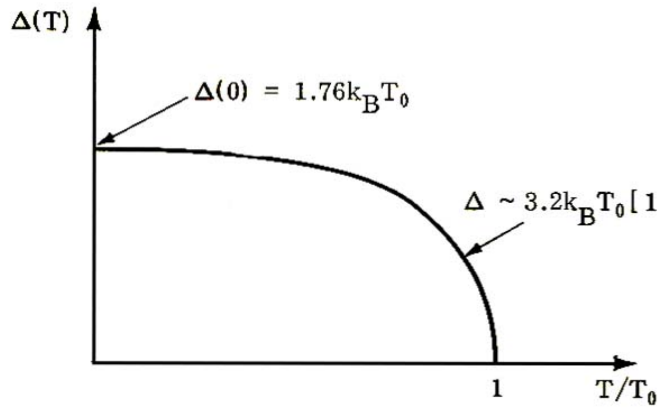

Figure 4-4
Variation of the order parameter Δ with temperature in the BCS approximation.

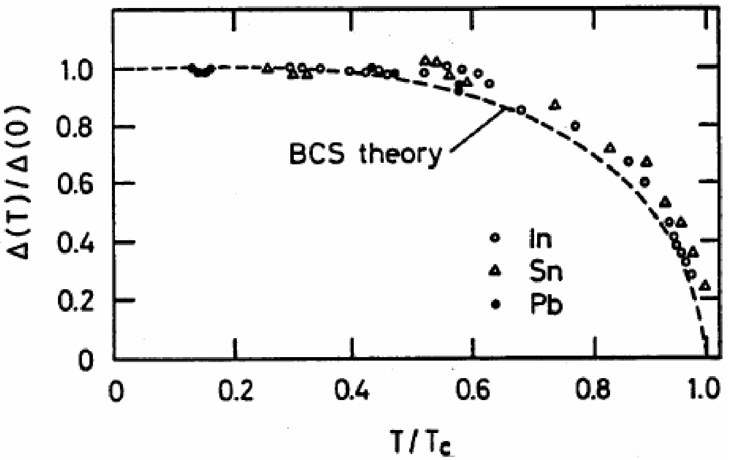

BCS Excited States

Energy of excited states:

$$\varepsilon_k = 2\sqrt{\xi_k^2 + \Delta_0^2}$$

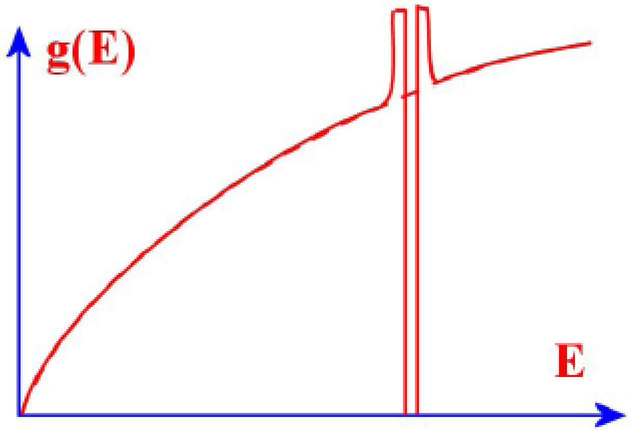

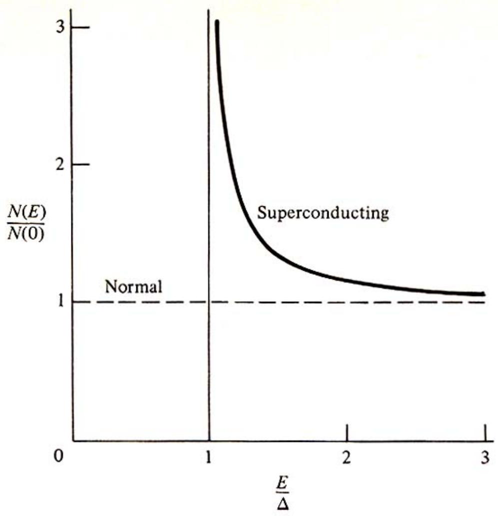

FIGURE 2-4
Density of states in superconducting compared to normal state. All **k** states whose energies fall in the gap in the normal metal are raised in energy above the gap in the superconducting state.

BCS Specific Heat

Specific heat

$$C_{es} \simeq \quad \exp\left(-\frac{\Delta}{kT}\right) \text{ for } T < \frac{T_c}{10}$$

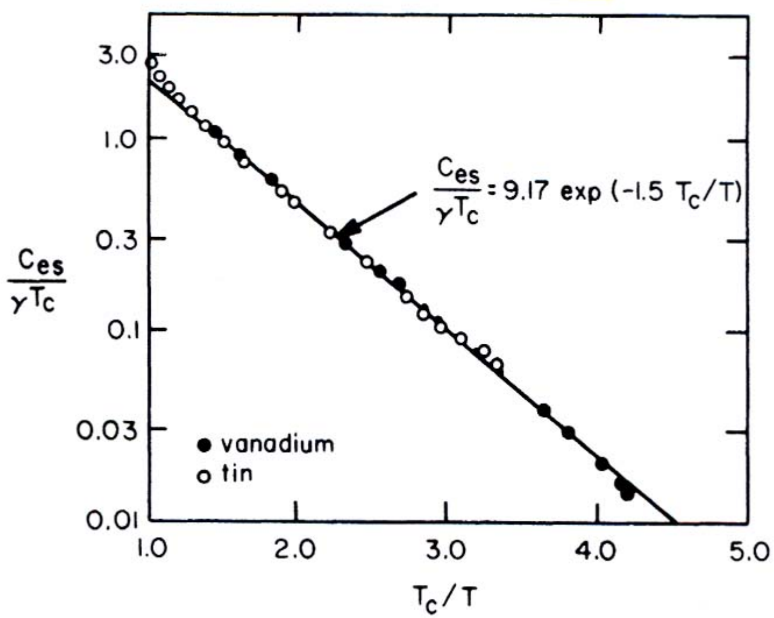

Fig. 22. Reduced electronic specific heat in superconducting vanadium and tin. [From Biondi et al., (*150*).]

Electrodynamics and Surface Impedance in BCS Model

$$H_0\phi + H_{ex}\ \phi = i\hbar\frac{\partial\phi}{\partial t}$$

$$H_{ex} = \frac{e}{mc}\sum A(r_i,t)\,p_i$$

H_{ex} is treated as a small perturbation

$$H_{rf} << H_c$$

There is, at present, no model for superconducting surface resistance at high rf field

$$J \propto \int \frac{R[R\cdot A]\,I(\omega,R,T)\,e^{-\frac{R}{l}}}{R^4}\,dr$$

similar to Pippard's model

$$J(k) = -\frac{c}{4\pi}K(k)A(k)$$

$K(0)\neq 0:$ Meissner effect

Penetration Depth

$$\lambda = \frac{2}{\pi}\int \frac{dk}{K(k)+k^2}\,dk \qquad \text{(specular)}$$

Represented accurately by $\lambda \sim \dfrac{1}{\sqrt{1-\left(\dfrac{T_c}{T}\right)^4}}$ near T_c

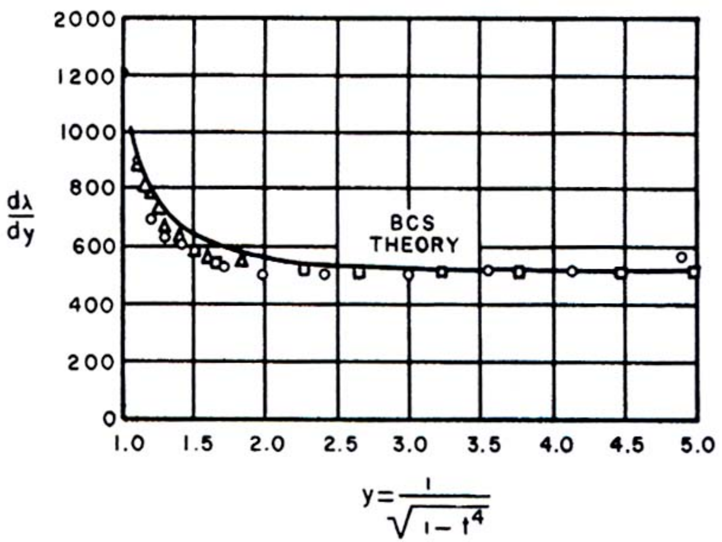

Fig. 30. Temperature dependence of $d\lambda/dy$ for tin obtained by Schawlow and Devlin (*207*) compared with the theoretical curve obtained from the BCS theory.

Surface Resistance

Temperature dependence

–close to T_c : dominated by change in $\lambda(t)$ $\quad \dfrac{t^4}{(1-t^2)^{3/2}}$

–for $T < \dfrac{T_c}{2}$: dominated by density of excited states $\sim e^{-\Delta/kT}$

$$R_s \sim \frac{A}{T}\omega^2 \exp\left(-\frac{\Delta}{kT}\right)$$

Frequency dependence

ω^2 is a good approximation

Surface Resistance

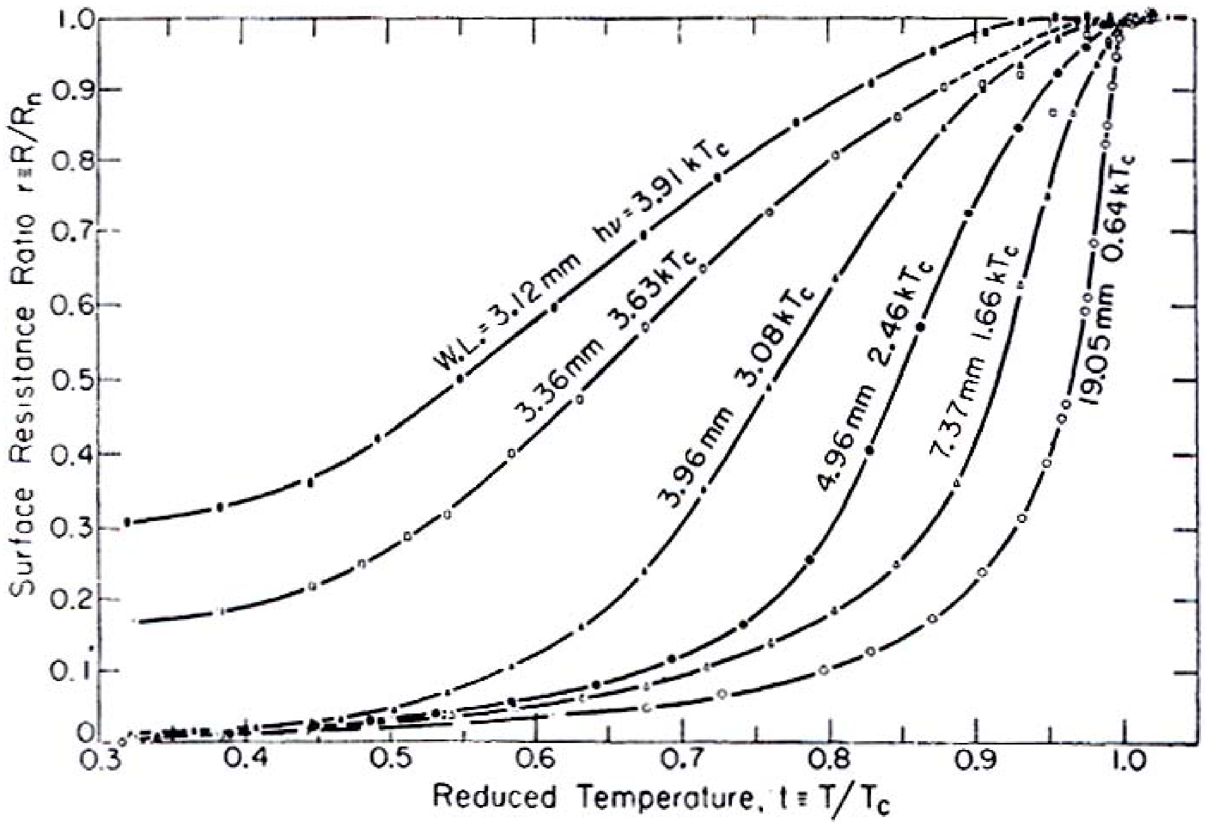

Fig. 1. Measured values of the surface resistance ratio r of superconducting aluminum as a function of the reduced temperature t at several representative wavelengths. The wavelengths and corresponding photon energies are indicated on the curves
[After Biondi and Garfunkel (*15*).]

Surface Resistance

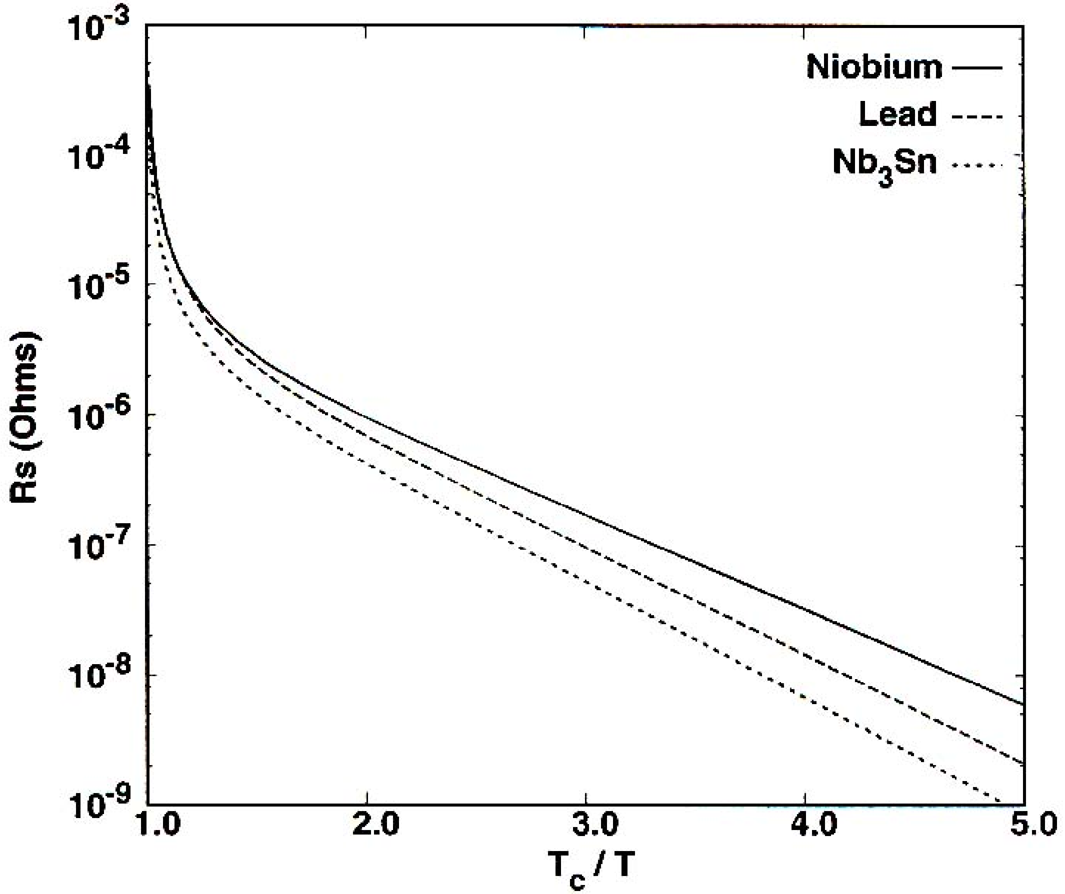

Figure 4.5: Theoretical surface resistance at 1.5 GHz of lead, niobium and Nb_3Sn as calculated from program [94]. The values given in Table 4.1 were used for the material parameters.

Surface Resistance

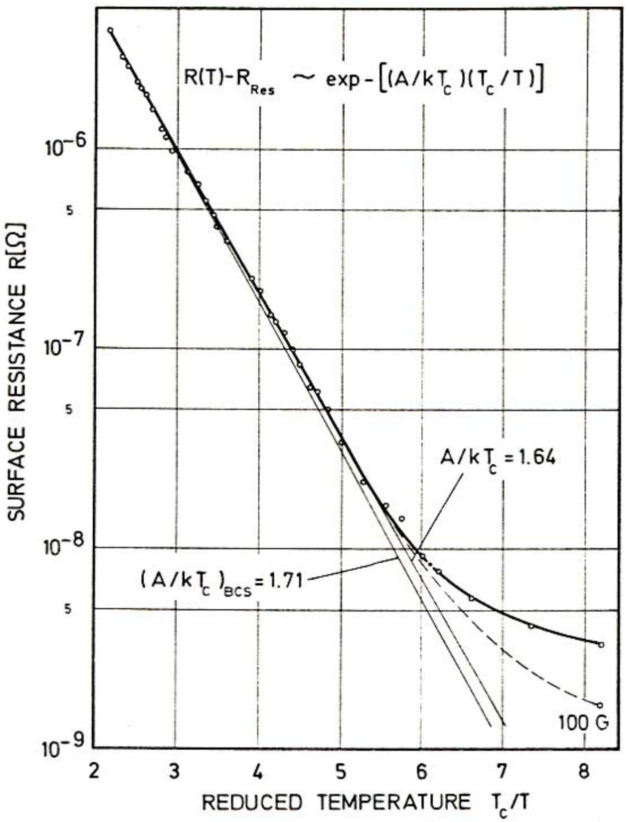

Fig. 2. Temperature dependence of surface resistance of niobium at 3.7 GHz measured in the TE_{011} mode at $H_{rf} \simeq 10$ G. The values computed with the BCS theory used the following material parameters:

$T_c = 9.25$ K; $\lambda_L(T=0, l=\infty) = 320$ Å;

$\Delta(0)/kT = 1.85$; $\xi_F(T=0, l=\infty) = 620$ Å; $l = 1000$ Å or 80 Å.

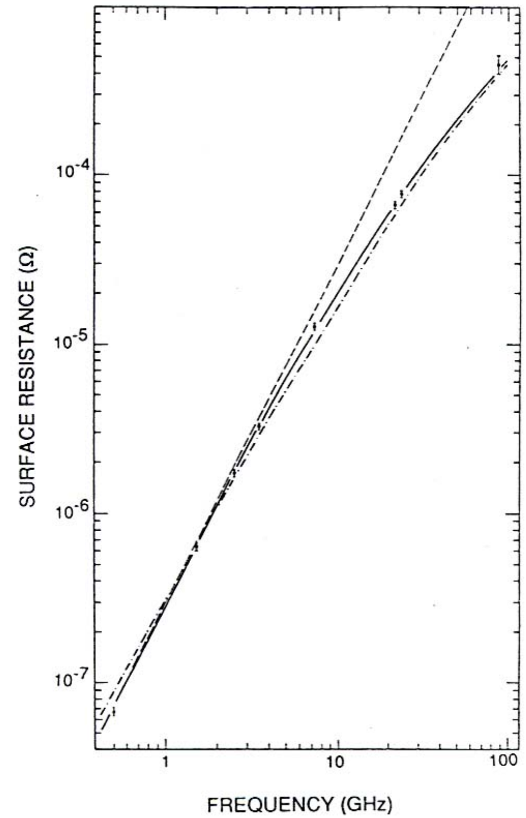

Fig. 5. The surface resistance of Nb at 4.2 K as a function of frequency [62,63]. Whereas the isotropic BCS surface resistance (– · – ·) resulted in $R \propto \omega^{1.8}$ around 1 GHz, the measurements fit better to ω^2 (– – –). The solid curve, which fits the data over the entire range, is a calculation based on the smearing of the BCS density-of-states singularity by the energy gap anisotropy in the presence of impurity scattering [61]. The authors thank G. Müller for providing this figure.

Surface Impedance - Definitions

- The electromagnetic response of a metal, whether normal or superconducting, is described by a complex surface impedance, $Z = R + iX$

R : Surface resistance

X : Surface reactance

Both R and X are real

Definitions

For a semi- infinite slab:

$$Z = \frac{E_x(0)}{\int_0^\infty J_x(z)\,dz}$$ Definition

$$= \frac{E_x(0)}{H_y(0)} = i\omega\mu_0 \frac{E_x(0)}{\partial E_x(z)/\partial z\big|_{z=0_+}}$$ From Maxwell

Definitions

The surface resistance is also related to the power flow into the conductor

$$Z = Z_0\ \vec{S}(0_+) / \vec{S}(0_-)$$

$$Z_0 = \left(\frac{\mu_0}{\varepsilon_0}\right)^{1/2} \simeq 377\Omega$$ Impedance of vacuum

$$\vec{S} = \vec{E} \times \vec{H}$$ Poynting vector

and to the power dissipated inside the conductor

$$P = \tfrac{1}{2} R\, H^2(0_-)$$

Normal Conductors (local limit)

Maxwell equations are not sufficient to model the behavior of electromagnetic fields in materials. Need an additional equation to describe material properties

$$\frac{\partial J}{\partial t} + \frac{J}{\tau} = \frac{\sigma}{\tau} E \qquad \Rightarrow \sigma(\omega) = \frac{\sigma_0}{1 - i\omega\tau}$$

For Cu at 300 K, $\tau = 3 \times 10^{-14}$ sec

so for wavelengths longer than infrared $J = \sigma E$

Normal Conductors (local limit)

In the local limit $\vec{J}(z) = \sigma \vec{E}(z)$

The fields decay with a characteristic length (skin depth) $\delta = \left(\dfrac{2}{\mu_0 \omega \sigma} \right)^{1/2}$

$$E_x(z) = E_x(0) e^{-z/\delta} e^{-iz/\delta}$$

$$H_y(z) = \frac{(1-i)}{\mu_0 \omega \delta} E_x(z)$$

$$Z = \frac{E_x(0)}{H_y(0)} = \frac{(1+i)}{2} \mu_0 \omega \delta = \frac{(1+i)}{\sigma \delta} = (1+i) \left(\frac{\mu_0 \omega}{2\sigma} \right)^{1/2}$$

Normal Conductors (anomalous limit)

- At low temperature, experiments show that the surface resistance becomes independent of the conductivity
- As the temperature decreases, the conductivity σ increases
  - The skin depth decreases $$\delta = \left(\frac{2}{\mu_0 \omega \sigma} \right)^{1/2}$$
  - The skin depth (the distance over which fields vary) can become less then the mean free path of the electrons (the distance they travel before being scattered)
  - The electrons do not experience a constant electric field over a mean free path
  - The local relationship between field and current is not valid $$\vec{J}(z) \neq \sigma \vec{E}(z)$$

Normal Conductors (anomalous limit)

Introduce a new relationship where the current is related to the electric field over a volume of the size of the mean free path (*l*)

$$\vec{J}(\vec{r},t) = \frac{3\sigma}{4\pi l}\int_V d\vec{r}\,' \frac{\vec{R}\left[\vec{R}\cdot\vec{E}(\vec{r}\,',t-\vec{R}/v_F)\right]}{R^4}e^{-R/l} \quad \text{with} \quad \vec{R}=\vec{r}\,'-\vec{r}$$

Specular reflection: Boundaries act as perfect mirrors

Diffuse reflection: Electrons forget everything

Normal Conductors (anomalous limit)

In the extreme anomalous limit

$$\left(\frac{3}{2} \frac{l^2}{\delta_{cl}^2} \gg 1 \right)$$

$$\tfrac{9}{8} Z_{p=1} = Z_{p=0} = \left(\frac{\sqrt{3}\,\mu_0^2\,\omega^2 l}{16\pi\sigma} \right)^{1/3} \left(1 + i\sqrt{3}\right)$$

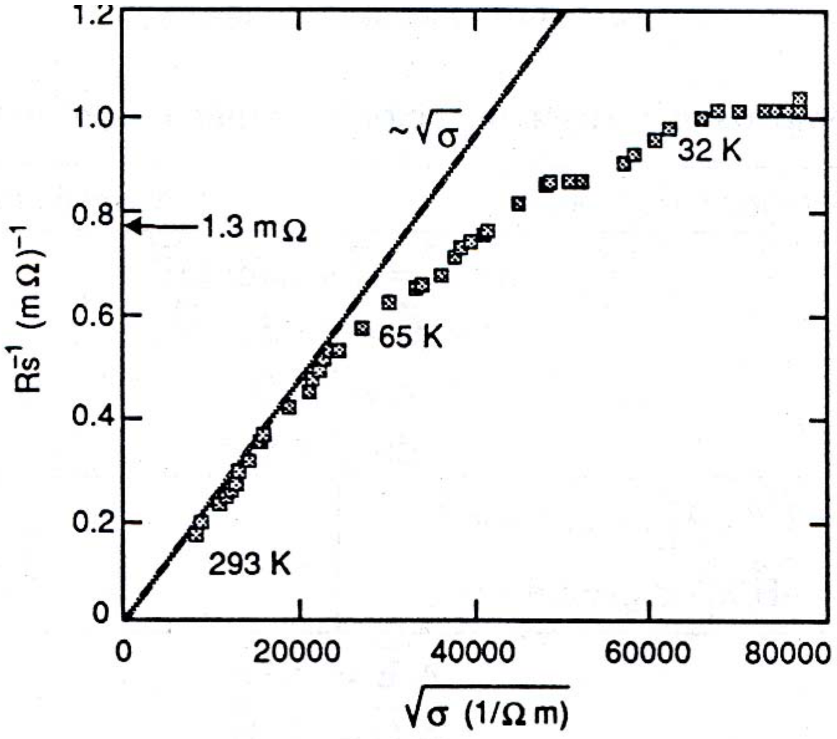

Fig. 2 Anomalous skin effect in a 500 MHz Cu cavity

p : fraction of electrons specularly scattered at surface

$1-p$: fraction of electrons diffusively scattered

Normal Conductors (anomalous limit)

$$R(l \to \infty) = 3.79 \times 10^{-5} \omega^{2/3} \left(\frac{l}{\sigma} \right)^{1/3}$$

For Cu: $l / \sigma = 6.8 \times 10^{-16}\ \Omega \cdot \mathrm{m}^2$

$$\frac{R(4.2\ \mathrm{K}, 500\ \mathrm{MHz})}{R(273\ \mathrm{K}, 500\ \mathrm{MHz})} = \frac{3.79 \times 10^{-5} \omega^{2/3} \left(\frac{l}{\sigma} \right)^{1/3}}{\sqrt{\frac{\mu_0 \omega}{2\sigma}}} \approx 0.12$$

Does not compensate for the Carnot efficiency

Surface Resistance of Superconductors

Superconductors are free of power dissipation in static fields.

In microwave fields, the time-dependent magnetic field in the penetration depth will generate an electric field.

$$\vec{\nabla} \times \vec{E} = -\frac{\partial \vec{B}}{\partial t}$$

The electric field will induce oscillations in the normal electrons, which will lead to power dissipation

Surface Impedance in the Two-Fluid Model

In a superconductor, a time-dependent current will be carried by the Copper pairs (superfluid component) and by the unpaired electrons (normal component)

$$J = J_n + J_s$$

$$J_n = \sigma_n E_0 e^{-i\omega t}$$ (Ohm's law for normal electrons)

$$J_s = i\frac{2n_c e^2}{m_e \omega} E_0 e^{-i\omega t}$$ $(m_e \dot{v}_c = -eE_0 e^{-i\omega t})$

$$J = \sigma E_0 e^{-i\omega t}$$

$\sigma = \sigma_n + i\sigma_s$ with $\sigma_s = \frac{2n_c e^2}{m_e \omega} = \frac{1}{\mu_0 \lambda_L^2 \omega}$

Surface Impedance in the Two-Fluid Model

For normal conductors

$$R_s = \frac{1}{\sigma\delta}$$

For superconductors

$$R_s = \Re\left[\frac{1}{\lambda_L\left(\sigma_n + i\sigma_s\right)}\right] = \frac{1}{\lambda_L}\frac{\sigma_n}{\sigma_n^2 + \sigma_s^2} \simeq \frac{1}{\lambda_L}\frac{\sigma_n}{\sigma_s^2}$$

The superconducting state surface resistance is proportional to the normal state conductivity

Surface Impedance in the Two-Fluid Model

$$R_s \simeq \frac{1}{\lambda_L}\frac{\sigma_n}{\sigma_s^2}$$

$$\sigma_n = \frac{n_n e^2 l}{m_e v_F} \propto l \ \exp\left[-\frac{\Delta(T)}{kT}\right] \qquad \sigma_s = \frac{1}{\mu_0 \lambda_L^2 \omega}$$

$$\boxed{R_s \propto \lambda_L^3 \, \omega^2 \, l \exp\left[-\frac{\Delta(T)}{kT}\right]}$$

This assumes that the mean free path is much larger than the coherence length

Surface Impedance in the Two-Fluid Model

For niobium we need to replace the London penetration depth with

$$\Lambda = \lambda_L \sqrt{1 + \xi / l}$$

As a result, the surface resistance shows a minimum when

$$\xi \approx l$$

Surface Resistance of Niobium

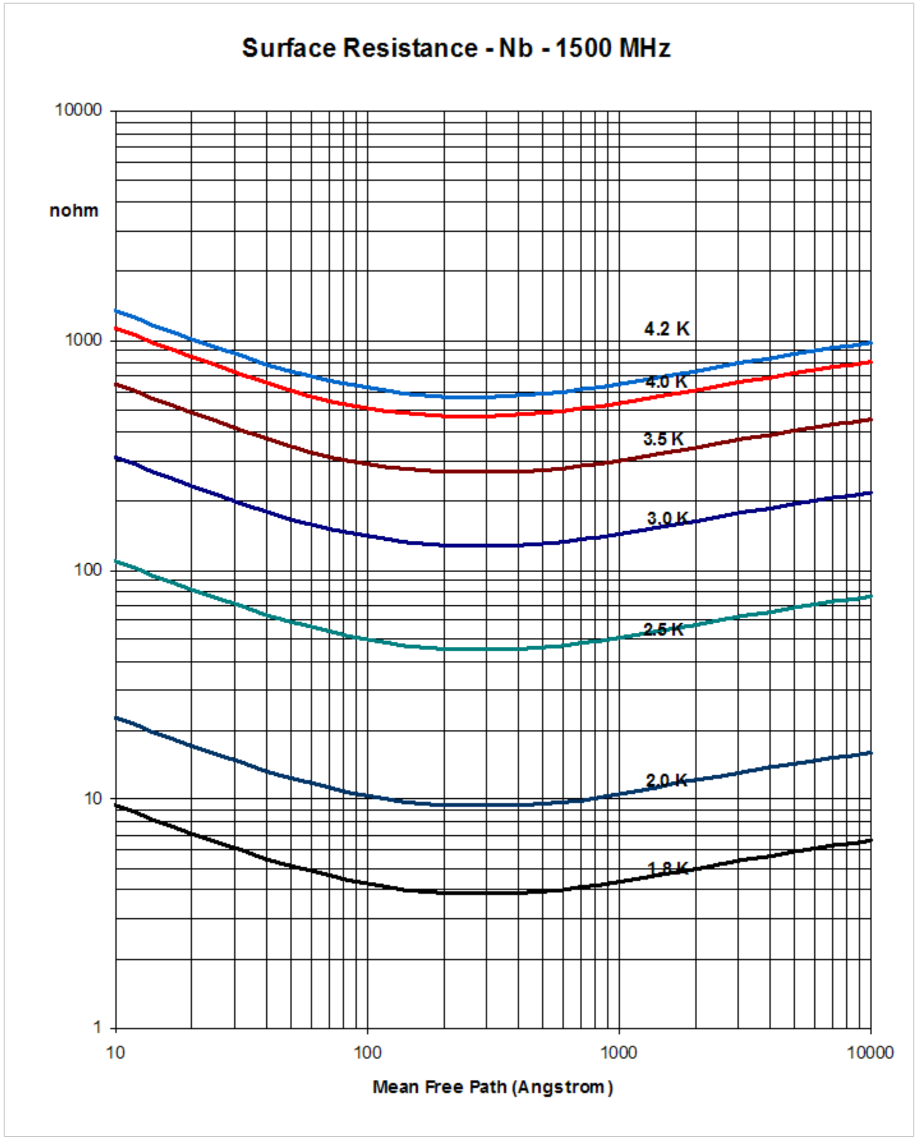

Electrodynamics and Surface Impedance in BCS Model

$$H_0\phi + H_{ex}\ \phi = i\hbar\frac{\partial\phi}{\partial t}$$

$$H_{ex} = \frac{e}{mc}\sum A\left(r_i,t\right)p_i$$

H_{ex} is treated as a small perturbation $H_{rf} << H_c$

There is, at present, no model for superconducting surface resistance at high rf field

$$J \propto \int \frac{R\left[R\cdot A\right] I\left(\omega,R,T\right) e^{-\frac{R}{l}}}{R^4} dr$$

similar to Pippard's model

$$J\left(k\right) = -\frac{c}{4\pi}K\left(k\right)A\left(k\right)$$

$K\left(0\right) \neq 0:$ Meissner effect

Surface Resistance of Superconductors

Temperature dependence

–close to T_c :

dominated by change in $\lambda(t)$ $\dfrac{t^4}{\left(1-t^2\right)^{3/2}}$

–for $T < \dfrac{T_c}{2}$:

dominated by density of excited states $\sim e^{-\Delta/kT}$

$$R_s \sim \frac{A}{T}\omega^2 \exp\left(-\frac{\Delta}{kT}\right)$$

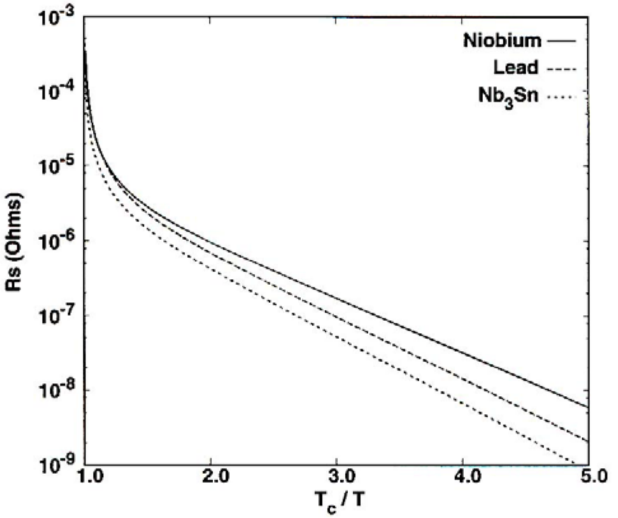

Figure 4.5: Theoretical surface resistance at 1.5 GHz of lead, niobium and Nb_3Sn as calculated from program [94]. The values given in Table 4.1 were used for the material parameters.

Frequency dependence

ω^2 is a good approximation

Surface Resistance of Superconductors

- The surface resistance of superconductors depends on the frequency, the temperature, and a few material parameters
  - Transition temperature
  - Energy gap
  - Coherence length
  - Penetration depth
  - Mean free path

- A good approximation for $T<T_c/2$ and $\omega<<\Delta/h$ is

$$R_s \sim \frac{A}{T}\omega^2 \exp\left(-\frac{\Delta}{kT}\right) + R_{res}$$

Surface Resistance of Superconductors

$$R_s \sim \frac{A}{T}\omega^2 \exp\left(-\frac{\Delta}{kT}\right) + R_{res}$$

In the dirty limit $l \ll \xi_0$ $R_{BCS} \propto l^{-1/2}$

In the clean limit $l \gg \xi_0$ $R_{BCS} \propto l$

R_{res}:

Residual surface resistance

No clear temperature dependence

No clear frequency dependence

Depends on trapped flux, impurities, grain boundaries, …

Surface Resistance of Superconductors

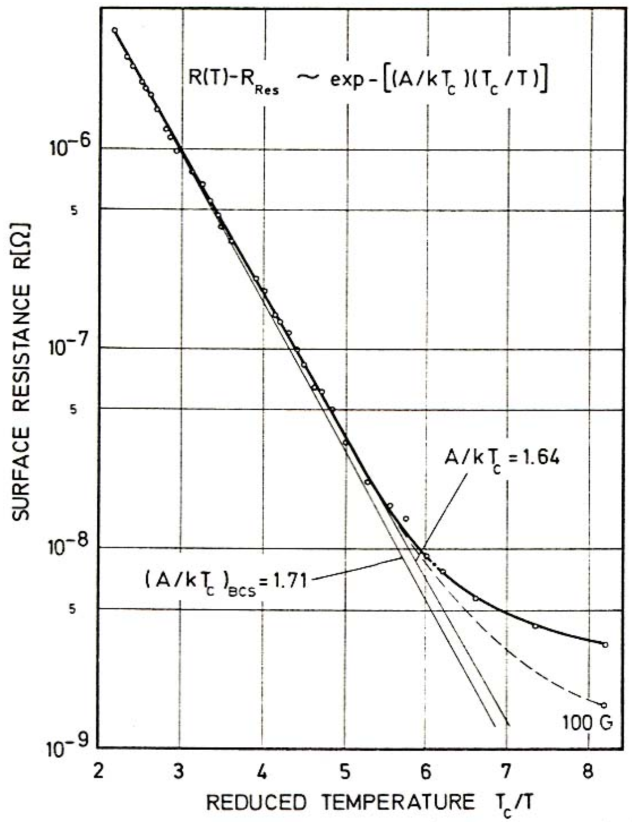

Fig. 2. Temperature dependence of surface resistance of niobium at 3.7 GHz measured in the TE_{011} mode at $H_{rf} \simeq 10$ G. The values computed with the BCS theory used the following material parameters:

$T_c = 9.25$ K; $\lambda_L(T=0, l=\infty) = 320$ Å;
$\Delta(0)/kT = 1.85$; $\xi_F(T=0, l=\infty) = 620$ Å; $l = 1000$ Å or 80 Å.

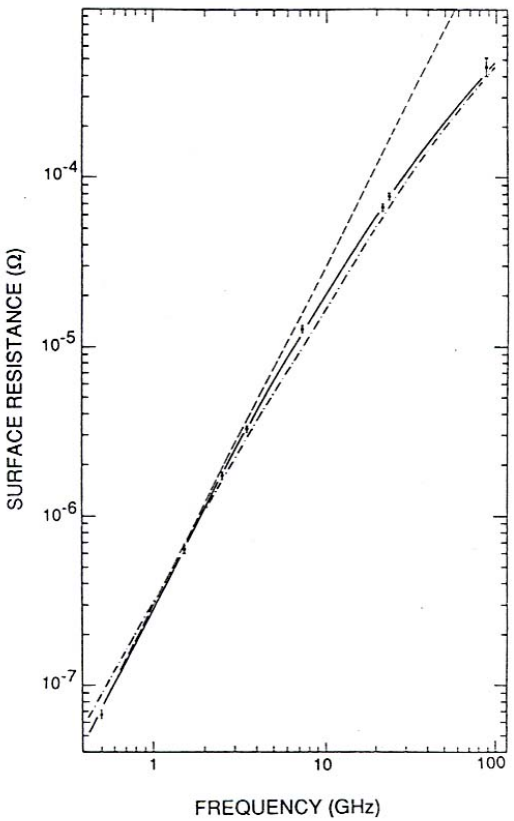

Fig. 5. The surface resistance of Nb at 4.2 K as a function of frequency [62,63]. Whereas the isotropic BCS surface resistance (– · – ·) resulted in $R \propto \omega^{1.8}$ around 1 GHz, the measurements fit better to ω^2 (– – –). The solid curve, which fits the data over the entire range, is a calculation based on the smearing of the BCS density-of-states singularity by the energy gap anisotropy in the presence of impurity scattering [61]. The authors thank G. Müller for providing this figure.

Surface Resistance of Niobium

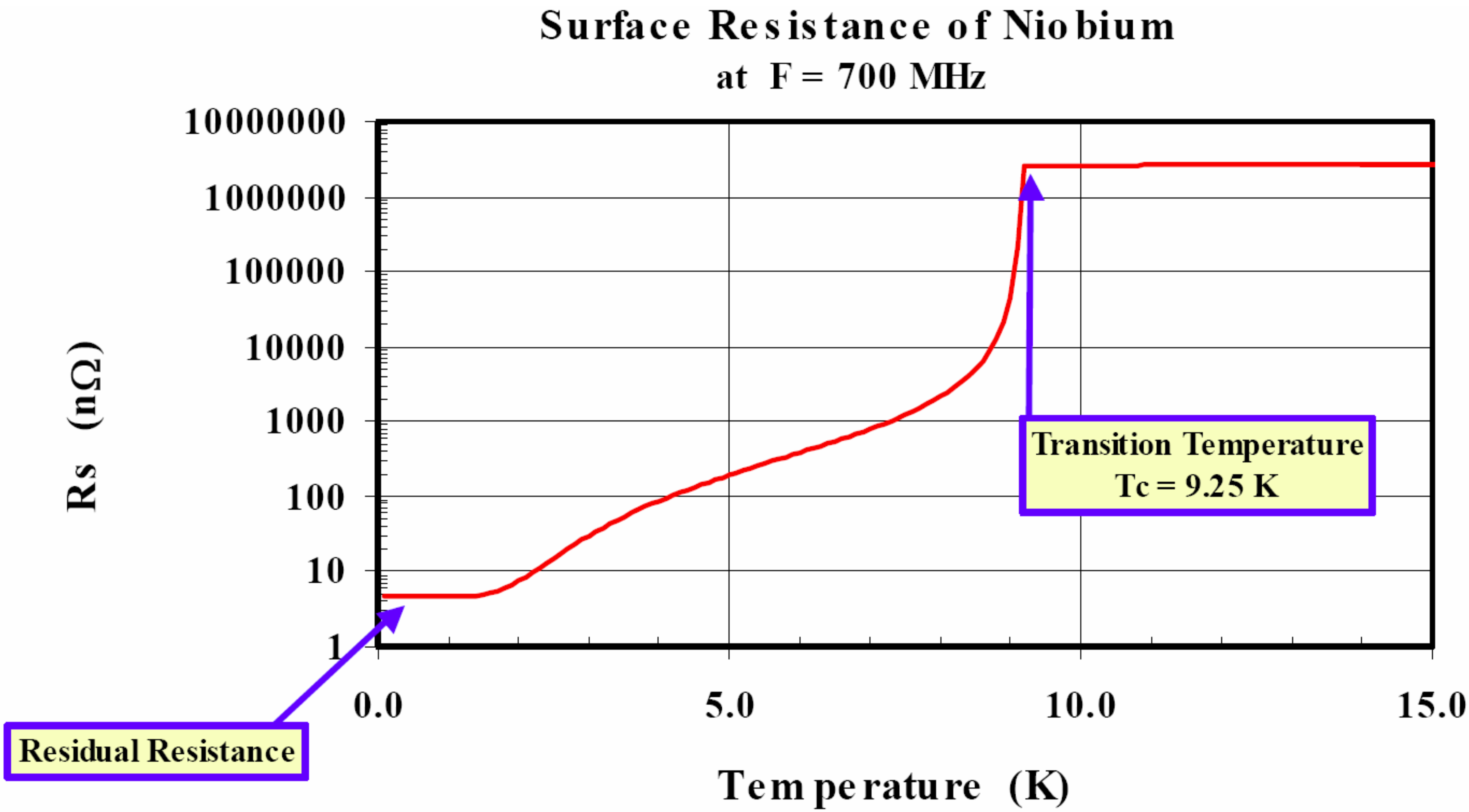

Surface Resistance of Niobium

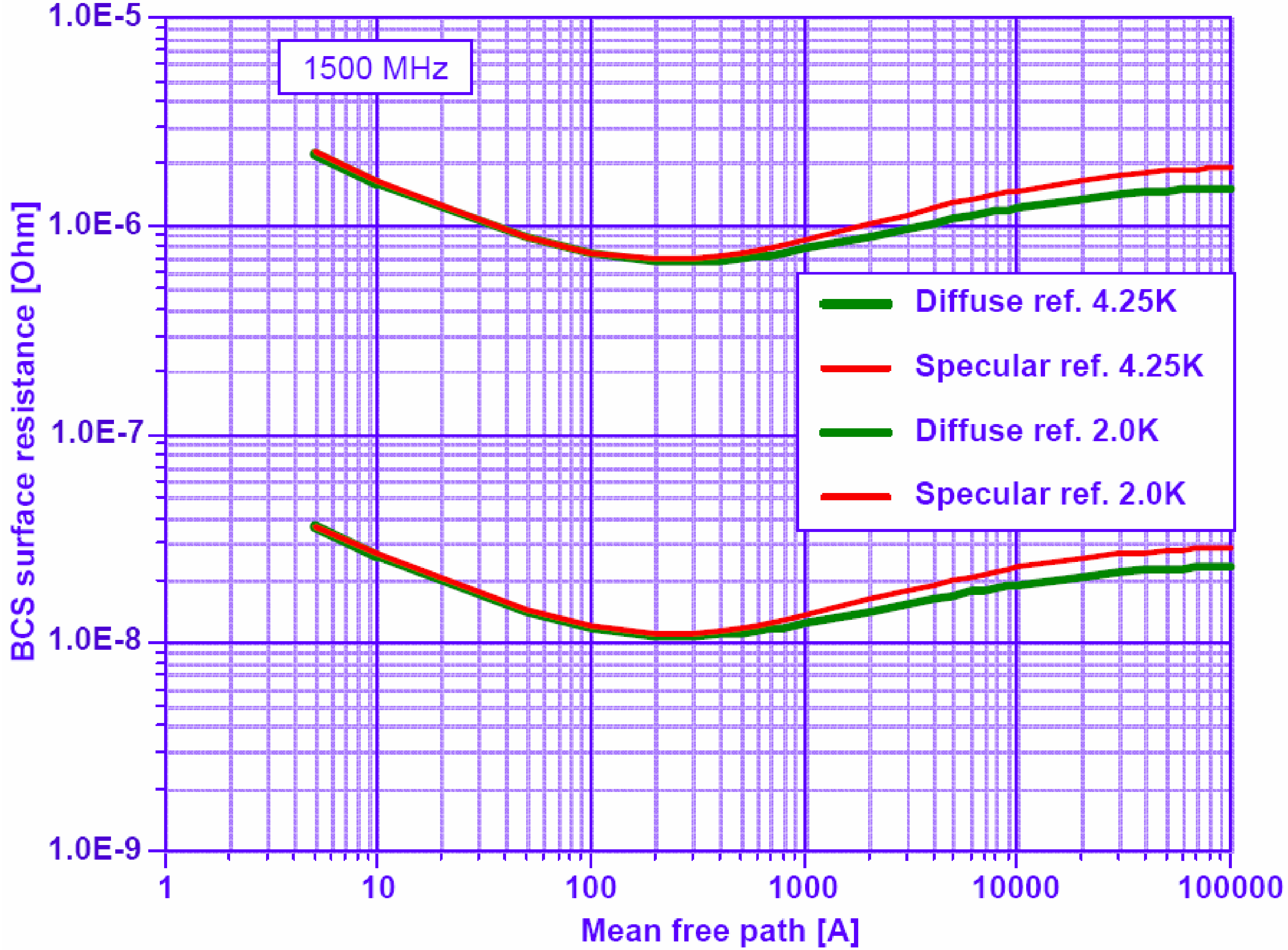

Super and Normal Conductors

- Normal Conductors
  - Skin depth proportional to $\omega^{-1/2}$
  - Surface resistance proportional to $\omega^{1/2 \rightarrow 2/3}$
  - Surface resistance independent of temperature (at low T)
  - For Cu at 300K and 1 GHz, R_s=8.3 mΩ

- Superconductors
  - Penetration depth independent of ω
  - Surface resistance proportional to ω^2
  - Surface resistance strongly dependent of temperature
  - For Nb at 2 K and 1 GHz, $R_s \approx 7$ nΩ

However: do not forget Carnot

RF Cavity

- Mode transformer (TEM→TM)
- Impedance transformer (Low Z→High Z)
- Space enclosed by conducting walls that can sustain an infinite number of resonant electromagnetic modes
- Shape is selected so that a particular mode can efficiently transfer its energy to a charged particle
- An isolated mode can be modeled by an LRC circuit

RF Cavity

Lorentz force $$\vec{F} = q(\vec{E} + \vec{v} \times \vec{B})$$

An accelerating cavity needs to provide an electric field E longitudinal with the velocity of the particle

Magnetic fields provide deflection but no acceleration

DC electric fields can provide energies of only a few MeV

Higher energies can be obtained only by transfer of energy from traveling waves →resonant circuits

Transfer of energy from a wave to a particle is efficient only is both propagate at the same velocity

Equivalent Circuit for an rf Cavity

Simple LC circuit representing an accelerating resonator

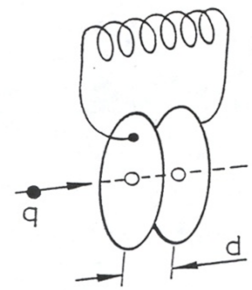

Simple lumped L-C circuit repesenting an accelerating resonator.
$\omega_o^2 = 1/LC$

Metamorphosis of the LC circuit into an accelerating cavity

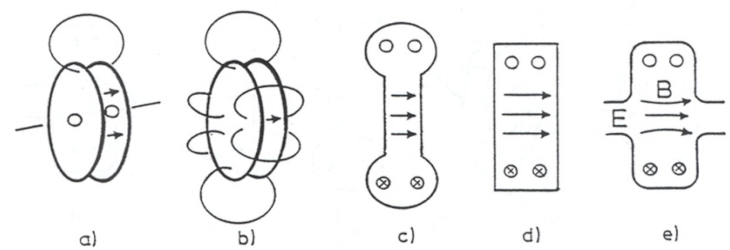

Metamorphosis of the L-C circuit of Fig. 1 into an accelerating cavity (after R.P.Feynman[33]). Fig. 5d shows the cylindrical "pillbox cavity" and Fig. 5e a slightly modified pillbox cavity with beam holes (typical β between 0.5 and 1.0). Fig. 5c resembles a low β version of the pillbox variety ($0.2<\beta<0.5$).

Chain of weakly coupled pillbox cavities representing an accelerating module

Chain of coupled pendula as its mechanical analog

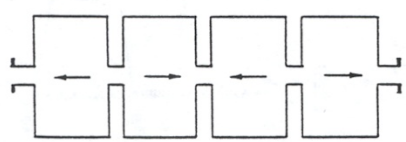

Chain of weakly-coupled pillbox cavities representing an accele-rating module

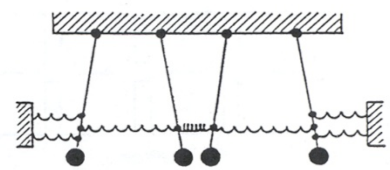

Chain of coupled pendula as a mechanical analogue to Fig. 6a

Electromagnetic Modes

Electromagnetic modes satisfy Maxwell equations

$$\left(\nabla^2 - \frac{1}{c^2}\frac{\partial^2}{\partial t^2}\right)\begin{Bmatrix}\vec{E}\\ \vec{H}\end{Bmatrix} = 0$$

With the boundary conditions (assuming the walls are made of a material of low surface resistance)

no tangential electric field $\vec{n} \times \vec{E} = 0$

no normal magnetic field $\vec{n} \bullet \vec{H} = 0$

Electromagnetic Modes

Assume everything $\sim e^{-i\omega t}$

$$\left(\nabla^2 + \frac{\omega^2}{c^2}\right)\begin{Bmatrix}\vec{E} \\ \vec{H}\end{Bmatrix} = 0$$

For a given cavity geometry, Maxwell equations have an infinite number of solutions with a sinusoidal time dependence

For efficient acceleration, choose a cavity geometry and a mode where:

Electric field is along particle trajectory

Magnetic field is 0 along particle trajectory

Velocity of the electromagnetic field is matched to particle velocity

Accelerating Field (gradient)

Voltage gained by a particle divided by a reference length

$$E = \frac{1}{L}\int E_z(z)\cos(\omega z / \beta c)dz$$

For velocity-of-light particles $$L = \frac{N\lambda}{2}$$

For less-than-velocity-of-light cavities, there is no universally adopted definition of the reference length

Design Considerations

$\frac{H_{s,\max}}{E_{acc}}$	minimum	critical field
$\frac{E_{s,\max}}{E_{acc}}$	minimum	field emission
$\frac{< H_s^2 >}{E_{acc}^2}$	minimum	shunt impedance, current losses
$\frac{< E_s^2 >}{E_{acc}^2}$	minimum	dielectric losses
$\frac{U}{E_{acc}^2}$	minimum maximum	control of microphonics voltage drop for high charge per bunch

Energy Content

Energy density in electromagnetic field:

$$u = \frac{1}{2}\left(\varepsilon_0 \mathbf{E}^2 + \mu_0 \mathbf{H}^2\right)$$

Because of the sinusoidal time dependence and the 90º phase shift, he energy oscillates back and forth between the electric and magnetic field

Total energy content in the cavity:

$$U = \frac{\varepsilon_0}{2}\int_V dV\,|\mathbf{E}|^2 = \frac{\mu_0}{2}\int_V dV\,|\mathbf{H}|^2$$

Power Dissipation

Power dissipation per unit area

$$\frac{dP}{da} = \frac{\mu_0 \omega \delta}{4} \left| \mathbf{H}_{\parallel} \right|^2 = \frac{R_s}{2} \left| \mathbf{H}_{\parallel} \right|^2$$

Total power dissipation in the cavity walls

$$P = \frac{R_s}{2} \int_A da \left| \mathbf{H}_{\parallel} \right|^2$$

Quality Factor

Quality Factor Q_0:

$$Q_0 \equiv \frac{\text{Energy stored in cavity}}{\text{Energy dissipated in cavity walls per radian}} = \frac{\omega_0 U}{P_{diss}}$$

$$= \omega_0 \tau_0 = \frac{\omega_0}{\Delta\omega_0}$$

$$Q_0 = \frac{\omega\mu_0}{R_s} \frac{\int_V dV \, |\mathbf{H}|^2}{\int_A da \, |\mathbf{H}_{||}|^2}$$

Geometrical Factor

Geometrical Factor QRs (Ω)

Product of the Quality Factor and the surface resistance

Independent of size and material

Depends only on shape of cavity and electromagnetic mode

$$G = QR_s = \omega\mu_0 \frac{\int_V dV\,|\mathbf{H}|^2}{\int_A da\,|\mathbf{H}_{\|}|^2} = 2\pi\sqrt{\frac{\mu_0}{\varepsilon_0}}\frac{1}{\lambda}\frac{\int_V dV\,|\mathbf{H}|^2}{\int_A da\,|\mathbf{H}_{\|}|^2} = \frac{2\pi\eta}{\lambda}\frac{\int_V dV\,|\mathbf{H}|^2}{\int_A da\,|\mathbf{H}_{\|}|^2}$$

$\eta \approx 377\Omega$ Impedance of vacuum

Shunt Impedance, R/Q

Shunt impedance R_{sh}: $$R_{sh} \equiv \frac{V_c^2}{P_{diss}}$$ in Ω

V_c = accelerating voltage

Note: Sometimes the shunt impedance is defined as $\frac{V_c^2}{2P_{diss}}$ or quoted as impedance per unit length (ohm/m)

R/Q (in Ω)

$$\frac{R}{Q} = \frac{V^2}{P}\frac{P}{\omega U} = \frac{E^2}{U}\frac{L^2}{\omega}$$

Q – Geometrical Factor (Q R_s)

Q: $\dfrac{\text{Energy content}}{\text{Energy disspated during one radian}} = \omega \dfrac{U}{P} = \omega\tau = \dfrac{\omega}{\Delta\omega}$

Rough estimate (factor of 2) for fundamental mode

$$\omega = \frac{2\pi c}{\lambda} \simeq \frac{2\pi}{\sqrt{\varepsilon_0 \mu_0}} \frac{1}{2L} \qquad U = \frac{\mu_0}{2} \int H^2 dv \simeq \frac{\mu_0}{2} \frac{1}{2} H_0^2 \frac{\pi L^3}{6}$$

$$P = \frac{1}{2} R_s \int H^2 dA = \frac{1}{2} R_s \frac{1}{2} H_0^2 \pi L^2$$

$$QR_s \sim \frac{\pi}{6} \sqrt{\frac{\mu_0}{\varepsilon_0}} = 200\Omega$$

$G = QR_s$ is size (frequency) and material independent.

It depends only on the mode geometry

It is independent of number of cells

For superconducting elliptical cavities $QR_s \sim 275\Omega$

Shunt Impedance (R_{sh}), R_{sh} R_s, R/Q

$$R_{sh} = \frac{V^2}{P} \simeq \frac{E_z^2 L^2}{\frac{1}{2} R_s H_0^2 \pi L^2 \frac{1}{2}}$$

In practice for elliptical cavities

$R_{sh} R_s \simeq 33{,}000 \ \left(\Omega^2\right)$ per cell

$R_{sh} / Q \simeq 100\Omega$ per cell

$R_{sh}\, R_s$ and R_{sh} / Q

Independent of size (frequency) and material

Depends on mode geometry

Proportional to number of cells

Power Dissipated per Unit Length or Unit Area

$$\frac{P}{L} \propto \frac{1}{\frac{R}{Q} QR_S} \frac{E^2 R_S}{\omega}$$

For normal conductors $R_S \propto \omega^{1/2}$

$$\frac{P}{L} \propto \omega^{-\frac{1}{2}}$$

$$\frac{P}{A} \propto \omega^{\frac{1}{2}}$$

For superconductors $R_S \propto \omega^2$

$$\frac{P}{L} \propto \omega$$

$$\frac{P}{A} \propto \omega^2$$

External Coupling

- Consider a cavity connected to an rf source
- A coaxial cable carries power from an rf source to the cavity
- The strength of the input coupler is adjusted by changing the penetration of the center conductor
- There is a fixed output coupler, the transmitted power probe, which picks up power transmitted through the cavity. This is usually very weakly coupled

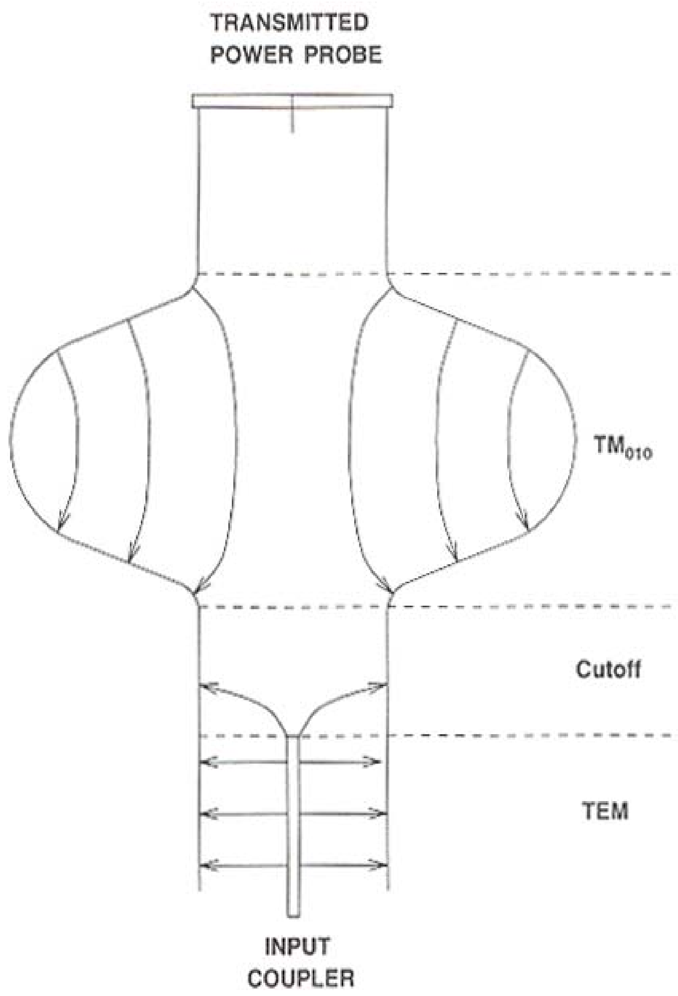

Cavity with External Coupling

Consider the rf cavity after the rf is turned off.
Stored energy *U* satisfies the equation:

$$\frac{dU}{dt} = -P_{tot}$$

Total power being lost, P_{tot}, is: $P_{tot} = P_{diss} + P_e + P_t$

P_e is the power leaking back out the input coupler.
P_t is the power coming out the transmitted power coupler.
Typically P_t is very small $\Rightarrow P_{tot} \approx P_{diss} + P_e$

Recall $Q_0 \equiv \frac{\omega_0 U}{P_{diss}}$

Similarly define a “loaded” quality factor Q_L: $Q_L \equiv \frac{\omega_0 U}{P_{tot}}$

Now $\frac{dU}{dt} = -\frac{\omega_0 U}{Q_L} \quad \Rightarrow \quad U = U_0 e^{-\frac{\omega_0 t}{Q_L}}$

$\therefore$ energy in the cavity decays exponentially with time constant: $\tau_L = \frac{Q_L}{\omega_0}$

Cavity with External Coupling

Equation
$$\frac{P_{tot}}{\omega_0 U} = \frac{P_{diss} + P_e}{\omega_0 U}$$

suggests that we can assign a quality factor to each loss mechanism, such that
$$\frac{1}{Q_L} = \frac{1}{Q_0} + \frac{1}{Q_e}$$

where, by definition,
$$Q_e \equiv \frac{\omega_0 U}{P_e}$$

Typical values for CEBAF 7-cell cavities: Q_0=1x10^{10}, $Q_e \approx Q_L$=2x10^{7}.

Cavity with External Coupling

- Define "coupling parameter": $$\beta \equiv \frac{Q_0}{Q_e}$$

  therefore $$\frac{1}{Q_L} = \frac{(1+\beta)}{Q_0}$$

  β is equal to: $$\beta = \frac{P_e}{P_{diss}}$$

- It tells us how strongly the couplers interact with the cavity. Large β implies that the power leaking out of the coupler is large compared to the power dissipated in the cavity walls.

Several Loss Mechanisms

$P = \sum P_i$ -wall losses

-power absorbed by beam

-coupling to outside world

Associate Q will each loss mechanism

$$Q_i = \omega \frac{U}{P_i}$$

(index 0 is reserved for wall losses)

Loaded Q: Q_L

$$\frac{1}{Q_L} = \frac{\sum P_i}{\omega U} = \sum \frac{1}{Q_i}$$

Coupling coefficient:

$$\beta_i = \frac{Q_0}{Q_i} = \frac{P_i}{P_0}$$

$$Q_L = \frac{Q_0}{1 + \sum \beta_i}$$

Equivalent Circuit for an rf Cavity

Simple LC circuit representing an accelerating resonator

Metamorphosis of the LC circuit into an accelerating cavity

Chain of weakly coupled pillbox cavities representing an accelerating cavity

Chain of coupled pendula as its mechanical analogue

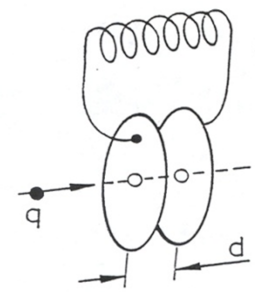

Simple lumped L-C circuit repesenting an accelerating resonator.
$\omega_o^2 = 1/LC$

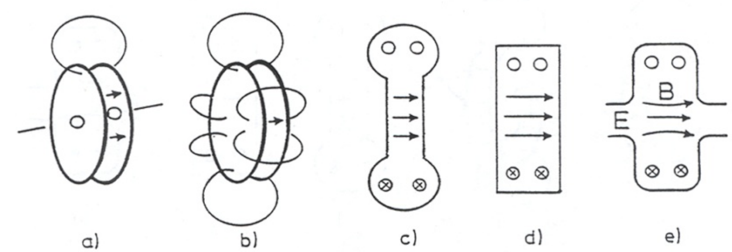

Metamorphosis of the L-C circuit of Fig. 1 into an accelerating cavity (after R.P.Feynman[33]). Fig. 5d shows the cylindrical "pillbox cavity" and Fig. 5e a slightly modified pillbox cavity with beam holes (typical β between 0.5 and 1.0). Fig. 5c resembles a low β version of the pillbox variety ($0.2<\beta<0.5$).

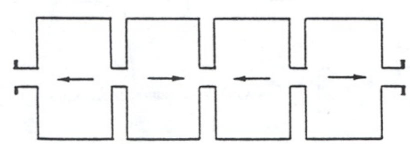

Chain of weakly-coupled pillbox cavities representing an accelerating module

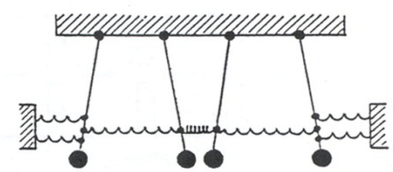

Chain of coupled pendula as a mechanical analogue to Fig. 6a

Parallel Circuit Model of an Electromagnetic Mode

- Power dissipated in resistor R:

$$P_{diss} = \frac{1}{2}\frac{V_c^2}{R}$$

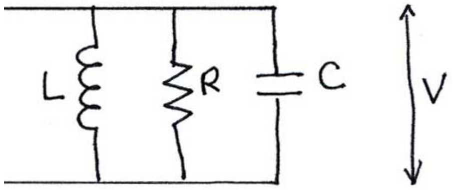

- Shunt impedance:

$$R_{sh} \equiv \frac{V_c^2}{P_{diss}} \qquad \Rightarrow \quad R_{sh} = 2R$$

- Quality factor of resonator:

$$Q_0 \equiv \frac{\omega_0 U}{P_{diss}} = \omega_0 CR = \frac{R}{L\omega_c} = R\left(\frac{C}{L}\right)^{1/2}$$

$$\tilde{Z} = R\left[1 + iQ_0\left(\frac{\omega}{\omega_0} - \frac{\omega_0}{\omega}\right)\right]^{-1}$$

$$\omega \approx \omega_0 \ , \qquad \tilde{Z} \approx R\left[1 + 2iQ_0\left(\frac{\omega - \omega_0}{\omega_0}\right)\right]^{-1}$$

1-Port System

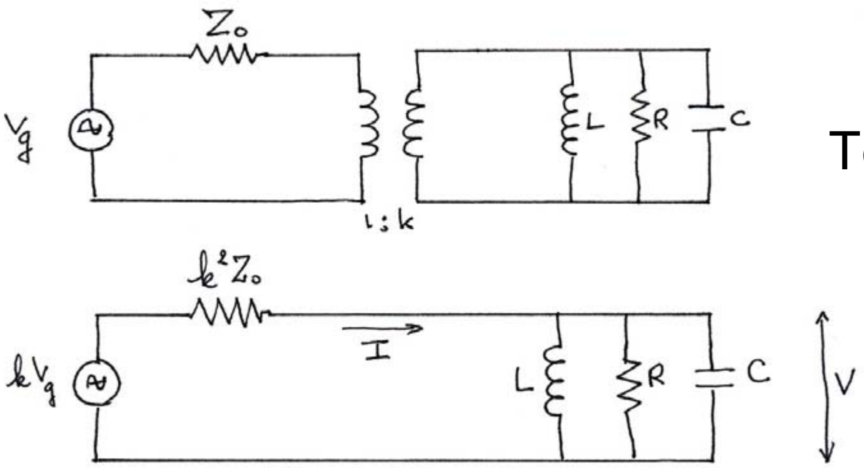

Total impedance: $$k^2 Z_0 + \frac{R}{1 + 2i\dfrac{Q_0}{\omega_0}\Delta\omega}$$

$$I = \frac{kV_g}{k^2 Z_0 + \dfrac{R}{1 + 2i\dfrac{Q_0}{\omega_0}\Delta\omega}} \qquad V = kV_g \frac{R}{R + k^2 Z_0 \left(1 + 2i\dfrac{Q_0}{\omega_0}\Delta\omega\right)}$$

1-Port System

Energy content $U=\frac{1}{2}CV^2=\frac{1}{2}\frac{Q_0}{\omega R}V^2$

$$=\frac{1}{2}\frac{Q_0}{\omega R}\;k^2V_g^2\;\frac{R^2}{\left(R+k^2Z_0\right)^2+4k^4Z_0^2Q_0^2\left(\frac{\Delta\omega}{\omega_0}\right)^2}$$

Incident power: $P_{inc}=\frac{V_g^2}{8Z_0}$

Define coupling coefficient: $\beta=\frac{R}{k_0^2Z_0}$

$$\frac{U}{P_{inc}}=\frac{Q_0}{\omega_0}\frac{4\beta}{(1+\beta)^2}\frac{1}{1+\left(\frac{2Q_0}{1+\beta}\right)^2\left(\frac{\Delta\omega}{\omega_0}\right)^2}$$

1-Port System

Power dissipated

$$P_{diss} = \frac{\omega U}{Q_0} = P_{inc} \frac{4\beta}{(1+\beta)^2} \frac{1}{1+\left(\frac{2Q_0}{1+\beta}\right)^2 \left(\frac{\Delta\omega}{\omega_0}\right)^2}$$

Optimal coupling: $\frac{U}{P_{inc}}$ maximum or $P_{diss} = P_{inc}$

$\Rightarrow \Delta\omega = 0, \qquad \beta = 1$: critical coupling

Reflected power

$$P_{ref} = P_{inc} - P_{diss} = P_{mc}\left[1 - \frac{4\beta}{(1+\beta)^2} \frac{1}{1+\left(\frac{2Q_0}{1+\beta}\frac{\Delta\omega}{\omega_0}\right)^2}\right]$$

1-Port System

At resonance

$$U = \frac{Q_0}{\omega_0} \frac{4\beta}{(1+\beta)^2} P_{inc}$$

$$P_{diss} = \frac{4\beta}{(1+\beta)^2} P_{inc}$$

$$P_{ref} = \left(\frac{1-\beta}{1+\beta}\right)^2 P_{inc}$$

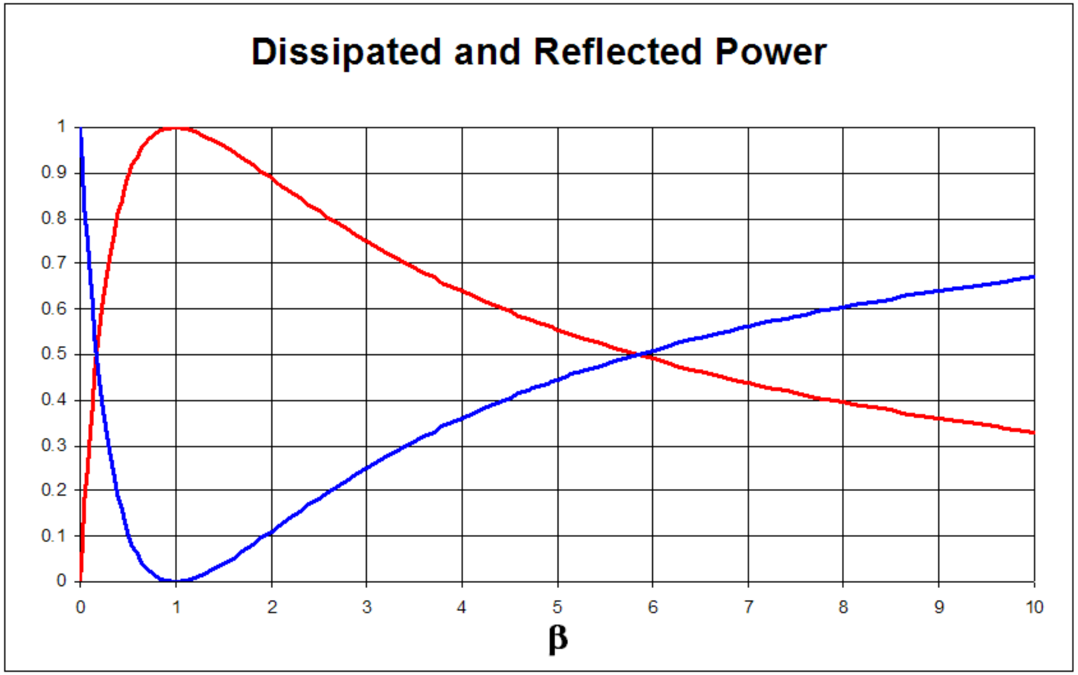

Equivalent Circuit for a Cavity with Beam

- Beam in the rf cavity is represented by a current generator.
- Equiv

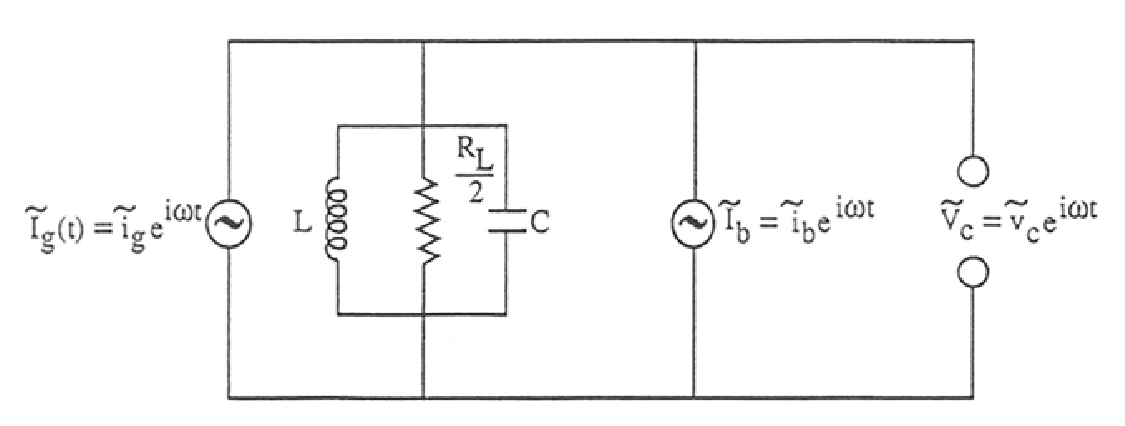

$$R_L = \frac{R_{sh}}{(1+\beta)}$$

$\tilde{i}_b$ produces $\tilde{V}_b$ with phase ψ (detuning angle)

$\tilde{i}_g$ produces $\tilde{V}_g$ with phase ψ

$$\tilde{V}_c = \tilde{V}_g - \tilde{V}_b$$

$$\tan \psi = -2\frac{Q_0}{1+\beta}\frac{\Delta\omega}{\omega_0}$$

Equivalent Circuit for a Cavity with Beam

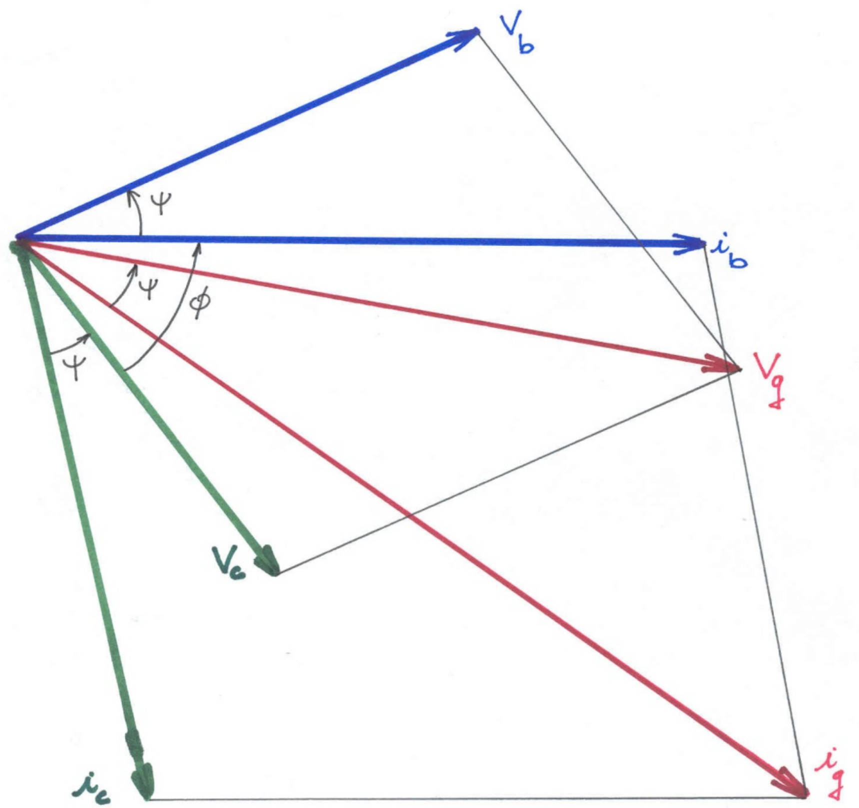

$$V_g = (P_g R_{sh})^{1/2} \frac{2\beta^{1/2}}{1+\beta} \cos\psi$$

$$V_b = \frac{i_b R_{sh}}{2(1+\beta)} \cos\psi$$

$$i_b = 2i_0 \frac{\sin\frac{\theta_b}{2}}{\frac{\theta_b}{2}}$$

i_b: beam rf current

i_0: beam dc current

θ_b: beam bunch length

Equivalent Circuit for a Cavity with Beam

$$\boxed{P_g = \frac{V_c^2}{R_{sh}} \frac{1}{4\beta} \left\{ (1+\beta+b)^2 + \left[(1+\beta)\tan\psi - b\tan\phi \right]^2 \right\}}$$

$$b = \frac{\text{Power absorbed by the beam}}{\text{Power dissipated in the cavity}} = \frac{R_{sh} i_0 \cos\phi}{V_c}$$

Minimize P_g :

$$(1+\beta_{opt})\tan\psi_{opt} = b \ \tan\phi$$

$$\beta_{opt} = |1+b|$$

$$P_g^{opt} = \frac{V_c^2}{R_{sh}} \frac{|1+b| + (1+b)}{2}$$

Frequency Control

Energy gain $$W = qV\cos\phi$$

Energy gain error $$\frac{\delta W}{W} = \frac{\delta V}{V} - \delta\phi \tan\phi$$

The fluctuations in cavity field amplitude and phase come mostly from the fluctuations in cavity frequency

Need for fast frequency control

Minimization of rf power requires matching of average cavity frequency to reference frequency

Need for slow frequency tuners

Some Definitions

- Ponderomotive effects: changes in frequency caused by the electromagnetic field (radiation pressure)
  - Static Lorentz detuning (cw operation)
  - Dynamic Lorentz detuning (pulsed operation)

- Microphonics: changes in frequency caused by connections to the external world
  - Vibrations
  - Pressure fluctuations

Note: The two are not completely independent.

When phase and amplitude feedbacks are active, ponderomotive effects can change the response to external disturbances

Cavity with Beam and Microphonics

- The detuning is now

$$\tan\psi = -2Q_L \frac{\delta\omega_0 \pm \delta\omega_m}{\omega_0} \qquad \tan\psi_0 = -2Q_L \frac{\delta\omega_0}{\omega_0}$$

where $\delta\omega_0$ is the static detuning (controllable)

and $\delta\omega_m$ is the random dynamic detuning (uncontrollable)

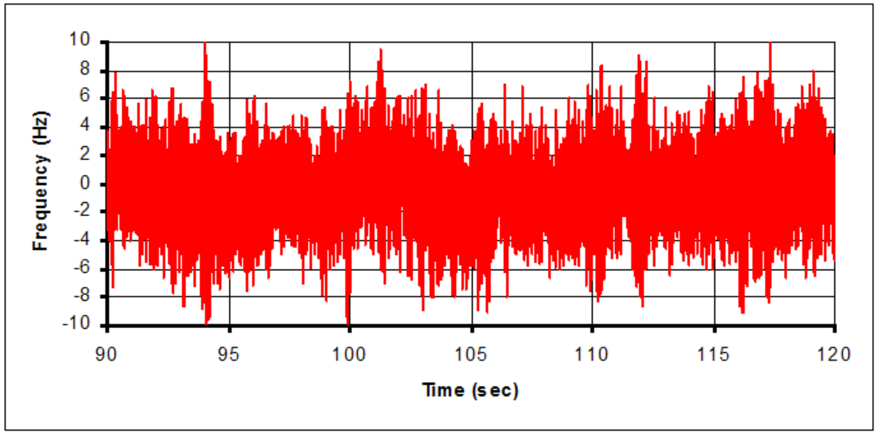

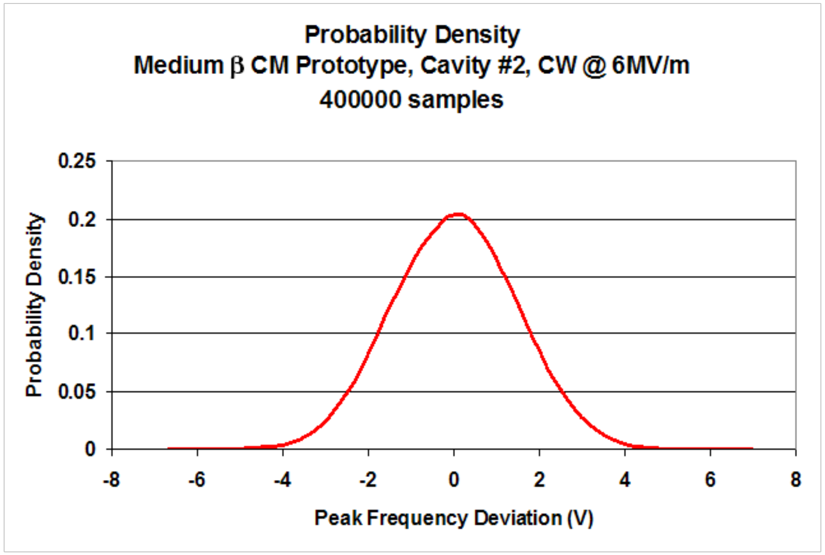

Q_{ext} Optimization with Microphonics

Condition for optimum coupling:

$$\beta_{opt} = \sqrt{(b+1)^2 + \left(2Q_0 \frac{\delta\omega_m}{\omega_0}\right)^2}$$

and

$$P_g^{opt} = \frac{V_c^2}{2R_{sh}}\left[(b+1) + \sqrt{(b+1)^2 + \left(2Q_0 \frac{\delta\omega_m}{\omega_0}\right)^2}\right]$$

In the absence of beam (b=0):

$$\beta_{opt} = \sqrt{1 + \left(2Q_0 \frac{\delta\omega_m}{\omega_0}\right)^2}$$

and

$$P_g^{opt} = \frac{V_c^2}{2R_{sh}}\left[1 + \sqrt{1 + \left(2Q_0 \frac{\delta\omega_m}{\omega_0}\right)^2}\right]$$

$\simeq U\ \delta\omega_m$ If $\delta\omega_m$ is very large

Example

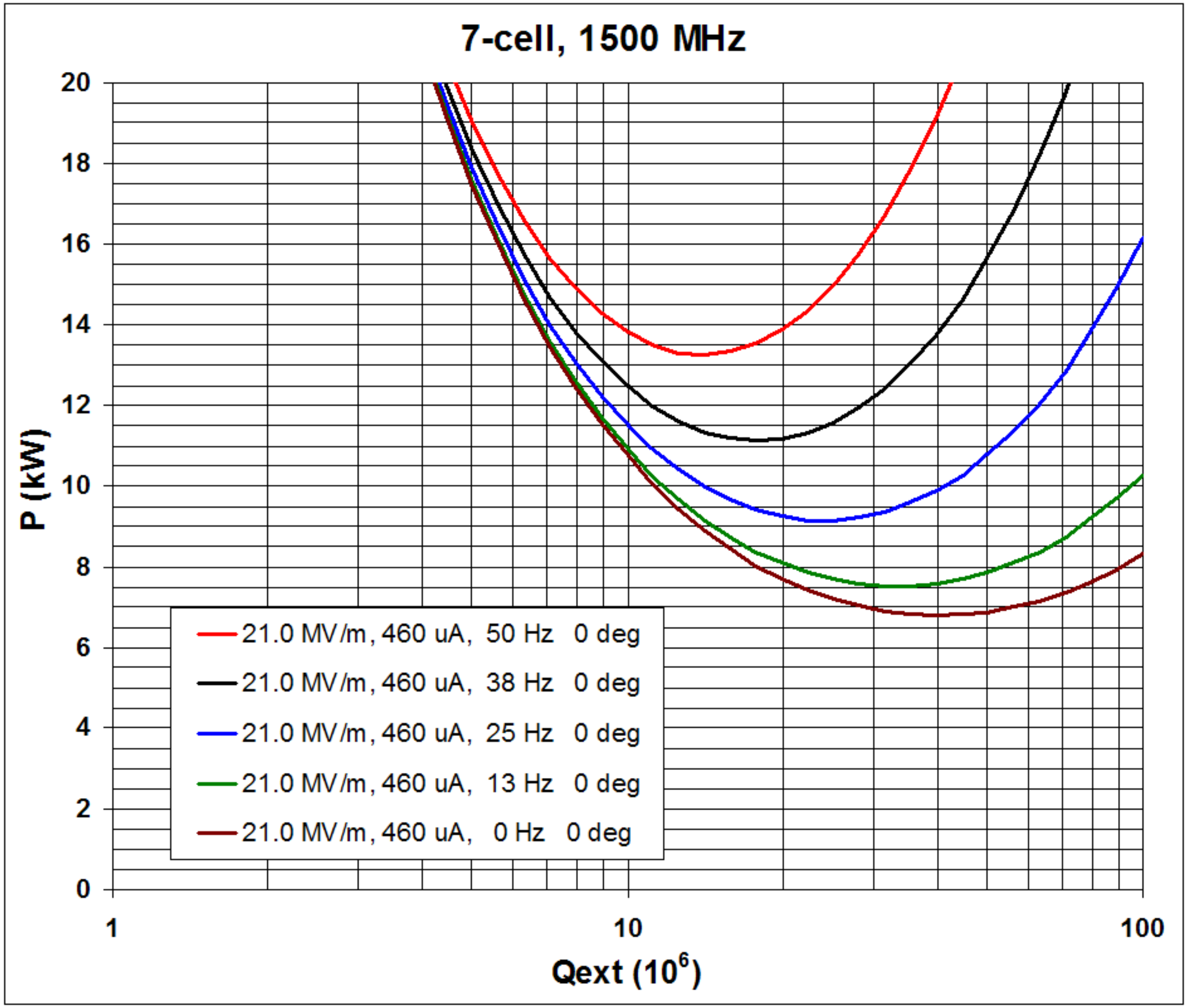

7-cell, 1500 MHz
20
18
16
14
12
10
8
6
4
2
0
P (kW)
1
10
100
Qext (10^6)
21.0 MV/m, 460 uA, 50 Hz 0 deg
21.0 MV/m, 460 uA, 38 Hz 0 deg
21.0 MV/m, 460 uA, 25 Hz 0 deg
21.0 MV/m, 460 uA, 13 Hz 0 deg
21.0 MV/m, 460 uA, 0 Hz 0 deg

Example

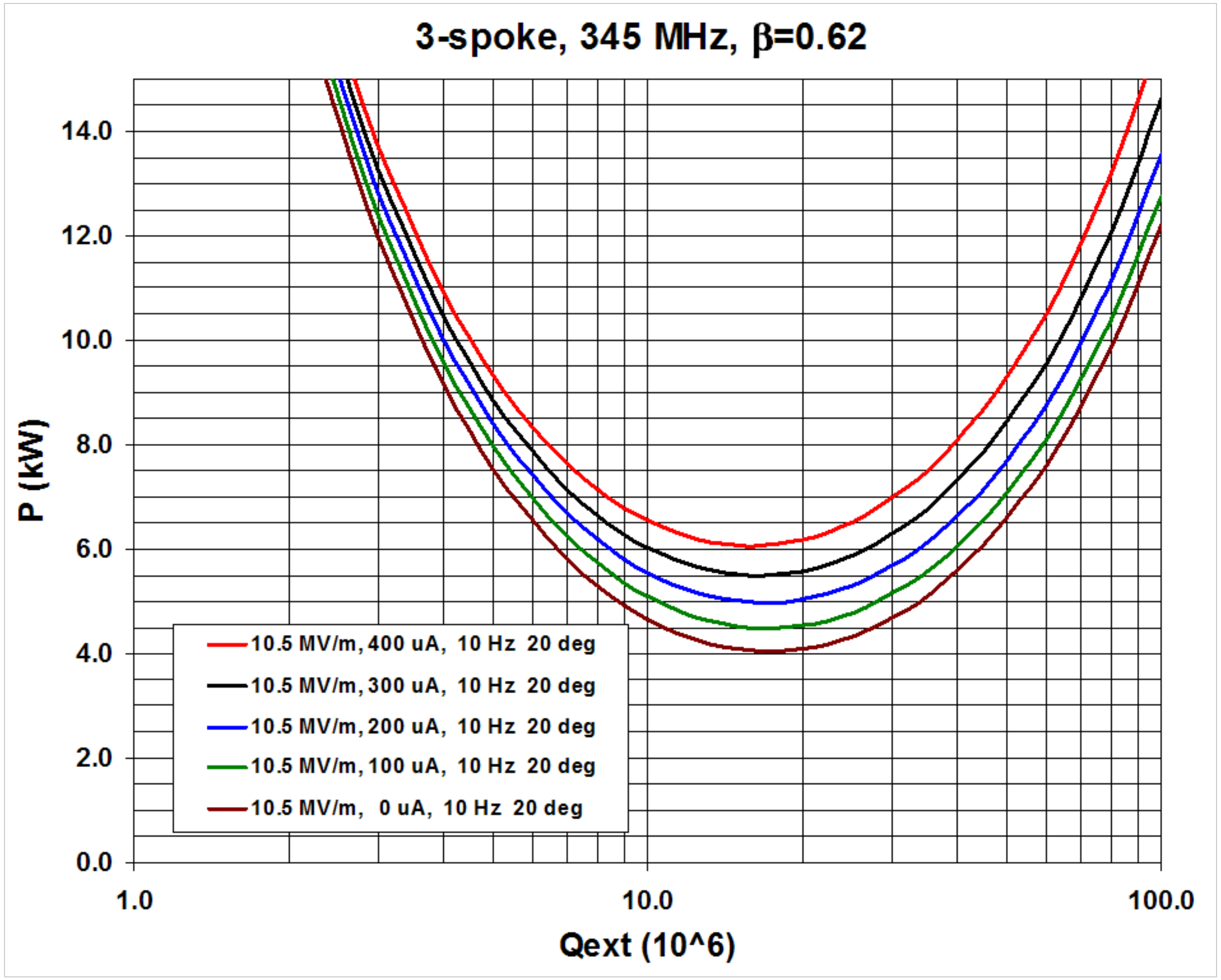

3-spoke, 345 MHz, β=0.62
P (kW)
14.0
12.0
10.0
8.0
6.0
4.0
2.0
0.0
1.0
10.0
100.0
Qext (10^6)
10.5 MV/m, 400 uA, 10 Hz 20 deg
10.5 MV/m, 300 uA, 10 Hz 20 deg
10.5 MV/m, 200 uA, 10 Hz 20 deg
10.5 MV/m, 100 uA, 10 Hz 20 deg
10.5 MV/m, 0 uA, 10 Hz 20 deg

Lorentz Detuning

Pressure deforms the cavity wall:

RF power produces radiation pressure:

$$P = \frac{\mu_0 H^2 - \varepsilon_0 E^2}{4}$$

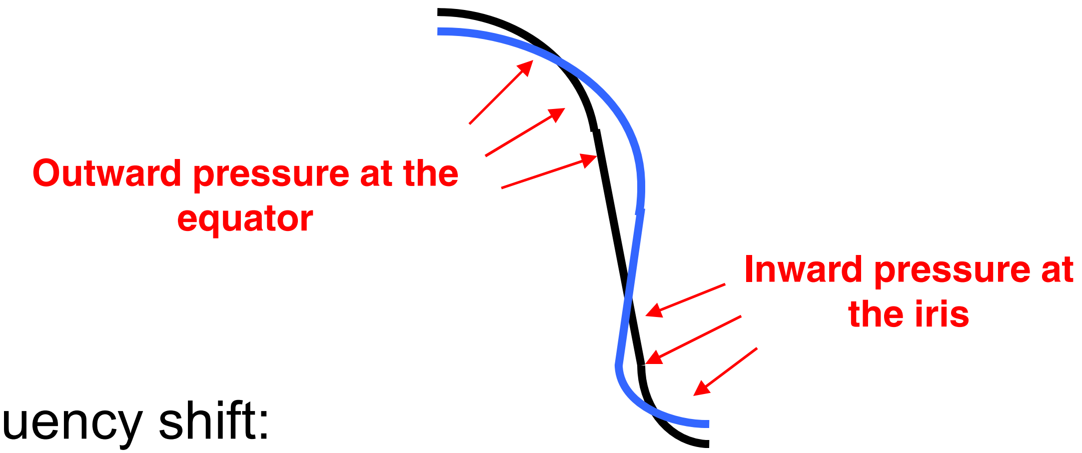

Deformation produces a frequency shift:

$$\Delta f = -k_L E_{acc}^2$$

Lorentz Detuning

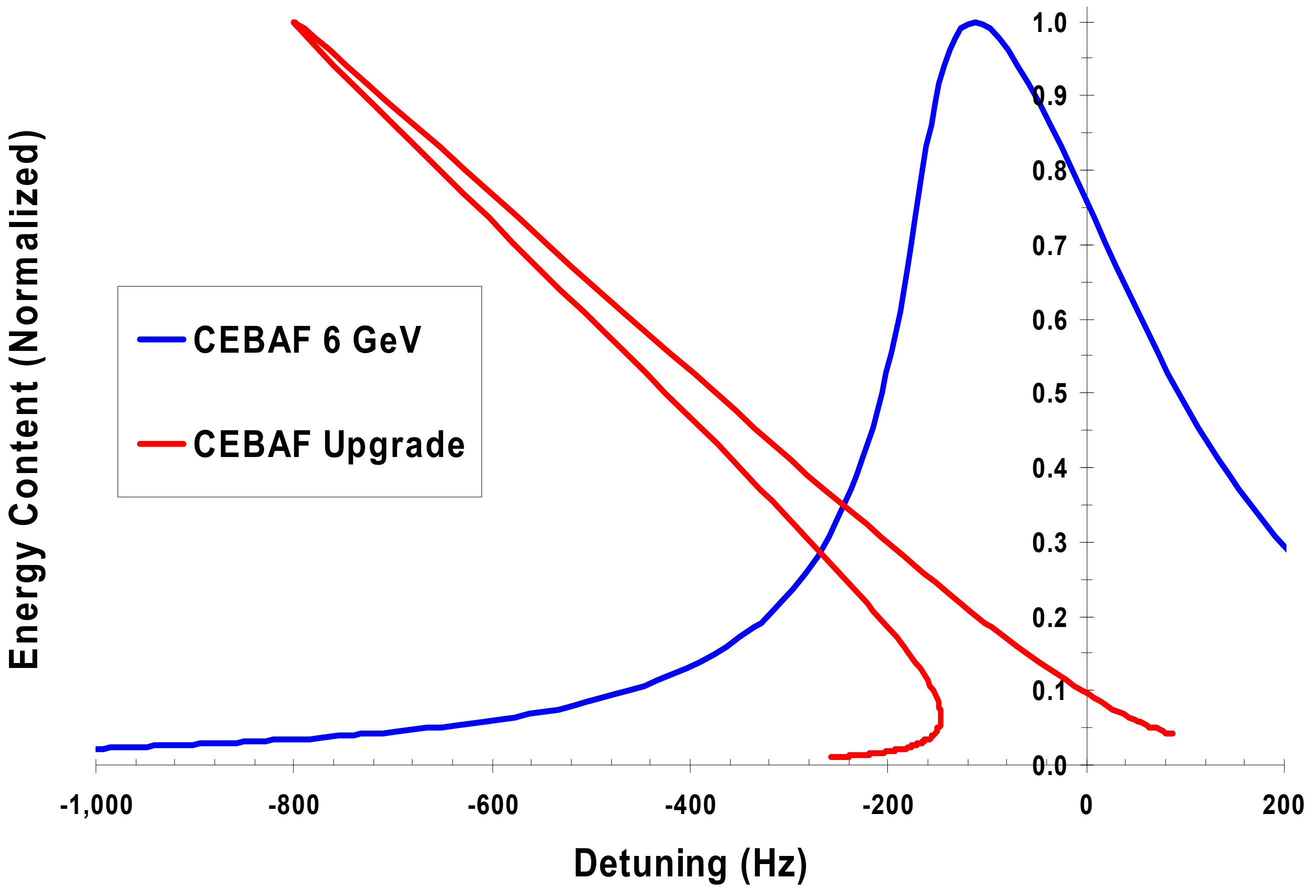

Microphonics

- **Total detuning**

$$\delta\omega_0 + \delta\omega_m$$

where $\delta\omega_0$ is the static detuning (controllable)

and $\delta\omega_m$ is the random dynamic detuning (uncontrollable)

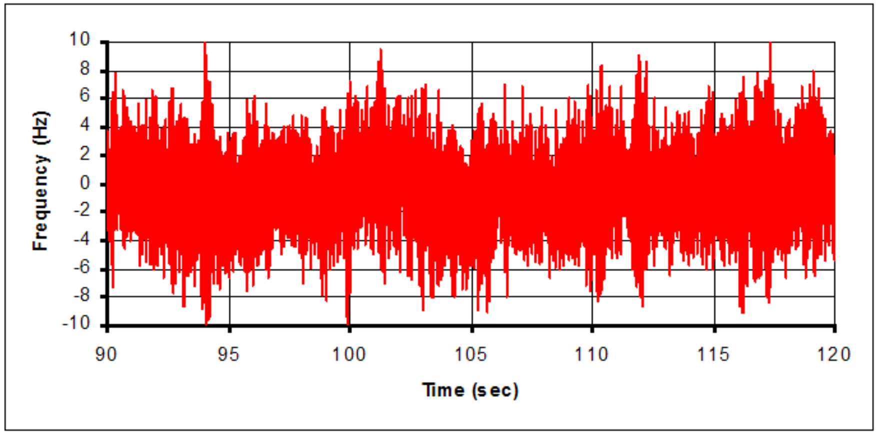

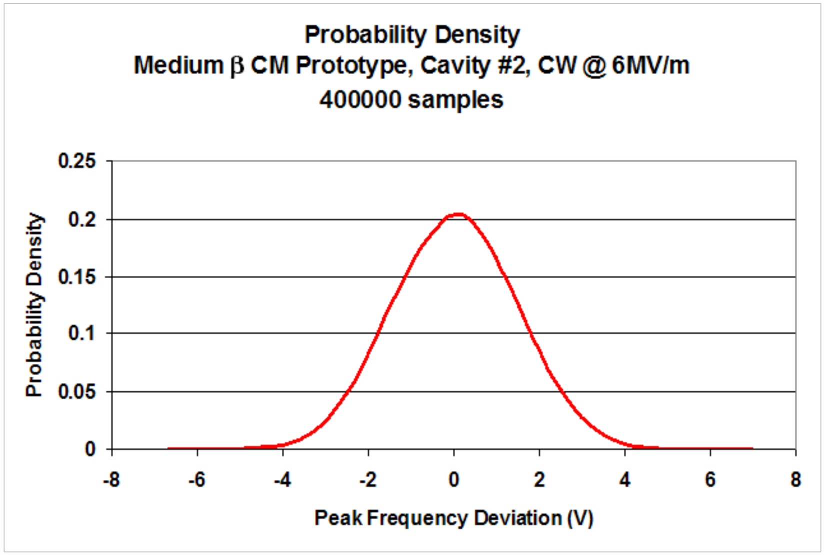

Ponderomotive Effects

- **Adiabatic theorem applied to harmonic oscillators (Boltzmann-Ehrenfest)**

If $\varepsilon = \frac{1}{\omega^2}\frac{d\omega}{dt} \ll 1$, then $\frac{U}{\omega}$ is an adiabatic invariant to all orders

$$\Delta\left(\frac{U}{\omega}\right) \Big/ \left(\frac{U}{\omega}\right) \sim o(e^{-d/\varepsilon}) \quad \Rightarrow \quad \boxed{\frac{\Delta\omega}{\omega} = \frac{\Delta U}{U}} \qquad \text{(Slater)}$$

Quantum mechanical picture: the number of photons is constant: $U = N\hbar\omega$

$$U = \int_V dv \left[\frac{\mu_0}{4} H^2(\vec{r}) + \frac{\varepsilon_0}{4} E^2(\vec{r})\right] \text{ (energy content)}$$

$$\Delta U = -\int_S dS\, \vec{n}(\vec{r}) \cdot \vec{\xi}(\vec{r}) \left[\frac{\mu_0}{4} H^2(\vec{r}) - \frac{\varepsilon_0}{4} E^2(\vec{r})\right] \text{ (work done by radiation pressure)}$$

Ponderomotive Effects

$$\frac{\Delta\omega}{\omega} = -\frac{\int_S dS\, \vec{n}(\vec{r})\cdot\vec{\xi}(\vec{r}) \left[\frac{\mu_0}{4}H^2(\vec{r}) - \frac{\varepsilon_0}{4}E^2(\vec{r})\right]}{\int_V dv \left[\frac{\mu_0}{4}H^2(\vec{r}) + \frac{\varepsilon_0}{4}E^2(\vec{r})\right]}$$

Expand wall displacements and forces in normal modes of vibration $\phi_\mu(\vec{r})$ of the resonator

$$\int_S dS\, \phi_\mu(\vec{r})\, \phi_\nu(\vec{r}) = \delta_{\mu\nu}$$

$$\xi(\vec{r}) = \sum_\mu q_\mu \phi_\mu(\vec{r}) \qquad q_\mu = \int_S \xi(\vec{r})\, \phi_\mu(\vec{r})\, dS$$

$$F(\vec{r}) = \sum_\mu F_\mu \phi_\mu(\vec{r}) \qquad F_\mu = \int_S F(\vec{r})\, \phi_\mu(\vec{r})\, dS$$

Ponderomotive Effects

Equation of motion of mechanical mode μ

$$\frac{d}{dt}\frac{\partial L}{\partial \dot{q}_\mu} - \frac{\partial L}{\partial q_\mu} + \frac{\partial \Phi}{\partial \dot{q}_\mu} = F_\mu \qquad L = T - U \qquad \text{(Euler-Lagrange)}$$

$$U = \frac{1}{2}\sum_\mu c_\mu q_\mu^2$$ (elastic potential energy) c_μ: elastic constant

$$T = \frac{1}{2}\sum_\mu c_\mu \frac{\dot{q}_\mu^2}{\Omega_\mu^2}$$ (kinetic energy) Ω_μ: frequency

$$\Phi = \sum_\mu \frac{c_\mu}{\tau_\mu}\frac{\dot{q}_\mu^2}{\Omega_\mu^2}$$ (power loss) τ_μ: decay time

$$\boxed{\ddot{q}_\mu + \frac{2}{\tau_\mu}\dot{q}_\mu + \Omega_\mu^2 q_\mu = \frac{\Omega_\mu^2}{c_\mu}F_\mu}$$

Ponderomotive Effects

The frequency shift $\Delta\omega_\mu$ caused by the mechanical mode μ is proportional to q_μ

$$\boxed{\Delta\ddot{\omega}_\mu + \frac{2}{\tau_\mu}\Delta\dot{\omega}_\mu + \Omega_\mu^2 \Delta\omega_\mu = -\frac{\omega_0}{c_\mu}\left(\frac{F_\mu}{U}\right)^2 \Omega_\mu^2 U = -k_\mu \Omega_\mu^2 V^2}$$

Total frequency shift: $\Delta\omega(t) = \sum_\mu \Delta\omega_\mu(t)$

Static frequency shift: $\Delta\omega_0 = \sum_\mu \Delta\omega_{\mu 0} = -V^2 \sum_\mu k_\mu$

Static Lorentz coefficient: $k = \sum_\mu k_\mu$

Ponderomotive Effects – Mechanical Modes

$$\Delta\ddot{\omega}_\mu + \frac{2}{\tau_\mu}\Delta\dot{\omega}_\mu + \Omega_\mu{}^2\Delta\omega_\mu = -\Omega_\mu^2 k_\mu V_0{}^2 + \cancel{n(t)}$$

Fluctuations around steady state:

$$\Delta\omega_\mu = \Delta\omega_{\mu o} + \delta\omega_\mu$$

$$V = V_0(1+\delta v)$$

Linearized equation of motion for mechanical mode:

$$\delta\ddot{\omega}_\mu + \frac{2}{\tau_\mu}\delta\dot{\omega}_\mu + \Omega_\mu^2\delta\omega_\mu = -2\Omega_\mu^2 k_\mu V_0{}^2\delta v$$

The mechanical mode is driven by fluctuations in the electromagnetic mode amplitude.

Variations in the mechanical mode amplitude causes a variation of the electromagnetic mode frequency, which can cause a variation of its amplitude.

→Closed feedback system between electromagnetic and mechanical modes, that can lead to instabilities.

Lorentz Transfer Function

$$\delta\ddot{\omega}_{\mu} + \frac{2}{\tau_{\mu}}\delta\dot{\omega}_{\mu} + \Omega_{\mu}^{2}\delta\omega_{\mu} = -2\Omega_{\mu}^{2}k_{\mu}V_{0}^{\ 2}\delta v$$

$$\delta\omega_{\mu}(\omega) = \frac{-2\Omega_{\mu}^{2}k_{\mu}V_{0}^{\ 2}}{\left(\Omega_{\mu}^{2} - \omega^{2}\right) + \frac{2}{\tau_{\mu}}i\omega}\delta v(\omega)$$

TEM-class cavities
ANL, single-spoke, 354 MHz, β=0.4

simple spectrum with few modes

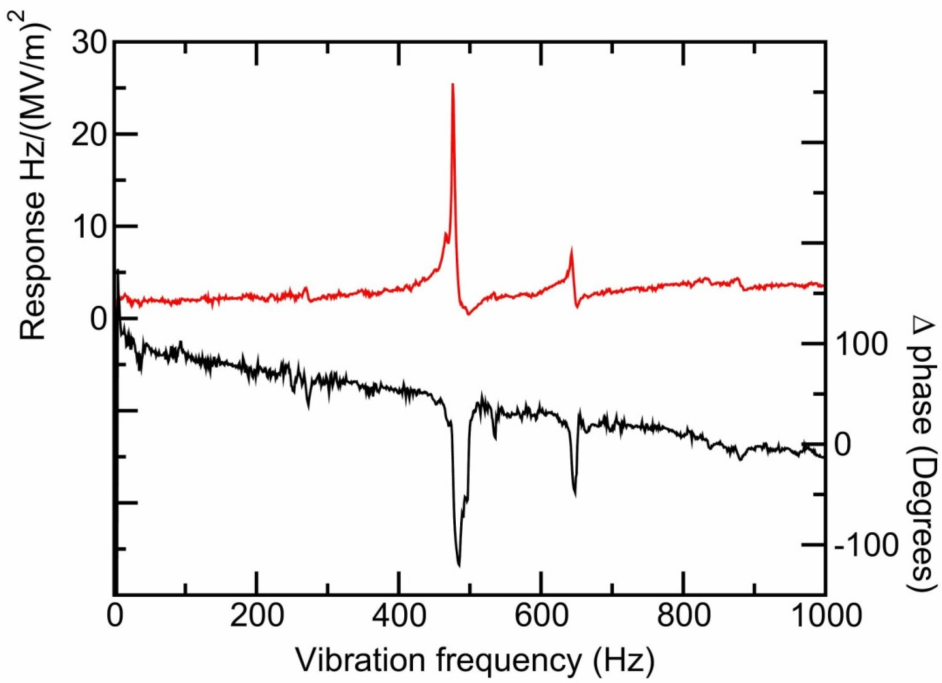

Lorentz Transfer Function

TM-class cavities (Jlab, 6-cell elliptical, 805 MHz, β=0.61)

Rich frequency spectrum from low to high frequencies

Large variations between cavities

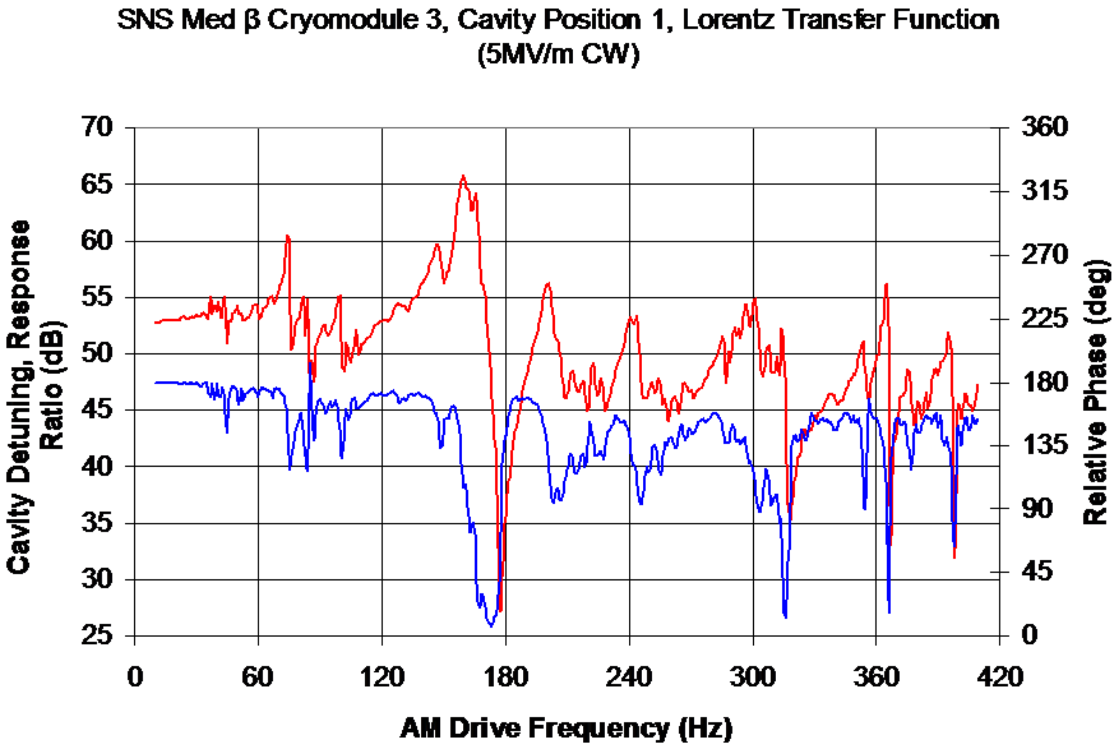

GDR and SEL

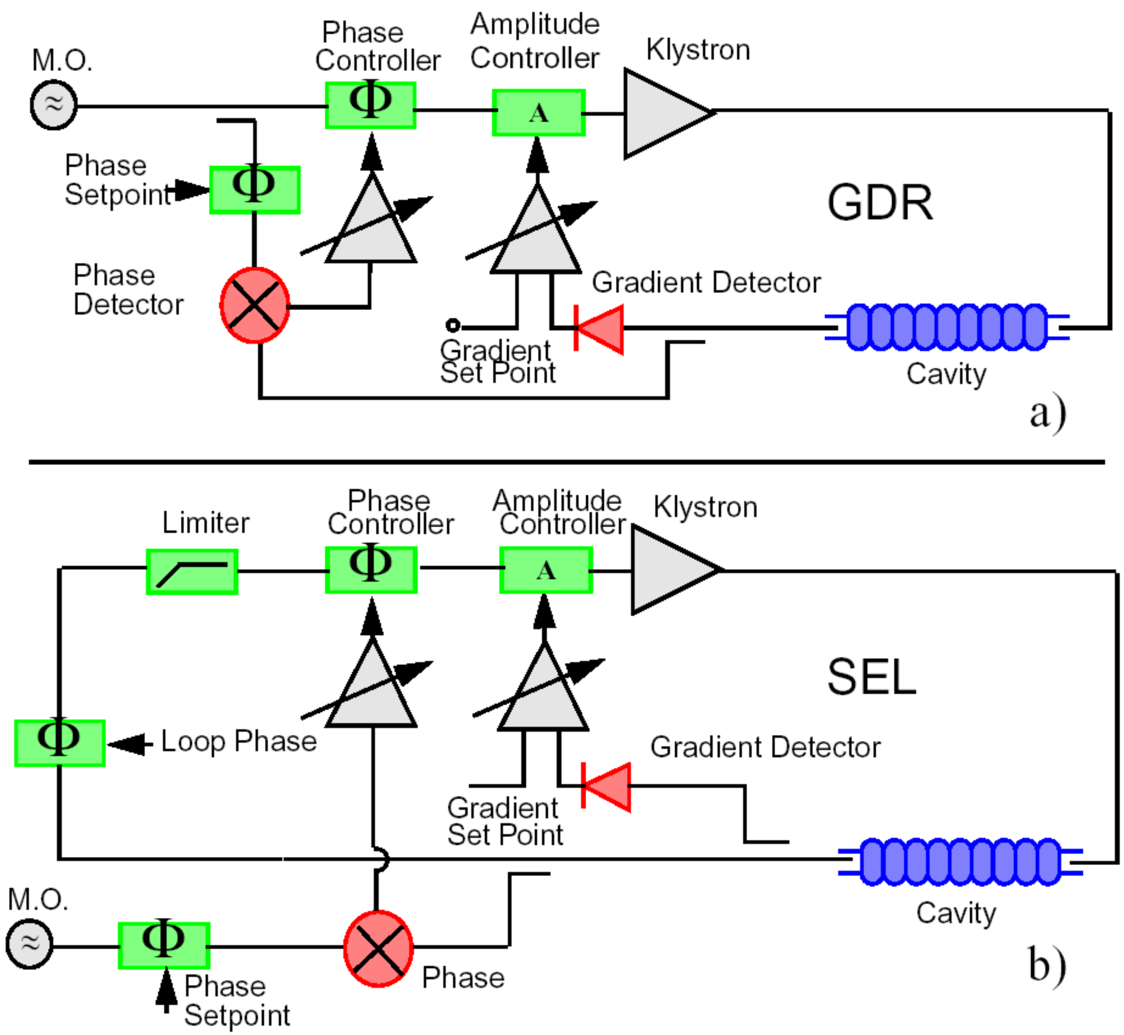
M.O.
Phase Controller
Amplitude Controller
Klystron
Phase Setpoint
GDR
Phase Detector
Gradient Detector
Gradient Set Point
Cavity
a)
Limiter
Phase Controller
Amplitude Controller
Klystron
SEL
Loop Phase
Gradient Detector
Gradient Set Point
M.O.
Cavity
Phase
b)
Phase Setpoint

Generator-Driven Resonator

- In a generator-driven resonator the coupling between the electromagnetic and mechanical modes can lead to two ponderomotive instabilities

- Monotonic instability : Jump phenomenon where the amplitudes of the electromagnetic and mechanical modes increase or decrease exponentially until limited by non-linear effects

- Oscillatory instability : The amplitudes of both modes oscillate and increase at an exponential rate until limited by non-linear effects

Self-Excited Loop-Principle of Stabilization

Controlling the external phase shift θ_l can cc
fluctuations in the cavity frequency ω_c so the
external frequency reference ω_r.

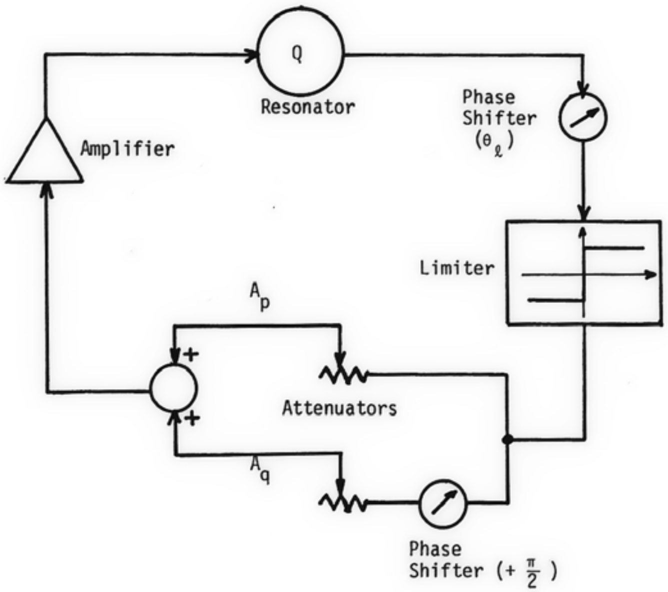

$$\omega = \omega_c + \frac{\omega_c}{2Q}\tan\theta_l$$

Instead of introducing an additional external
this is usually done by adding a signal in quadrature

→ The cavity field amplitude is unaffected by the phase stabilization even in the absence of amplitude feedback.

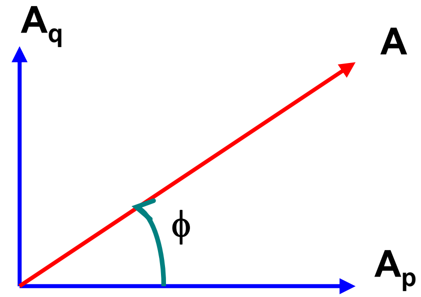

Self-Excited Loop

- Resonators operated in self-excited loops in the absence of feedback are free of ponderomotive instabilities. An SEL is equivalent to the ideal VCO.
  - Amplitude is stable
  - Frequency of the loop tracks the frequency of the cavity
- Phase stabilization can reintroduce instabilities, but they are easily controlled with small amount of amplitude feedback

Input-Output Variables

- **Generator - driven cavity**

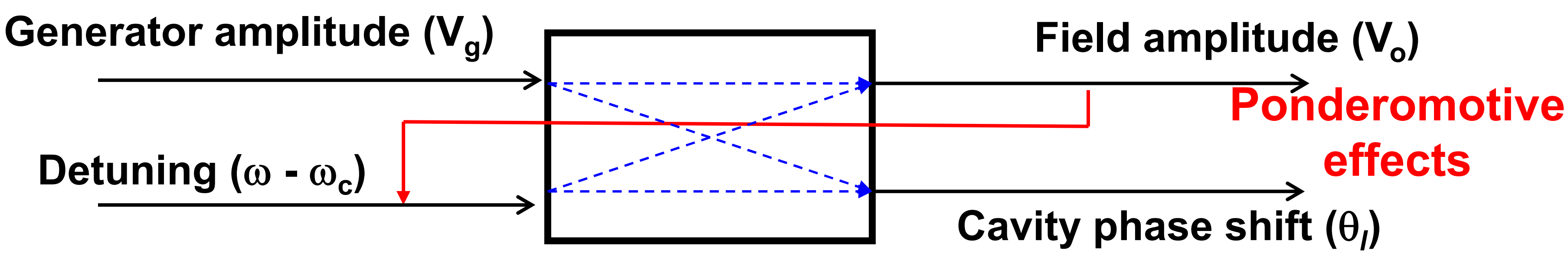

- **Cavity in a self-excited loop**

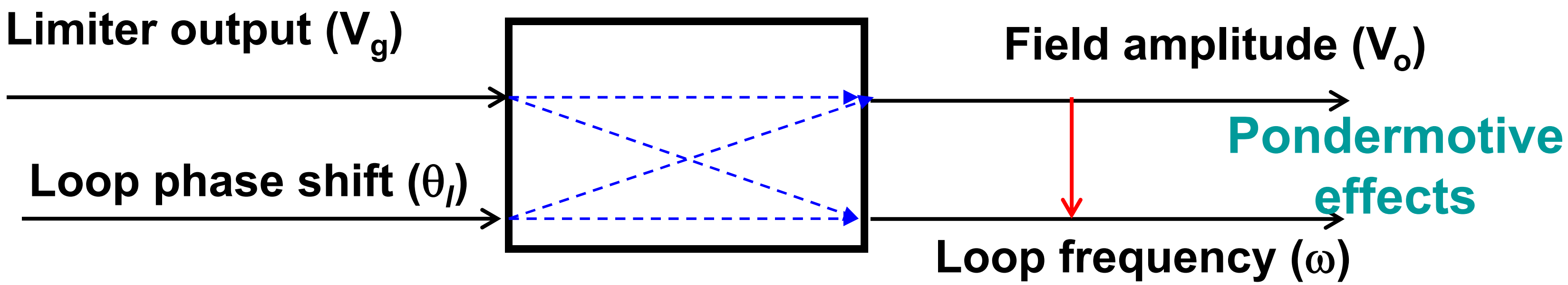

Lorentz Detuning

During transient operation (rise time and decay time) the loop frequency automatically tracts the resonator frequency. Lorentz detuning has no effect and is automatically compensated

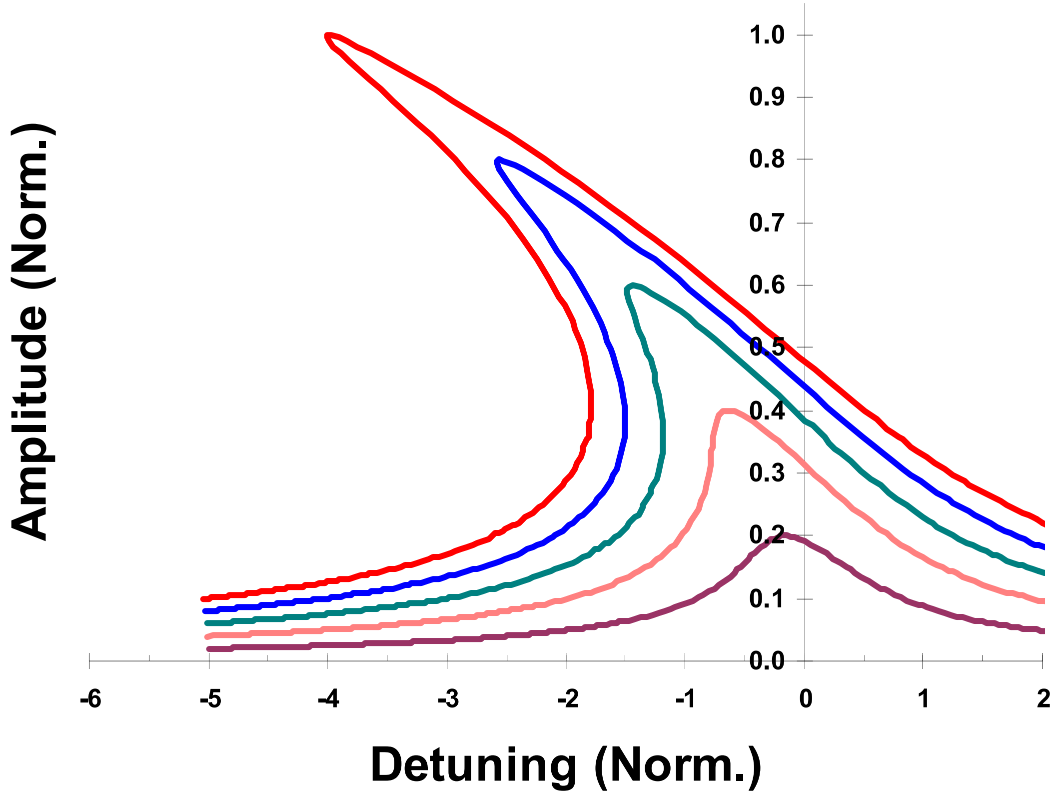

Microphonics

- Microphonics: changes in frequency caused by connections to the external world
  - Vibrations
  - Pressure fluctuations

When phase and amplitude feedbacks are active, ponderomotive effects can change the response to external disturbances

$$\delta\ddot{\omega}_\mu + \frac{2}{\tau_\mu}\delta\dot{\omega}_\mu + \Omega_\mu{}^2\delta\omega_\mu = -2\Omega_\mu^2 k_\mu V_0{}^2\delta v + n(t)$$

Microphonics

Two extreme classes of driving terms:

- Deterministic, monochromatic
  - Constant, well defined frequency
  - Constant amplitude
- Stochastic
  - Broadband (compared to bandwidth of mechanical mode)
  - Will be modeled by gaussian stationary white noise process

Microphonics (probability density)

Single gaussian	Bimodal	Multi-gaussian
Noise driven	Single-frequency driven	Non-stationary noise

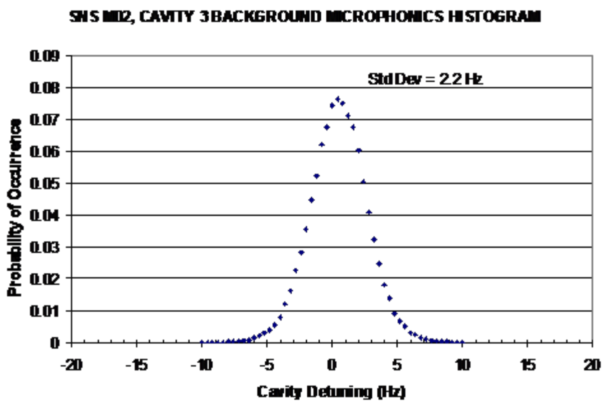

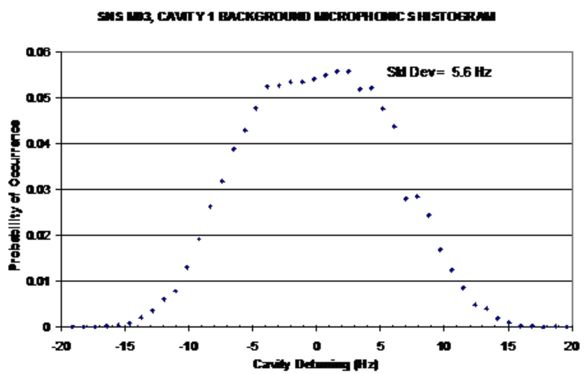

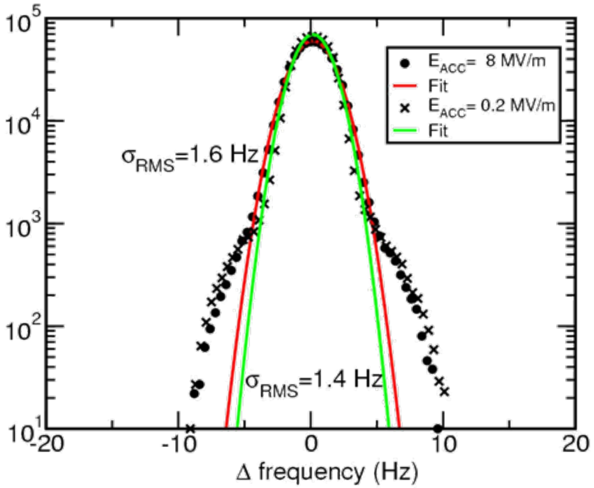

805 MHz TM	805 MHz TM	172 MHz TEM

Microphonics (frequency spectrum)

TM-class cavities (JLab, 6-cell elliptical, 805 MHz, β=0.61)

- **Rich frequency spectrum from low to high frequencies**
- **Large variations between cavities**

TEM-class cavities (ANL, single-spoke, 354 MHz, β=0.4)

- **Dominated by low frequency (<10 Hz) from pressure fluctuations**
- **Few high frequency mechanical modes that contribute little to microphonics level.**

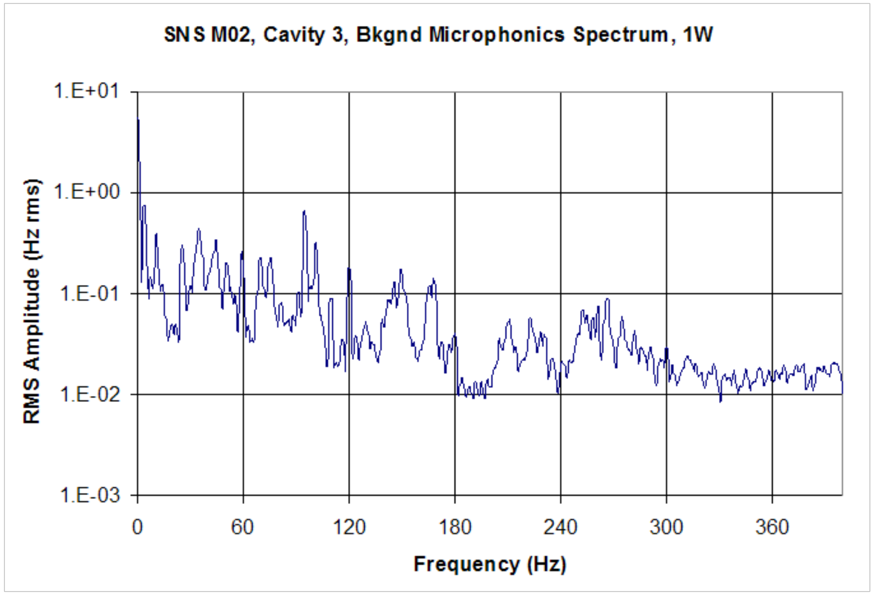

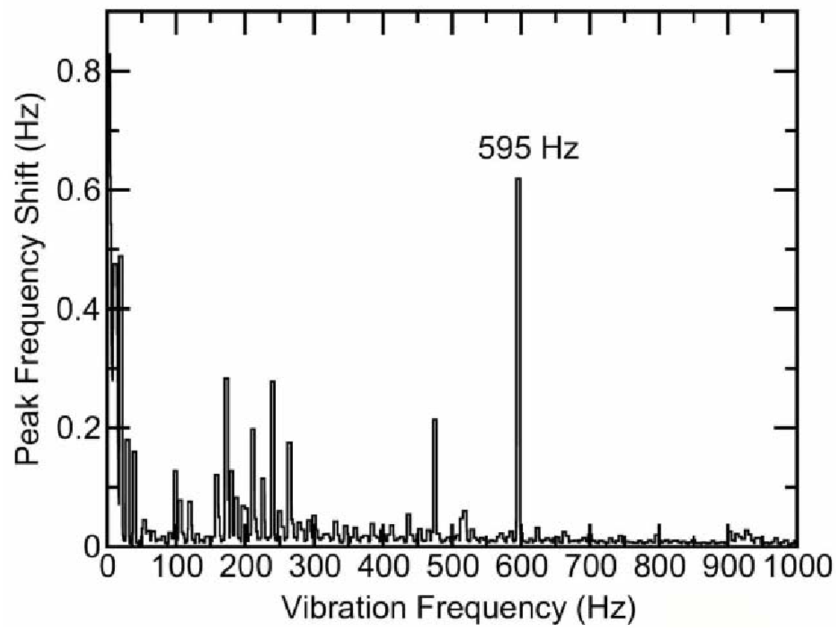

Probability Density (histogram)

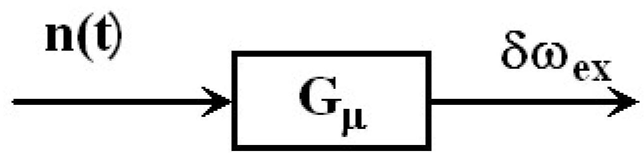

Harmonic oscillator (Ω_μ,τ_μ) driven by:

Single frequency, constant amplitude

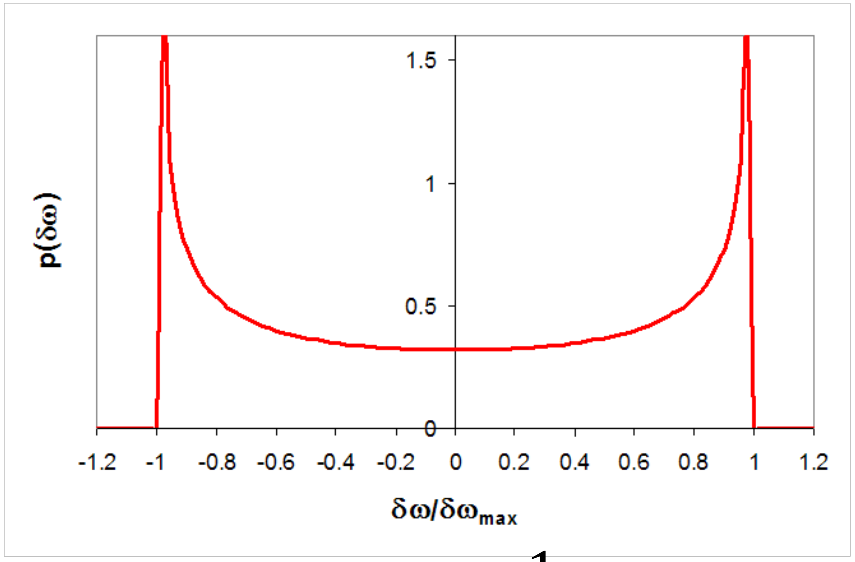

$$p(\delta\omega) = \frac{1}{\pi\sqrt{\delta\omega_{\max}^2 - \delta\omega^2}}$$

White noise, gaussian

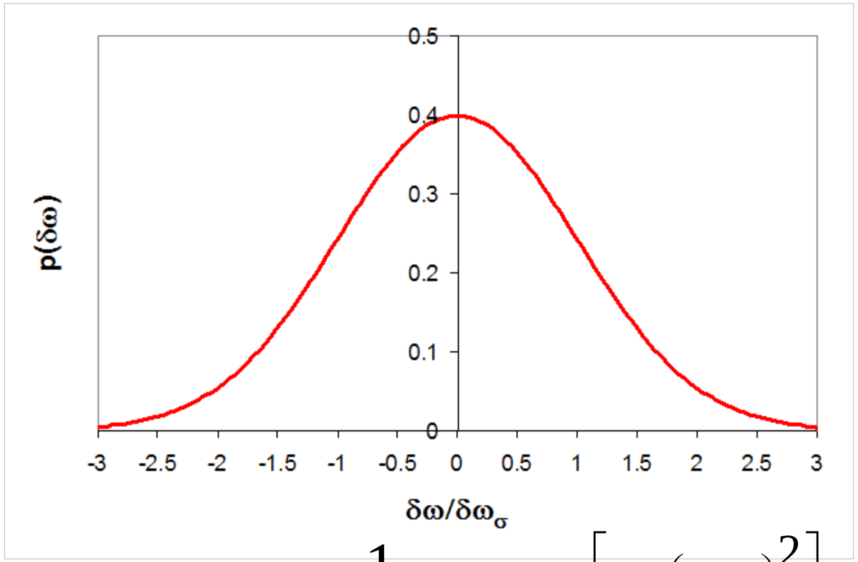

$$p(\delta\omega) = \frac{1}{\sigma_\omega\sqrt{2\pi}}\exp\left[-\frac{1}{2}\left(\frac{\delta\omega}{\sigma_\omega}\right)^2\right]$$

Autocorrelation Function

$$R_x(\tau) = \langle x(t)\, x(t+\tau) \rangle = \lim_{T\to\infty} \frac{1}{T} \int_0^T x(t)\, x(t+\tau)\, dt$$

Harmonic oscillator (Ω_μ, τ_μ) driven by:

Single frequency, constant amplitude

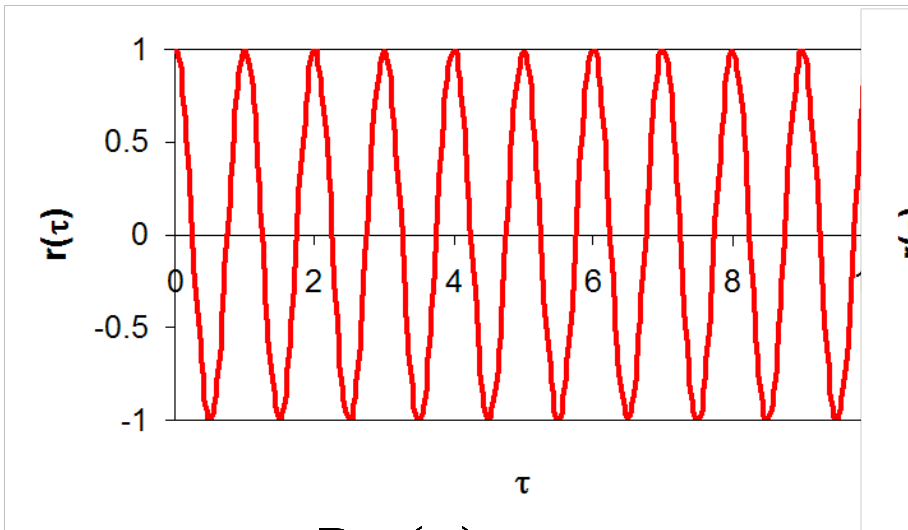

$$r_{\delta\omega}(\tau) = \frac{R_{\delta\omega}(\tau)}{R_{\delta\omega}(0)} = \cos(\omega_d \tau)$$

White noise, gaussian

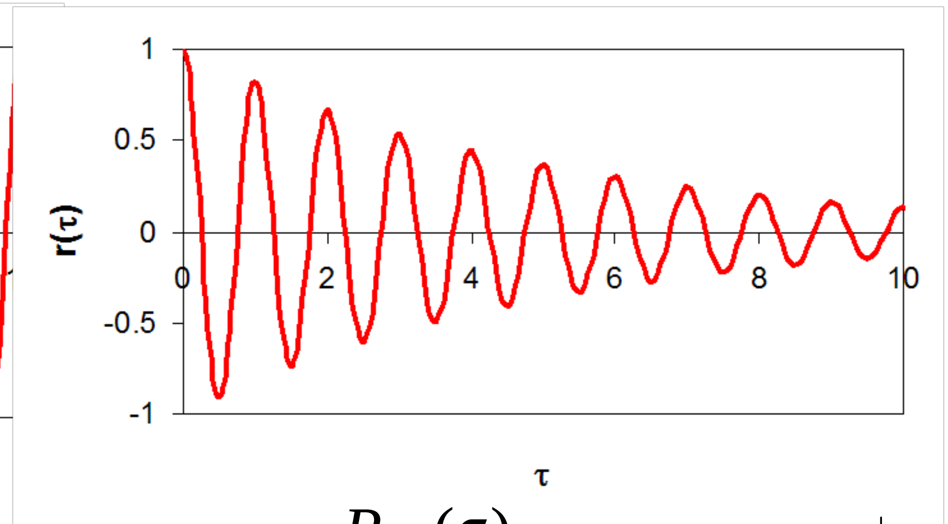

$$r_{\delta\omega}(\tau) = \frac{R_{\delta\omega}(\tau)}{R_{\delta\omega}(0)} = \cos(\Omega_\mu \tau) e^{-\left|\tau/\tau_\mu\right|}$$

Stationary Stochastic Processes

x(t): stationary random variable

Autocorrelation function:

$$R_x(\tau) = \langle x(t)\, x(t+\tau) \rangle = \lim_{T\to\infty} \frac{1}{T} \int_0^T x(t)\, x(t+\tau)\, dt$$

Spectral Density $S_x(\omega)$: Amount of power between ω and $d\omega$

$S_x(\omega)$ and $R_x(\tau)$ are related through the Fourier Transform (Wiener-Khintchine)

$$S_x(\omega) = \frac{1}{2\pi} \int_{-\infty}^{\infty} R_x(\tau)\, e^{-i\omega\tau}\, d\tau \qquad R_x(\tau) = \int_{-\infty}^{\infty} S_x(\omega)\, e^{i\omega\tau}\, d\omega$$

Mean square value:

$$\langle x^2 \rangle = R_x(0) = \int_{-\infty}^{\infty} S_x(\omega)\, d\omega$$

Stationary Stochastic Processes

For a stationary random process driving a linear system

$$x(t) \longrightarrow \boxed{T(i\omega)} \longrightarrow y(t)$$

$$\langle y^2 \rangle = R_y(0) = \int_{-\infty}^{+\infty} S_y(\omega)\, d\omega \qquad \langle x^2 \rangle = R_x(0) = \int_{-\infty}^{+\infty} S_x(\omega)\, d\omega$$

$R_y(\tau)$ $\left[R_x(\tau)\right]$: auto correlation function of $y(t)$ $[x(t)]$

$S_y(\omega)$ $\left[S_x(\omega)\right]$: spectral density of $y(t)$ $[x(t)]$

$$\boxed{S_y(\omega) = S_x(\omega)\left|T(i\omega)\right|^2}$$

$$\boxed{\langle y^2 \rangle = \int_{-\infty}^{+\infty} S_x(\omega)\left|T(i\omega)\right|^2 d\omega}$$

Performance of Control System

Residual phase and amplitude errors caused by microphonics

Can also be done for beam current amplitude and phase fluctuations

Assume a single mechanical oscillator of frequency Ω_μ and decay time τ_μ excited by white noise of spectral density A^2

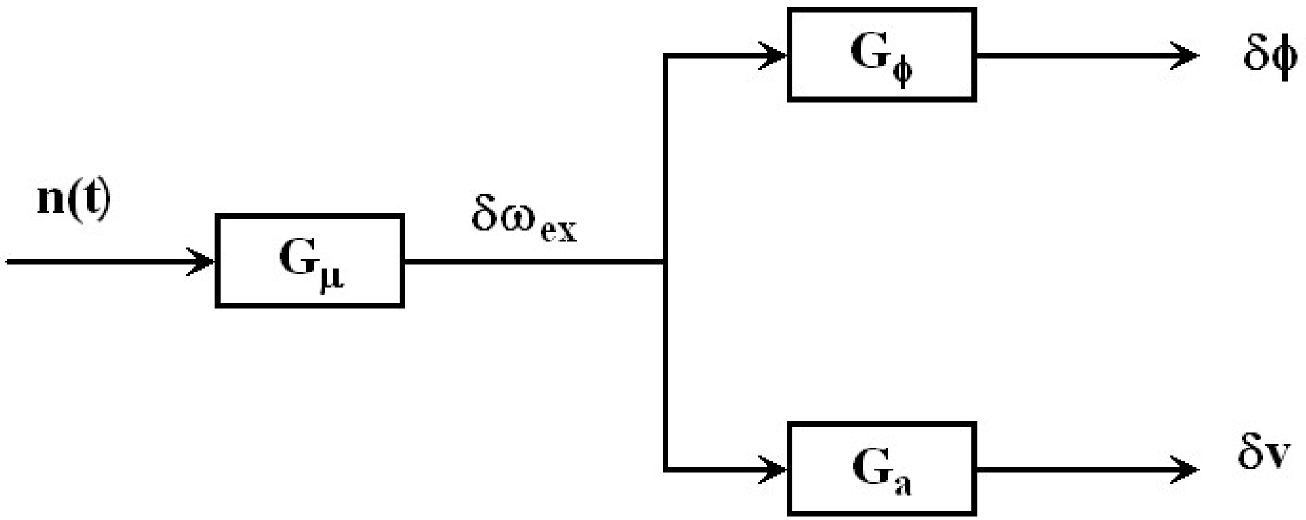

Performance of Control System

$$<\delta\omega_{ex}^2>=A^2\int_{-\infty}^{+\infty}\left|G_\mu(i\omega)\right|^2 d\omega = A^2\int_{-\infty}^{+\infty}\frac{d\omega}{\left|-\omega^2+\frac{2}{\tau_\mu}i\omega+\Omega_\mu^2\right|^2} = A^2\frac{\pi\tau_\mu}{2\Omega_\mu^2}$$

$$<\delta v^2>=A^2\int_{-\infty}^{+\infty}\left|G_\mu(i\omega)G_a(i\omega)\right|^2 d\omega = <\delta\omega_{ex}^2>\frac{2\Omega_\mu^2}{\pi\tau_\mu}\int_{-\infty}^{+\infty}\left|\frac{G_a(i\omega)}{-\omega^2+\frac{2}{\tau_\mu}i\omega+\Omega_\mu^2}\right|^2 d\omega$$

$$<\delta\varphi^2>=A^2\int_{-\infty}^{+\infty}\left|G_\mu(i\omega)G_\varphi(i\omega)\right|^2 d\omega = <\delta\omega_{ex}^2>\frac{2\Omega_\mu^2}{\pi\tau_\mu}\int_{-\infty}^{+\infty}\left|\frac{G_\varphi(i\omega)}{-\omega^2+\frac{2}{\tau_\mu}i\omega+\Omega_\mu^2}\right|^2 d\omega$$

The Real World

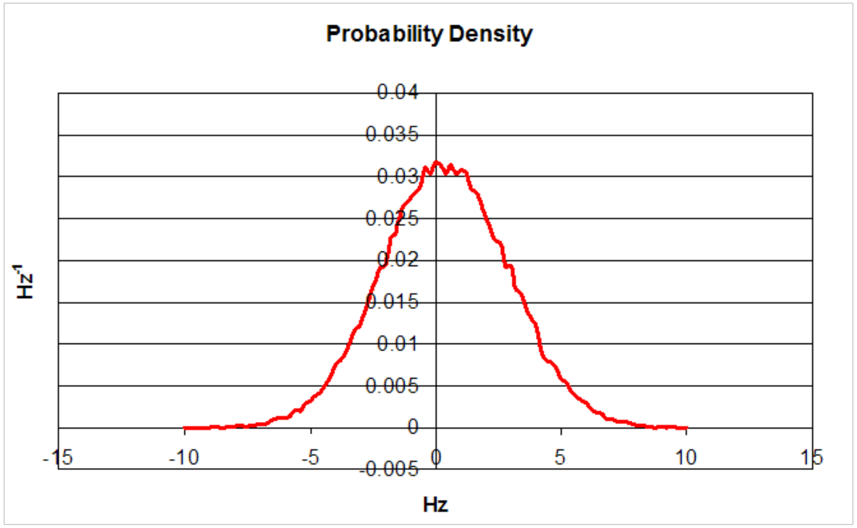

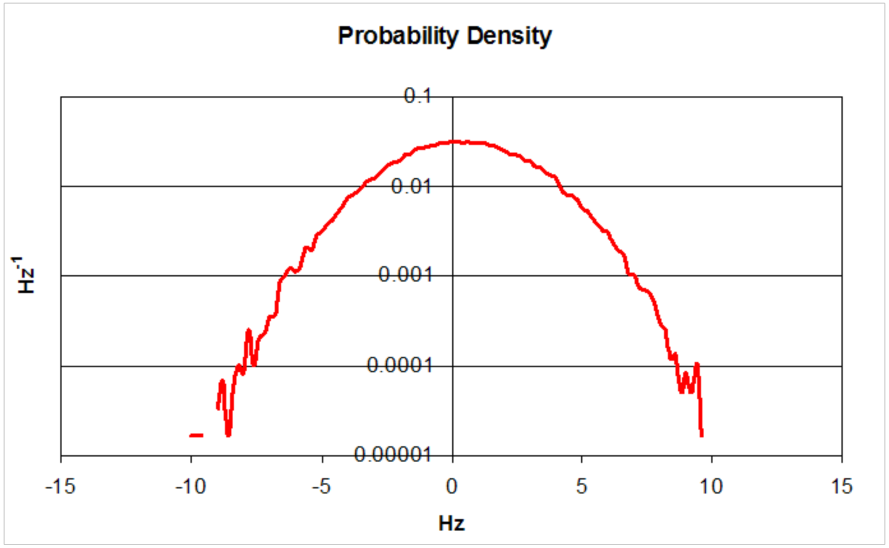

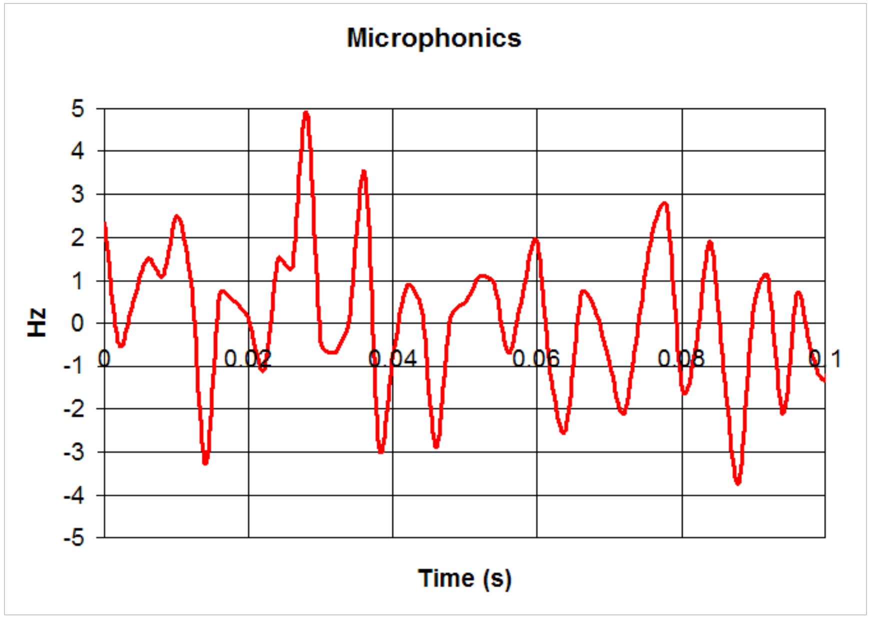

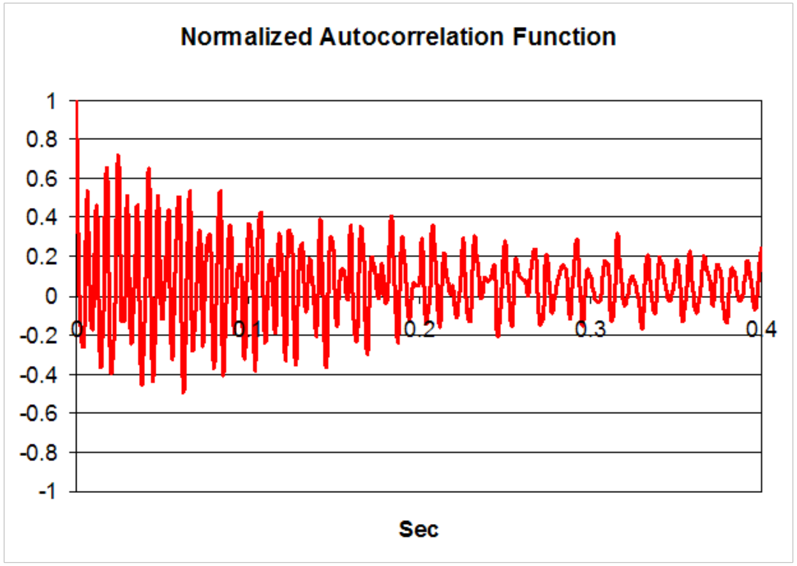

The Real World

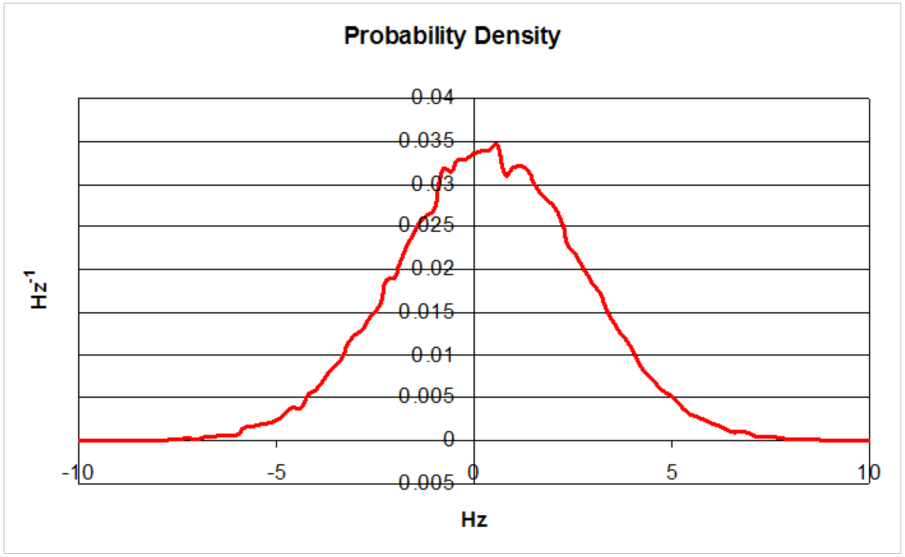

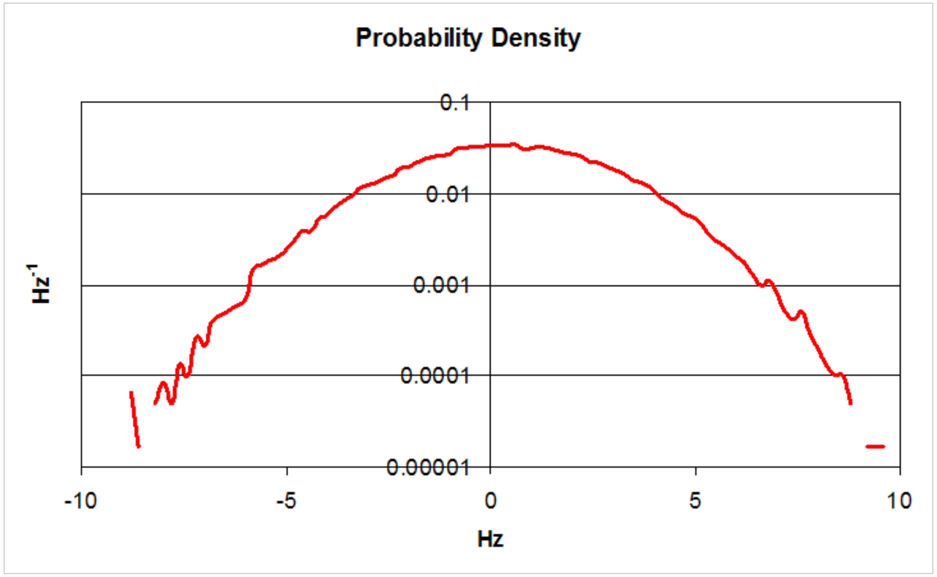

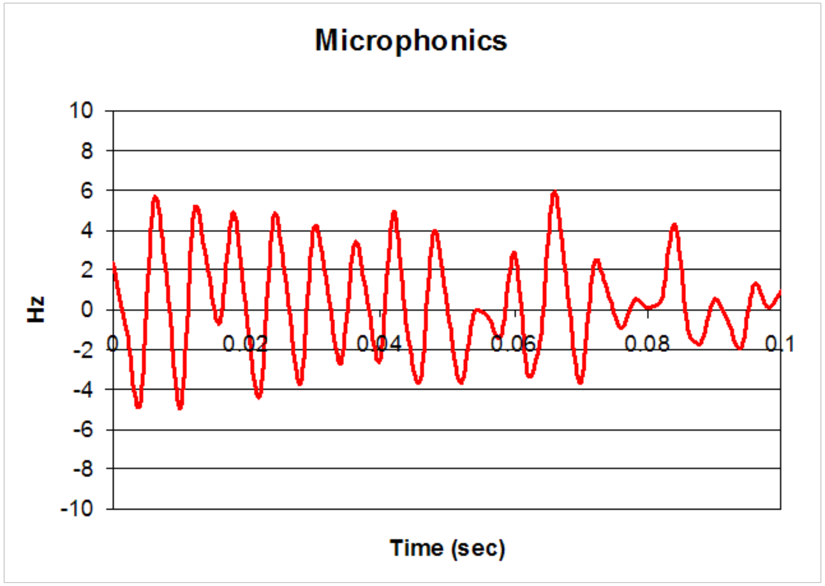

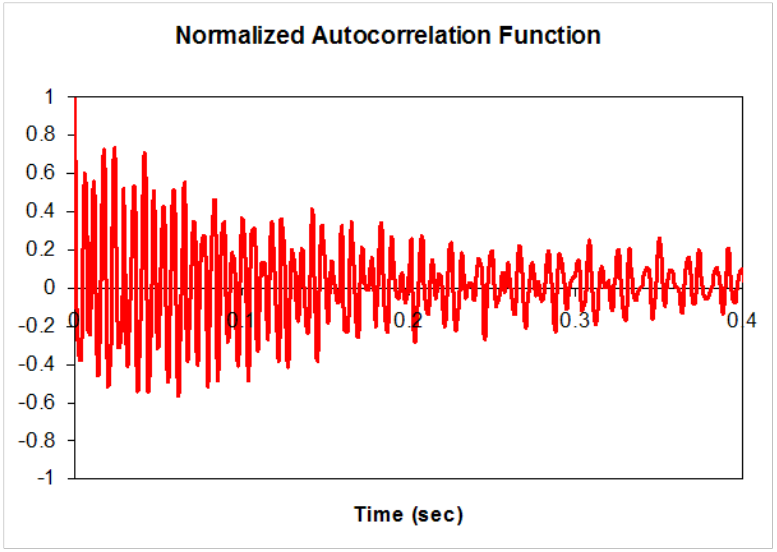

The Real World

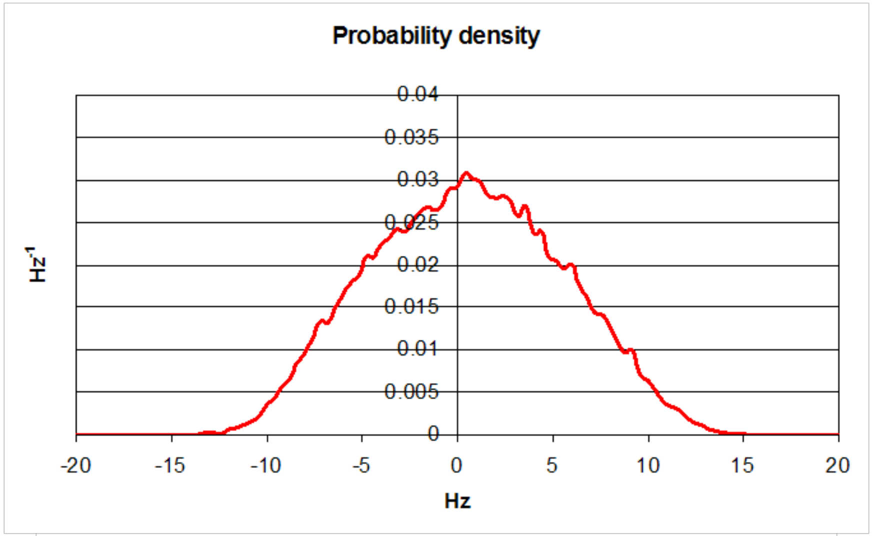

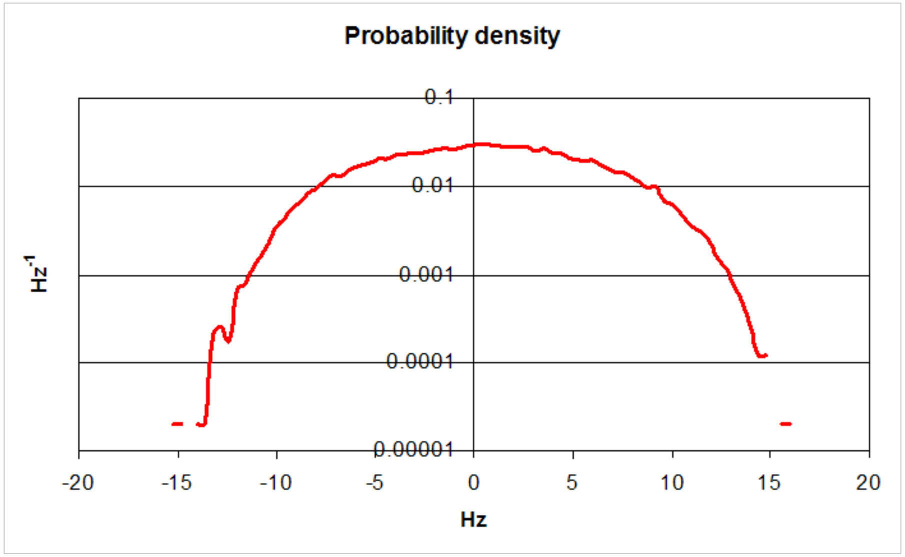

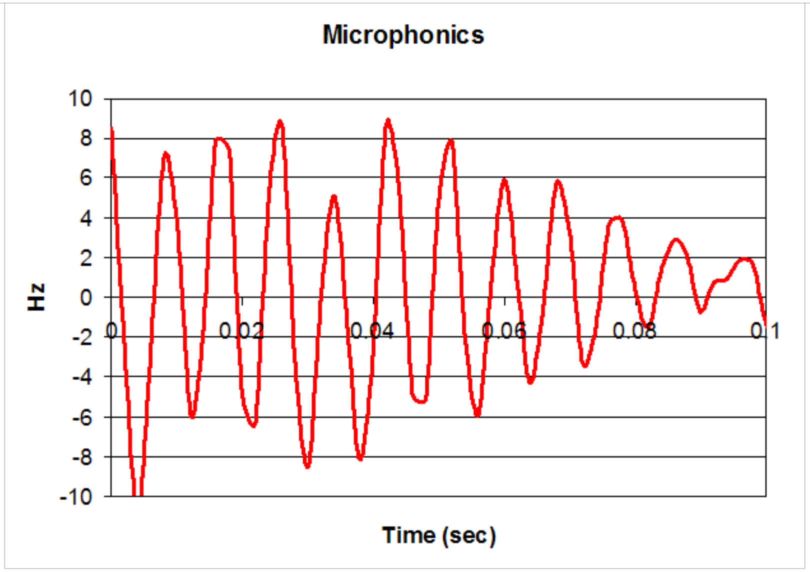

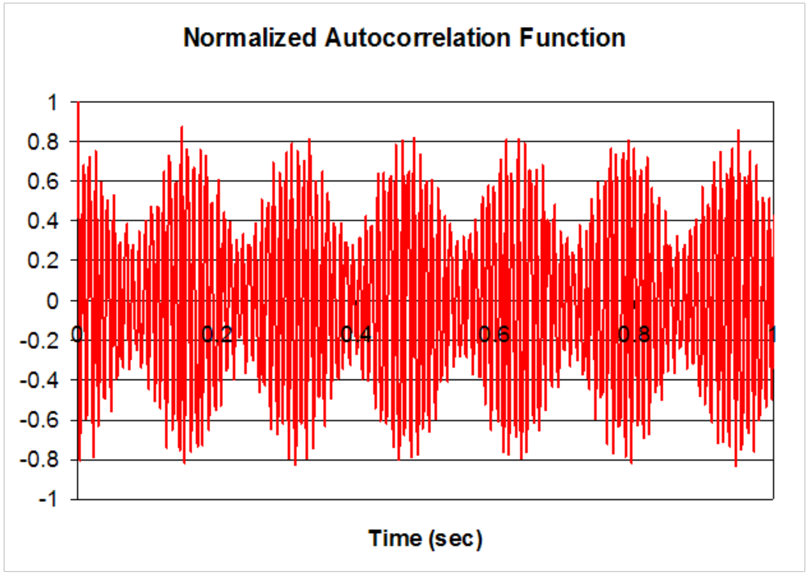

Piezo control of microphonics

MSU, 6-cell elliptical 805 MHz, β=0.49

Adaptive feedforward compensation

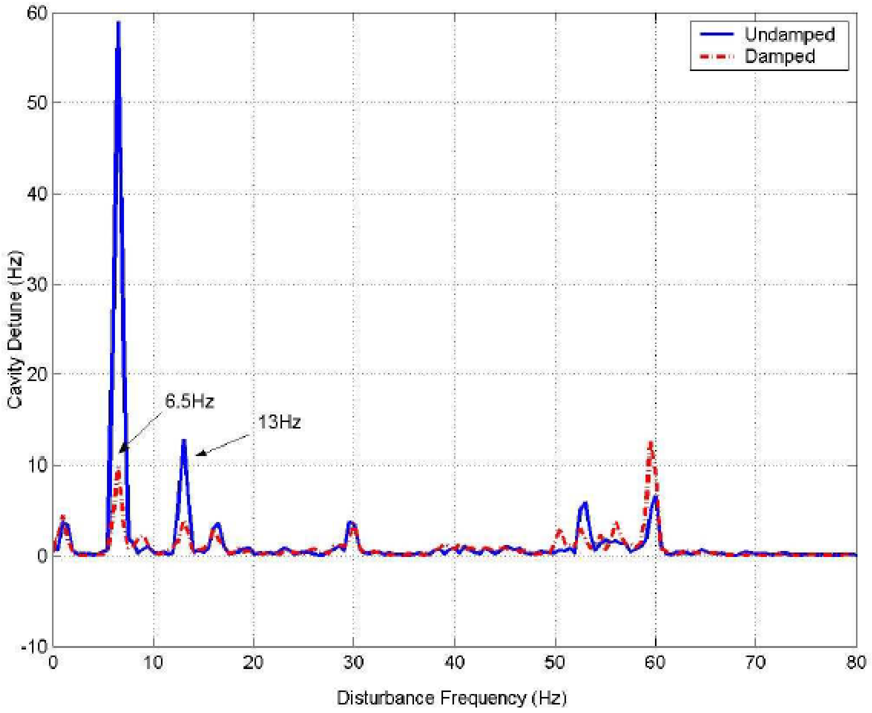

Figure 2. Active damping of helium oscillations at 2K.

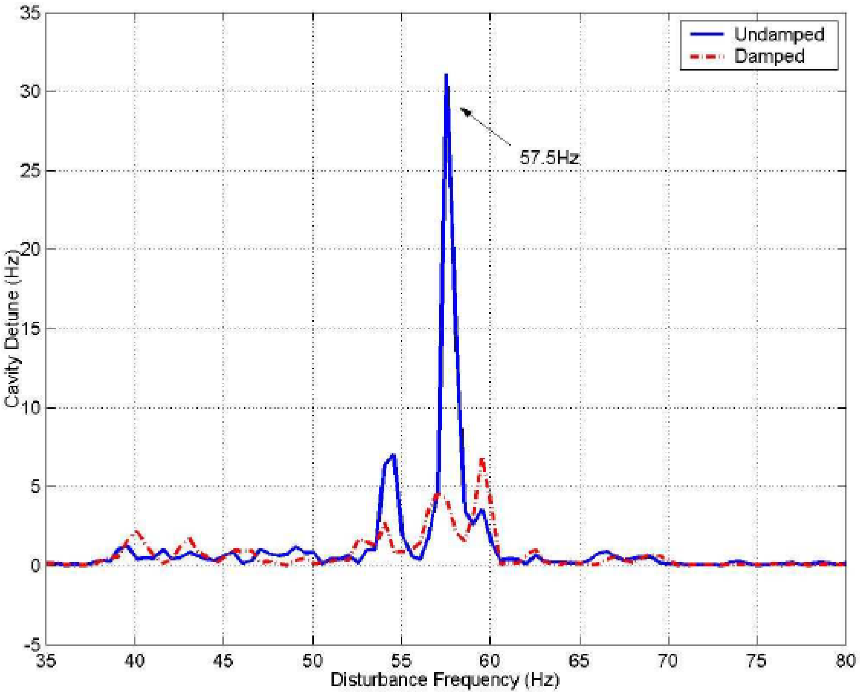

Figure 3. Active damping of external vibration at 2K.

Piezo Control of Microphonics

FNAL, 3-cell 3.9 GHz

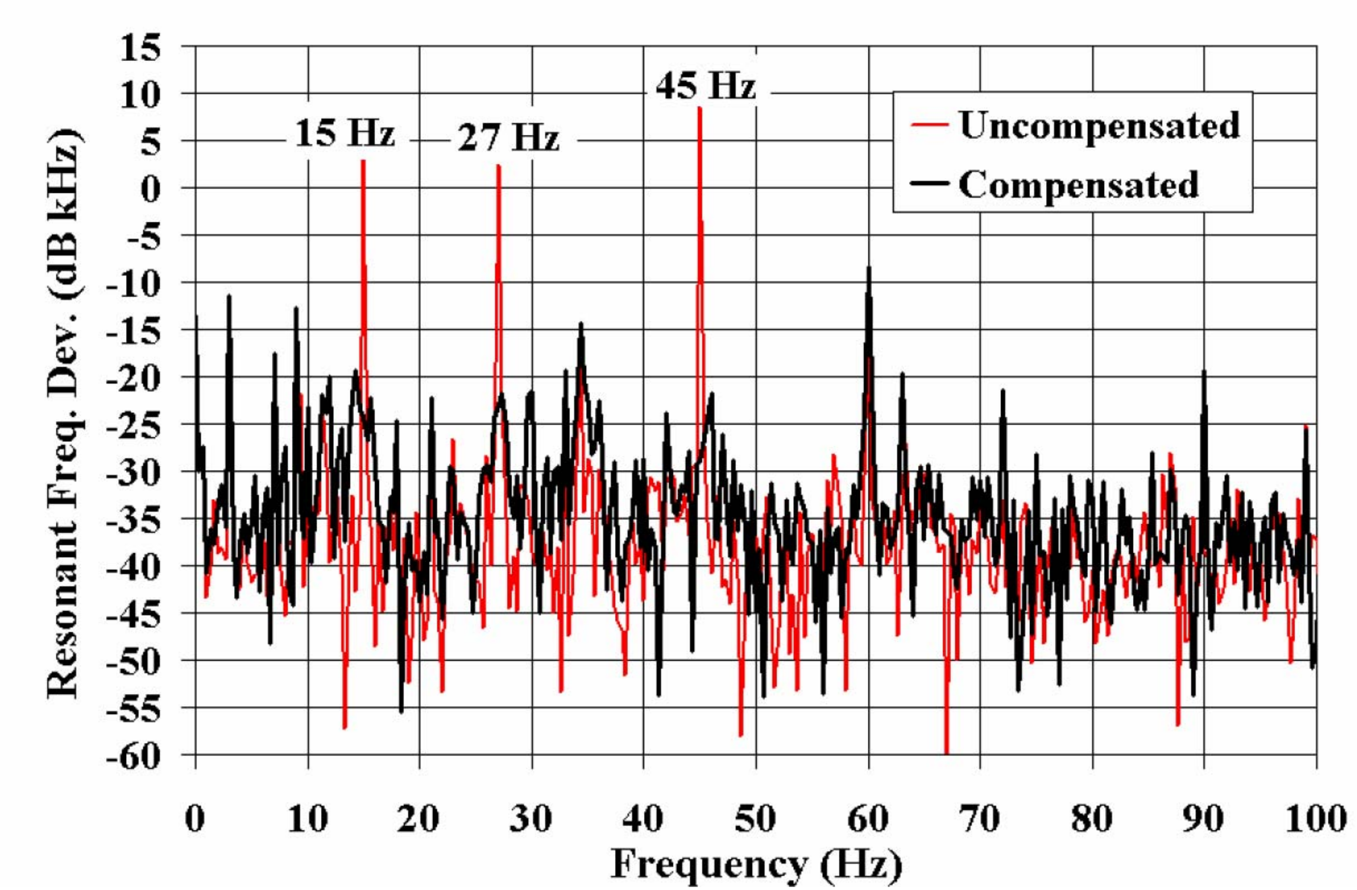

SEL and GDR

- SEL are best suited for high gradient, high-loaded Q cavities operated cw.
  - Well behaved with respect to ponderomotive instabilities
  - Unaffected by Lorentz detuning at power up
  - Able to run independently of external rf source
  - Rise time can be random and slow (starts from noise)

- GDR are best suited for low-Q cavities operated for short pulse length.
  - Fast predictable rise time
  - Power up can be hampered by Lorentz detuning

TESLA Control System

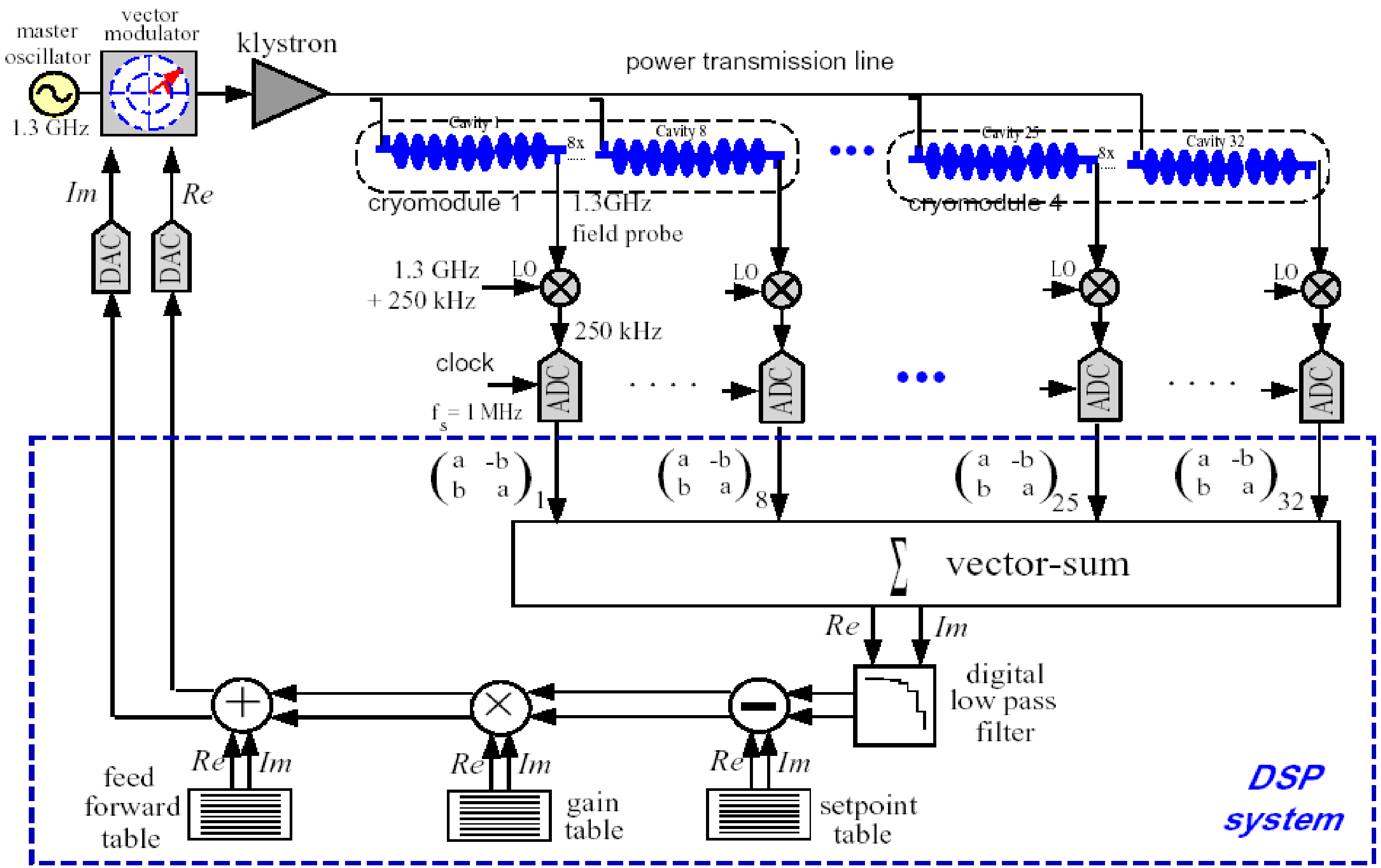

Basic LLRF Block Diagram

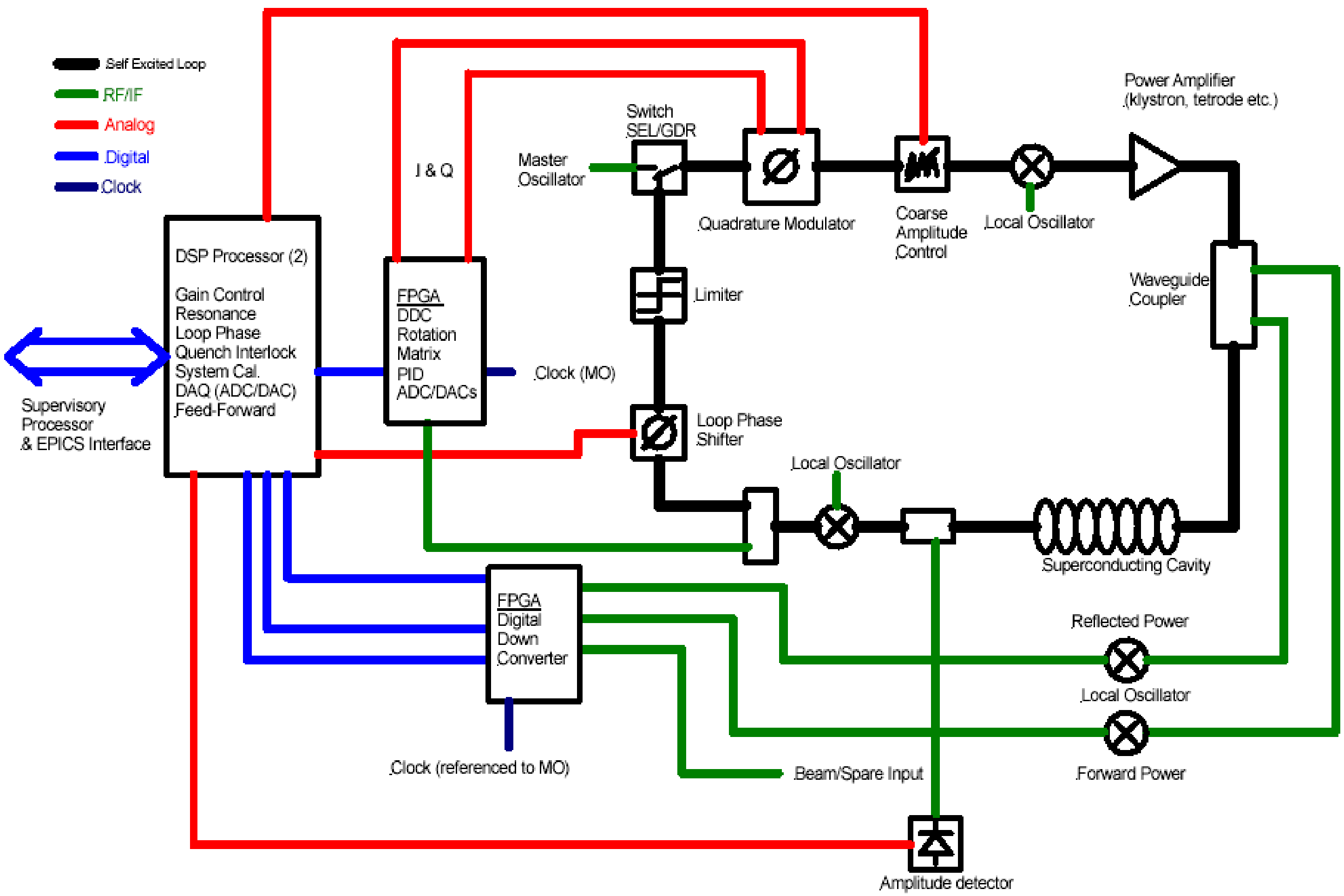

Low level rf control development

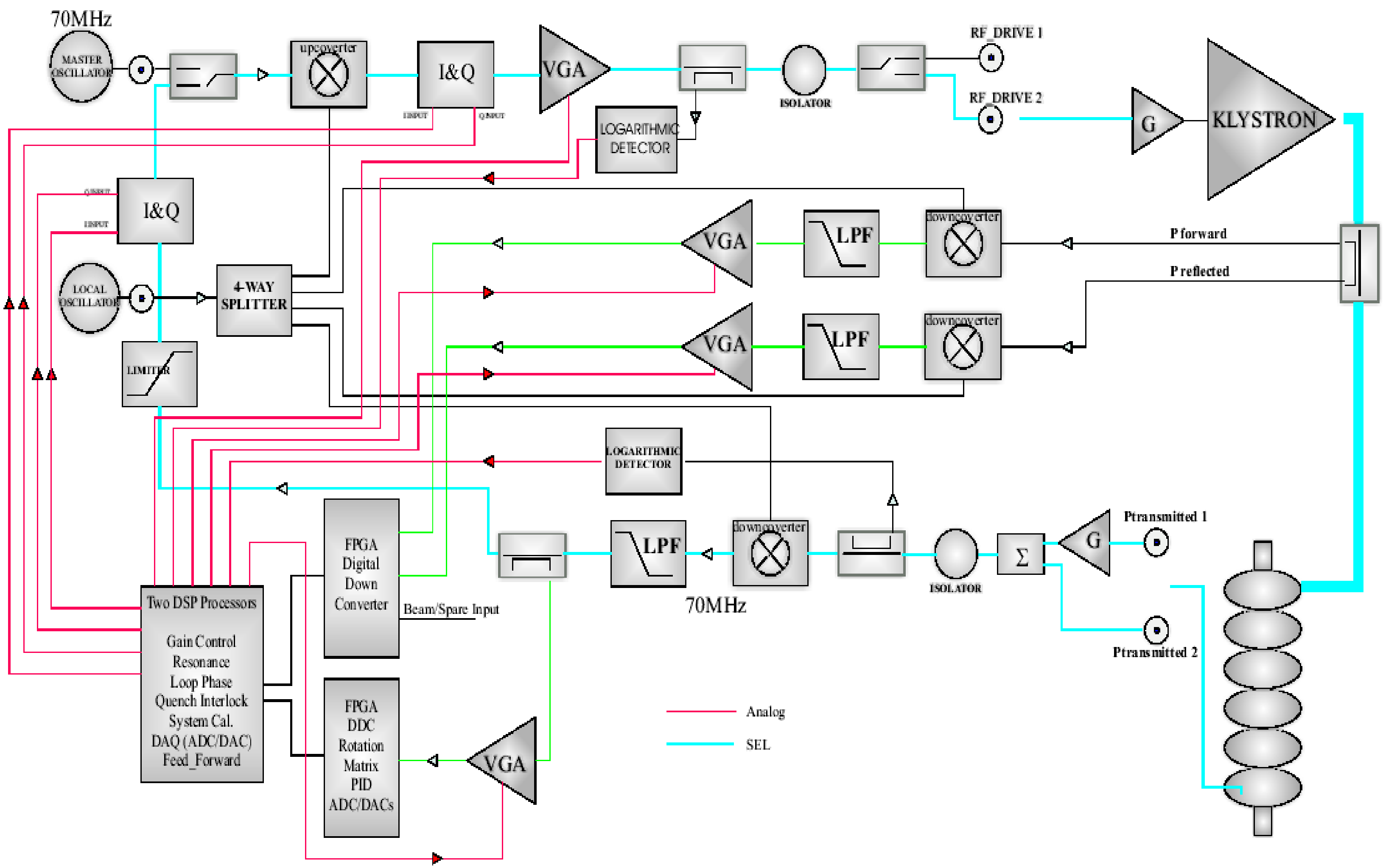

Concept for a LLRF control system

Pulsed Operation

- Under pulsed operation Lorentz detuning can have a complicated dynamic behavior

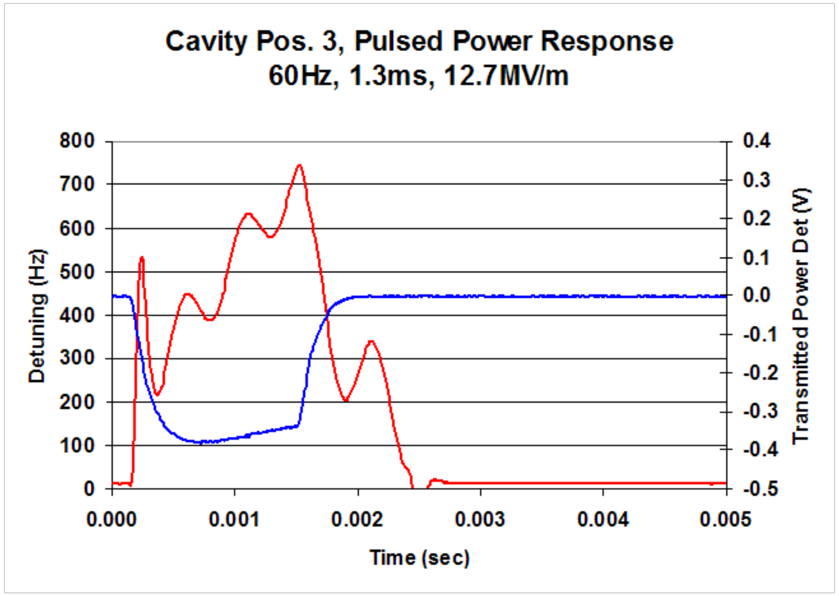

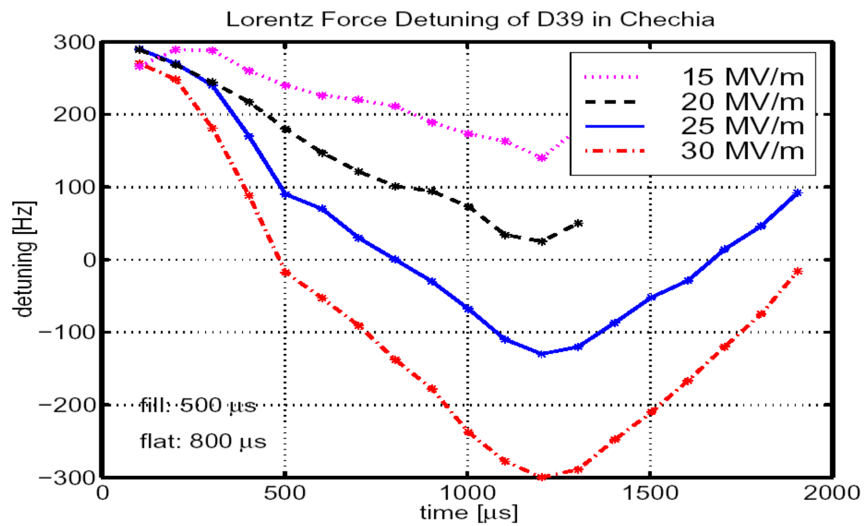

Fig. 2: Lorentz force detuning measured for a TESLA cavity at different gradients.

Pulsed Operation

- Fast piezoelectric tuners can be used to compensate the dynamic Lorentz detuning

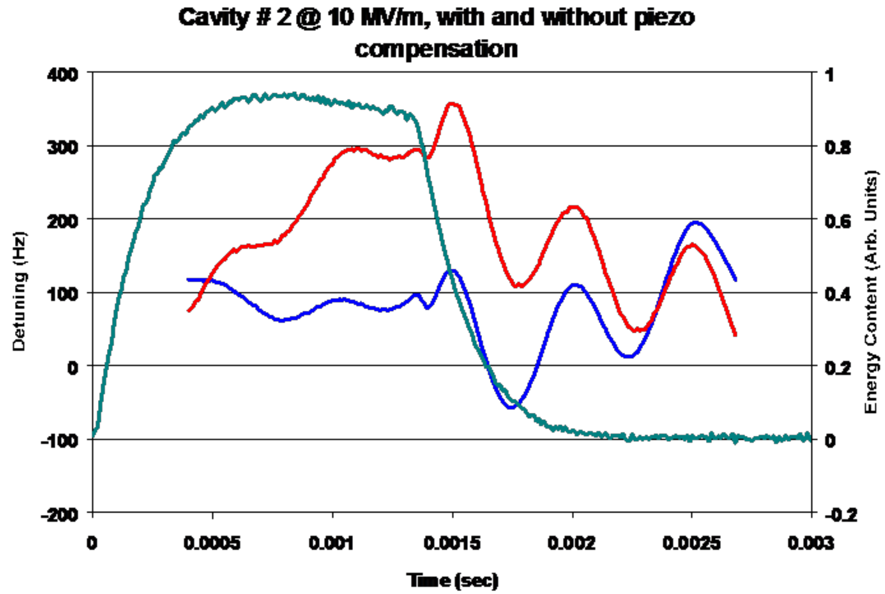

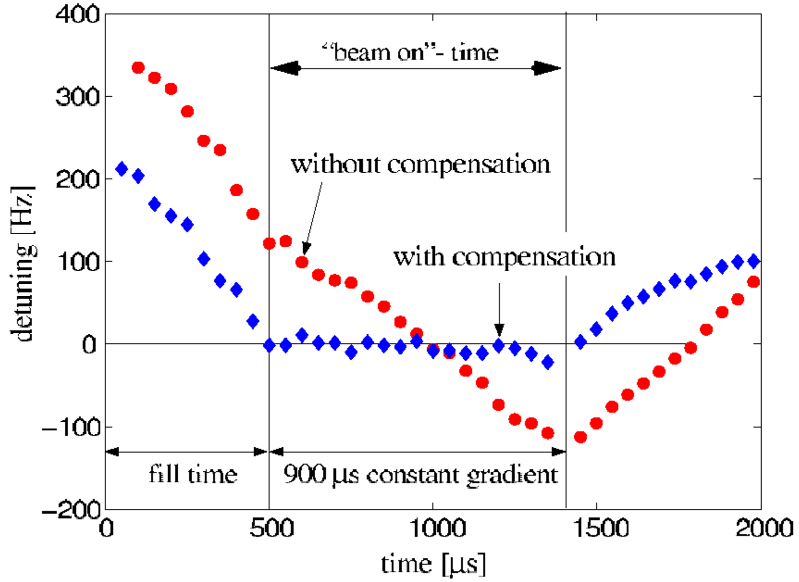

Figure 2. Lorentz force compensation at the TTF